UNIVERSIDAD DE COSTA RICA
SISTEMA DE ESTUDIOS DE POSGRADO

CONTENIDO Y REACTIVIDAD DE LOS MINERALES DE CARGA VARIABLE EN DOS SECUENCIAS TOPOGRÁFICAS DE SUELOS VOLCÁNICOS: IMPLICACIONES EN EL COMPORTAMIENTO DE ADSORCIÓN DE FÓSFORO

Tesis sometida a la consideración de la Comisión del Programa de Estudios de Posgrado en Ciencias Agrícolas y Recursos Naturales para optar al grado y título de Maestría Académica en Ciencias Agrícolas y Recursos Naturales con énfasis en Suelos

CINTYA BEATRIZ SOLANO SOLANO

Ciudad Universitaria Rodrigo Facio, Costa Rica

2025

DEDICATORIA

Agradezco profundamente a mi familia por todo el apoyo brindado durante este proceso, a mis padres por haberme inculcado deseos de superación y a Rolando Castillo Muñoz por ser mi mentor y fuente de inspiración quién me ha motivado para continuar formándome como profesional.

AGRADECIMIENTOS

Agradezco a mi comité de tesis conformado por el Dr. Juan Carlos Méndez Fernández, Dr. Manuel Ernesto Camacho Umaña y el Dr. Agustín Solano Arguedas por sus valiosas contribuciones y guía para mejorar el presente trabajo.

Agradezco a todo el personal del Centro de Investigaciones Agronómicas del Laboratorio de Suelos y Foliares que me brindaron su apoyo cuando hice uso de las instalaciones para elaborar el trabajo de laboratorio.

“Esta tesis fue aceptada por la Comisión del Programa de Estudios de Posgrado en Ciencias Agrícolas y Recursos Naturales de la Universidad de Costa Rica, como requisito parcial para optar al grado y título de Maestría Académica en Ciencias Agrícolas y Recursos Naturales con énfasis en Suelos.”

MARIO ALBERTO VILLATORO SANCHEZ (FIRMA)

Firmado digitalmente por MARIO ALBERTO VILLATORO SANCHEZ (FIRMA)
Fecha: 2025.11.03 17:25:11 -06'00'

Dr. Mario Villatoro Sánchez
Representante del Decano
Sistema de Estudios de Posgrado

JUAN CARLOS MENDEZ FERNANDEZ (FIRMA)

Firmado digitalmente por JUAN CARLOS MENDEZ FERNANDEZ (FIRMA)
Fecha: 2025.10.29 08:49:20 -06'00'

Dr. Juan Carlos Méndez Fernández
Director de tesis

MANUEL ERNESTO CAMACHO UMAÑA (FIRMA)

Firmado digitalmente por MANUEL ERNESTO CAMACHO UMAÑA (FIRMA)
Fecha: 2025.10.29 12:05:51 -06'00'

Dr. Manuel Ernesto Camacho Umaña
Asesor

AGUSTIN FRANCISCO SOLANO ARGUEDAS (FIRMA)

Firmado digitalmente por AGUSTIN FRANCISCO SOLANO ARGUEDAS (FIRMA)
Fecha: 2025.10.28 13:17:12 -06'00'

Dr. Agustín Francisco Solano Arguedas
Asesor

CATALINA SALAS DURAN (FIRMA)
PERSONA FISICA, CPF-01-1107-0374.
Fecha declarada: 04/11/2025 02:43:46 PM
Esta es una representación gráfica únicamente, verifique la validez de la firma.

Dra. Catalina Salas Durán
Directora
Programa Posgrado en Ciencias Agrícolas y Recursos Naturales

CINTYA BEATRIZ SOLANO SOLANO (FIRMA)

Digital unterschrieben von CINTYA BEATRIZ SOLANO SOLANO (FIRMA)
Datum: 2025.10.26 11:49:42 -06'00'

Cintya Beatriz Solano Solano
Candidata

TABLE OF CONTENTS

Contents

ABSTRACT

Volcanic soils are globally significant for agriculture and environmental purposes due to their unique mineralogical properties, particularly the abundance of short-range order (SRO) minerals, which influence both organic carbon stabilization and phosphorus (P) retention. This research was conducted on the southern flank of Irazú Volcano, Costa Rica, to investigate two key aspects: (i) the variation in SRO mineral content and composition along altitudinal gradients and depth, and (ii) the role of the reactive surface area (RSA) and associated to these minerals in modulating P adsorption in two soil toposequences with contrasting soil moisture conditions. The two soil toposequences were defined along an altitudinal range from 1734 to 2853 m asl for the East-South (ES) toposequence with a consistent Udic moisture regime, and from 1724 to 3178 m asl for the West-South (WS) toposequence with a transition from Udic to Ustic moisture regime. Soil chemical extractions using ammonium oxalate (AO), dithionite-citrate (DC) and sodium pyrophosphate (P_y) solutions were used to define operationally the content of Fe, Al, and Si present in soils as SRO minerals and to analyze changes in weathering intensity along the altitudinal gradients. The influence of SRO minerals on P behavior was assessed through extraction techniques such as oxalate-extractable phosphorus (P_{ox}) and Olsen extraction (P-Olsen), phosphate (PO_4^{3-}) and adsorption isotherms. The estimation of the RSA was determinate by implementing a method that uses soil phosphate as probe ion, followed by interpretation with Surface Complexation Model (SCM). The results shown that soils from the ES toposequence exhibit higher content of SRO aluminosilicates, RSA, P_{ox} and PO_4^{3-} sorption capacity (Q_{max}) compared with soils from the WS toposequence. Additionally, the ES toposequence with a consistent Udic moisture regime, showed an increasing downslope in SRO content, total carbon content, RSA, P_{ox}, and PO_4^{3-} sorption capacity (Q_{max}), associated with enhanced weathering with increasing temperature. Additionally, the formation and persistence of SRO minerals in the ES toposequence result from stable Udic moisture conditions maintained along the altitudinal gradient. In contrast, the WS toposequence exhibited no consistent altitudinal trend regarding the variables mentioned above, likely due to a transition from Udic to Ustic regimes that facilitated the transformation of SRO phases into more crystalline forms. Furthermore, for both toposequences, the plant-available P (P-Olsen) remained low across all samples (<10% of Pox), highlighting strong P fixation by SRO minerals. Calcium additions further enhanced P sorption, particularly in soils with low content of SRO and RSA. Overall, the findings demonstrate that both altitude and moisture regime significantly shape SRO formation, surface reactivity, and P availability in

volcanic soils. In summary, this research advances our understanding of the complex interactions between soil mineralogy, soil moisture regimes, landscape position, and P behavior in volcanic soils. The clear differences in PO_4^{3-} sorption capacity and P availability between the two toposequences highlight the need for differentiated land management practices to improve P use efficiency in agricultural activities. Future studies should explore the impact of agricultural practices, such as intensive fertilization and liming, under field conditions to optimize P management in these soils, considering the conditions in soil moisture regimes, mineralogy and reactivity, to accomplish agricultural and environmental objectives in volcanic regions.

RESUMEN

Los Andisoles son suelos formados a partir de diversos materiales volcánicos como depósitos de caída tipo tefra (ceniza volcánica), material volcaniclástico y lavas. En Costa Rica, aproximadamente una sexta parte del teriitorio nacional se encuentra cubierto por Andisoles. En ellos se desarrollan diversas actividades agrícolas de gran importancia económica y productiva para el país entre ellas la producción de cultivos hortícolas, cultivo de flores ornamentals, ganadería lechera y una parte importante del cultivo de café. A nivel mundial estos suelos volcánicos son muy importantes tanto para la agricultura como para el medio ambiente debido a que tienen propiedades mineralógicas únicas, en particular la abundancia de minerales de orden de corto alcance (SRO), que influyen tanto en la estabilización del carbono orgánico como en la retención de fósforo (P). Su alta capacidad de retención de fósforo (P), asociada principalmente a la presencia de fracciones minerales altamente reactivas de carga variable (minerales SRO) limitan la disponibilidad y recuperación de este nutriente por parte de las plantas. Por ello, en los sistemas agrícolas intensivos establecidos sobre estos suelos es común la aplicación de cantidades elevadas de fertilizantes fosfatados para mantener rendimientos adecuados. Sin embargo, aún con aportes significativos de fósforo, una fracción considerable de este nutriente queda retenida por componentes minerales reactivos, lo que representa un desafío agronómico y un costo económico importante para los productores. Esta investigación se llevó a cabo en la ladera sur del volcán Irazú, en Costa Rica, con el fin de estudiar dos aspectos clave: (i) la variación en el contenido y la composición de los minerales SRO a lo largo de los gradientes altitudinales y la profundidad, y (ii) el papel del área superficial reactiva (RSA) y su asociación con estos minerales en la modulación de la adsorción de P en dos toposecuencias de suelo con condiciones de humedad contrastantes. Las dos toposecuencias del suelo se definieron a lo largo de un rango altitudinal de 1734 a 2853 m s. n. m. para la toposecuencia Este-Sur (ES) con un régimen de humedad Údico constante, y de 1724 a 3178 m s. n. m. para la toposecuencia Oeste-Sur (WS) con una transición del régimen de humedad Údico a Ústico. Se utilizaron extracciones químicas del suelo con soluciones de oxalato de amonio (AO), ditionito-citrato (DC) y pirofosfato de sodio (Py) para definir operativamente el contenido de Fe, Al y Si presentes en los suelos como minerales SRO y para analizar los cambios en la intensidad de la meteorización a lo largo de los gradientes altitudinales. Se evaluó la influencia de los minerales SRO en el comportamiento de P mediante técnicas de extracción como el P extraíble con oxalato (P_{ox}) para todas las muestras de suelo, la extracción de Olsen (P-Olsen) y la capacidad de retención de P (CRP) para los dos primeros horizontes de los perfiles de suelo. Adicionalmente, se realizaron isotermas de adsorción de fosfato (PO_4^{3-}) en muestras de horizontes superficiales, cuyos datos

fueron interpretados utilizando un enfoque de Langmuir. También, se realizaron isotermas de adsorción de PO_4^{3-} con adición de calcio (Ca^{2+}), en muestras de suelo seleccionadas con características de reactividad contrastantes, con el fin de determinar el efecto de Ca^{2+} en la adsorción de PO_4^{3-}. La estimación del RSA se determinó mediante la aplicación de un método que utiliza el fosfato del suelo como ion sonda, seguido de la interpretación con el Modelo de Complejación Superficial (SCM). Los resultados mostraron que los suelos de la toposecuencia ES presentan un mayor contenido de aluminosilicatos SRO, RSA, P_{ox} y capacidad de sorción PO_4^{3-} (Q_{max}) en comparación con los suelos de la toposecuencia WS. Además, la toposecuencia ES, con un régimen de humedad Údico constante, mostró un aumento descendente en el contenido de minerales SRO, el contenido total de carbono, el RSA, el P_{ox} y la capacidad de sorción de PO_4^{3-} (Q_{max}). Estas tendencias de aumento con la altitud están asociadas a cambios en las condiciones ambientales como el aumento de la temperatura que promueve una mayor meteorización de los minerales primarios y la formación de minerales SRO. Además, la formación y persistencia de minerales SRO en la toposecuencia ES es el resultado de condiciones de humedad Údicas estables que se mantienen a lo largo del gradiente altitudinal, lo que favorece su preservación e inhibe su transformación a minerales más cristalinos menos reactivos. Por el contrario, la toposecuencia WS no mostró una tendencia altitudinal constante en relación con las variables mencionadas anteriormente, probablemente debido a una transición de regímenes Údico a Ústico que facilitó la transformación de las fases minerales SRO en formas más cristalinas. Además, en ambas toposecuencias, el P disponible para las plantas (P-Olsen) se mantuvo bajo en todas las muestras (<10 % de P_{ox}), lo que pone de relieve la fuerte fijación de P por los minerales SRO. Adicionalmente, se demostró que la adición de Ca^{2+} en general aumentó la adsorción de PO_4^{3-} en los suelos a través de la formación de complejos ternarios. Dicho efecto fue mayor en suelos caracterizados por tener un menor contenido mineral SRO y por ende una menor reactividad, por el contrario, fue menor en el suelo más reactivo (E3-1) del grupo de muestras seleccionadas. En general, los resultados demuestran que tanto la altitud como el régimen de humedad influyen significativamente en la formación y preservación de minerales SRO, la RSA, la adsorción y disponibilidad de P en los suelos volcánicos. En resumen, esta investigación amplía nuestro conocimiento sobre las complejas interacciones entre la mineralogía del suelo, los regímenes de humedad del suelo, la posición del paisaje y el comportamiento de adsorción de P en los suelos volcánicos. Las claras diferencias en la capacidad de sorción de PO_4^{3-} y la disponibilidad de P entre las dos toposecuencias ponen de relieve la necesidad de prácticas de gestión del suelo diferenciadas para mejorar la eficiencia del uso del P en las actividades agrícolas. Futuro estudios deberían explorar el impacto de las

prácticas agrícolas, como la fertilización intensiva y el encalado, en condiciones de campo para optimizar la gestión del P en estos suelos, teniendo en cuenta las condiciones de los regímenes de humedad del suelo, la mineralogía y la reactividad, con el fin de alcanzar los objetivos agrícolas y medioambientales en las regiones volcánicas.

INDEX OF TABLES

INDEX OF FIGURES

SUPPLEMENTARY INFORMATION

LIST OF ABBREVIATIONS

AC: Activated Carbon

ACCS: Asociación Costarricense de Ciencias del Suelo

AD: air-dried

Al: Aluminum

Al_{ox}: Aluminum extracted with ammonium oxalate

Alpy: Aluminum extracted with sodium pyrophosphate

AO: Ammonium Oxalate

Ca: Calcium

$CaCl_2$: Cloruro de calcio

CD-MUSIC: Charge Distribution Multisite Ion Complexation Model

Chi-sq: Chi-squared statistic

CIA: Centro de Investigaciones Agronómicas

DC: Dithionite-Citrate

ES: East-South

Fe: Iron

Fedc: Iron extracted with dithionite-citrate

Fe_{ox}: Iron extracted with ammonium oxalate

FIA: Flow Injection Analyzer

ICP-OES: Inductively Coupled Plasma – Optical Emission Spectroscopy

INII: Instituto de Investigaciones en Ingeniería

K_L: Langmuir affinity constant

MAE. Mean Absolute Error

MSE: Mean Squared Error

NaF: Fluoruro de sodio$NaNO_3$: Nitrato de sodio

NSSC: National Soil Survey Center

OD: oven-dried

P: Phosphorus

PO_4^{3-}: Phosphate

PRC: Phosphorus retention capacity

PSC: Phosphorus sorption capacity

PSDA: Particle size distribution analysis

Py: Pyrophosphate

PZC: Point of Zero Charge

Q_{max}: Maximum sorption capacity

RMSE: Root Mean Square Error

RSA: Reactive surface area

SCM: Surface Complexation Model

SD: Standard Deviation

SE: Standard errors

Si: Silicon

Si_{ox}: Silicon extracted with ammonium oxalate

SOC: Soil Organic Carbon

SOM: Soil Organic Matter

SRO: Short-range order

SSA: Specific surface area

SSR: Soil Solution Ratio

UCR: Universidad de Costa Rica

USDA: United States Department of Agriculture

WS: West-South

1. INTRODUCTION

In Costa Rica, approximately 14% of the surface territory is covered by soils derived from ashes and other volcanic materials called Andisols (Alvarado *et al*. 2001). Agricultural activities of great economic and productive importance for the country are developed on these soils, such as the production of horticultural crops, which are mainly concentrated in regions with soils derived from volcanic materials, as well as part of the national coffee production. These soils are characterized by high P retention associated mainly with the presence of highly reactive mineral fractions with variable charge. As a consequence, in these Andisols the availability and recovery rate of P by plants is low (Nanzyo 2002). Consequently, in intensive agriculture developed on these soils, large amounts of PO_4^{3-} fertilizers are usually applied in order to maintain adequate crop yields. However, even with intensive phosphate input, phosphate can be retained by reactive fractions of variable charge, which is a challenge for farmers with a significant economic cost.

Therefore, it is of great importance to study in detail the chemical processes and mechanisms that condition P availability in this type of volcanic soils. An example of these processes is the adsorption of PO_4^{3-} ions, which depends to a great extent on the content and reactive surface of the variable charge minerals. Both of the previously mentioned properties were investigated in the present study in order to quantify and understand their variability as a function of the degree of pedogenetic development of soils derived from volcanic materials, as well as the implications in terms of PO_4^{3-} adsorption behavior. The information obtained will allow a better understanding of the relationship between adsorption processes and the dominant mineralogical properties present in such soils, and their variation of this relationship with respect to changing environmental conditions such as temperature, precipitation and altitude. From a practical point of view, the information will allow proposing better management practices for the nutrient P in volcanic soils, based on the understanding of the chemical processes that condition the solubility of this element.

1.1. MINERALOGICAL CHARACTERISTICS

In general, Andisols are formed from primary minerals such as volcanic glass, quartz, pyroxenes, plagioclase, olivines, opaque minerals, hornblendes and biotites, present in materials such as tephras and lavas (Nanzyo 2002). Some of these primary minerals can be found in a slightly altered (poorly weathered) form in the larger soil grain size fractions, for example, in the sand

fraction. This alteration occurs by the weathering process, i.e., the chemical and physical mediated disintegration of these minerals.

Weathering processes of primary minerals release ions into solution (including Al, Fe, Si) which creates a condition of supersaturation with respect to secondary mineral phases, and subsequent formation of other solid phases (secondary minerals) occurs. Weathering of volcanic glass gives rise to the formation of secondary minerals of a weak degree of crystallinity, commonly referred to in literature as short-range-order (SRO) minerals. For example, aluminosilicate minerals such as allophane, proto-imogolite and imogolite, and iron (hydr)oxides like ferrihydrite and aluminum can originate from weathering of mafic and intermediate volcanic materials (Neall 2000).

The crystallinity of secondary minerals is influenced by environmental conditions such as temperature and humidity. Variations in these factors can alter both the composition and the transformation of these minerals, leading to changes from less crystalline to more crystalline phases (Candra *et al*. 2019; Tsai *et al*. 2010). Examples include the transformation of ferrihydrite to hematite or allophane/imogolite into gibbsite (Jongmans *et al*. 1995; Wada and Harward 1974). Toposequences, or soil topographic sequences, understood as a succession of soils and their transformation influenced by topography (Alves et al. 2024) provide a valuable approach for studying how factors such as altitude, temperature and precipitation affect edaphic processes. When such factors vary along the landscape, such environmental gradients can result in distinct mineralogical differences in the crystallinity of variable charge minerals. In volcanic soils, these variations can lead to significant changes in both the quantity and type of variable charge minerals, such as SRO, present along the toposequence, topic that was developed in the Chapter 1 of these thesis. Consequently, these changes also affect other factors like the RSA of the soils and PO_4^{3-} sorption capacity, topics that were further discussed in Chapter 2 of this thesis.

The SRO minerals have amphoteric properties, which means they possess variable type charge generated by deprotonation and protonation of functional groups exposed on their surfaces (Wada and Kawabata 1991). This charge is dependent on the chemical conditions of the soil solution, particularly pH and ionic strength. Generally, the pH corresponding to the point of zero charge (PZC) in these minerals is around 7 to 9 (Qafoku et al. 2004), so at the usual pH conditions in soils, these minerals have a net positive charge, making them capable of retaining anions and organic matter (Neall 2000).

Among the SRO aluminosilicates are allophane and imogolite, which have nanometer sizes with hollow spherical and tubular shapes (with diameters less than 3 to 5 nm and 1 to 2 nm,

respectively) and specific surface areas of approximately 1000 m^2 g (Neall 2000). According to Parfitt and Kimble (1989) the formation of aluminosilicate type allophane depends on both the parent material and the pH of the medium. Originally, allophane is formed from volcanic glass at pH (in water) between 5 and 7, and from feldspar/biotite at pH around 5 in soils with acidic and well-drained moisture regimes (Parfitt and Kimble 1989). In addition, these authors mention that silicon (Si)-rich allophane occurs in Si-enriched environments and Al-rich allophane forms in acid soils where Si tends to be low. Al-rich allophane formation is less frequent in soils with ustic, xeric and aridic moisture regimes because of less leaching (Parfitt and Kimble 1989). Also, allophane and imogolite have been found in soils formed from basalt saprolite in Hawaii, favored by conditions of high rainfall, good subsoil permeability, low pH and high organic content of the leaching solution (Wada *et al*. 1972).

Ferrihydrite is a secondary SRO iron mineral derived from weathering of volcanic materials as glass of mafic-intermediate composition and mafic crystals in the primary constituents of volcanic materials (Neall 2000). It is a variable charge mineral characterized by a large specific surface area similar to allophane and a high PO_4^{3-} binding capacity, contrary to imogolite which is less reactive with PO_4^{3-} (Hiemstra 2013, Nanzyo 2002, Wada 1989, Henmi *et al*. 1982). Ferrihydrite is an important precursor of other more stable and crystalline forms of iron oxides such as goethite and hematite which are often the last stage of transformation of these oxides (Cornell and Schwertmann 2003). Goethite and hematite are also characterized by variable charge, however, these minerals are less reactive than ferrihydrite due to their larger size and degree of crystallinity (Anschutz y Penn 2005).

Andisols are also characterized by the presence of metal–humus complexes (Al/Fe–humus) within their colloidal fraction. When the dominant form of active Al occurs as Al–humus complexes, these soils are typically classified as non-allophanic Andisols (Nanzyo, 2002). The high humus content in the surface horizons of such soils is primarily stabilized either through complexation with Al released during the weathering of volcanic materials (Takahashi and Dahlgren, 2016) or through coprecipitation and/or adsorption onto SRO minerals (Jamoteau *et al*. 2025). A key distinction between non-allophanic and allophanic Andisols is that the former exhibit stronger acidity and higher levels of exchangeable Al, which can lead to phytotoxicity in plants (Takahashi and Dahlgren, 2016).

1.2. SURFACE REACTIVITY

The colloidal fraction of Andisols is characterized by being very reactive and having a high specific surface area (Nanzyo 2002), mainly due to the presence of metastable nanocrystalline materials

such as allophanes, ferrihydrites and aluminum oxides. Specific surface area and surface charge density are two factors that determine the reactivity of a soil mineral/material (Uehara and Gillman 1980). This is related to adsorption processes between the solution and the surfaces of mineral particles or organic matter, where the bioavailability and mobility of ions depend on these interactions (Hiemstra *et al*. 2010a). Factors such as pH, ionic strength, presence or competition of promoter ions as well as the nature and amount of substrate affect the distribution of cations and anions over the solid and solution phase (Hiemstra *et al*. 2010a).

Surface complexation models (SCM) are used to estimate and predict the distribution of metals and oxyanions between solution and mineral surfaces (Hiemstra et al. 2010a). Any application of SCM to natural systems requires information about the RSA of the material involved in the adsorption process (Hiemstra et al. 2010a). Therefore, the evaluation of this important property is essential to study the mechanisms of ion adsorption that condition their availability in soils.

Recently, a methodology has been proposed that uses "native" soil phosphate as a probe ion to estimate the RSA of variably charged mineral fractions, with units of m^2 g of $soil^{-1}$. What occurs is a competitive interaction between phosphate and carbonate ions for adsorption to reactive groups on mineral surfaces which are interpreted by SCM (Hiemstra *et al*. 2010a). For such methodology, ferrihydrite has been proposed as a reference material for its already characterized reactivity properties and has proven to be a suitable indicator to consistently evaluate the reactive surface area (Mendez *et al*. 2020).

1.3. PHOSPHATE (PO_4^{3-}) RETENTION IN VOLCANIC SOILS

PO_4^{3-} is an oxyanion characterized by having low solubility in the soil. This makes it one of the most limiting elements for plant growth (Strawn et al. 2015). This anion tends to be strongly adsorbed by predominantly positively charged clay minerals in the soil (including Fe/Al oxides, SRO minerals such as allophane, imogolite and ferrihydrite) and also forms mineral precipitates with low solubility (Strawn *et al*. 2015). In soils derived from volcanic materials, P is usually a limiting nutrient in crops grown on such soils, and due to its high retention, large amounts of PO_4^{3-} fertilizers are applied in intensive agricultural systems (Nanzyo 2002).

The literature is extensive and diverse regarding the study of PO_4^{3-} retention related to variable charge mineral fraction in soils derived from volcanic materials (Strawn *et al*. 2015; Uchida *et al*. 2022; Theng *et al*. 1982; Hashimoto *et al*. 2012; Saunders 1965; Saunders 1959; Galvéz *et al*. 1999; Hiemstra *et al*. 2010a; Hiemstra and Zhao 2016; Koopmans *et al*. 2020; Liu *et al*. 2021; Li *et al*. 2022). Such mineral fractions of variable charge are the main colloids responsible for PO_4^{3-}

retention in volcanic ash-derived soils. However, these minerals have varying degrees of affinity for PO_4^{3-}. In this regard, there are studies suggesting that Al and allophane play a more important role than Fe (ferrihydrite) in P retention in Andisols (Uchida *et al*. 2022; Hashimoto *et al*. 2012).

The PO_4^{3-} retention capacity of Al and Fe minerals varies with respect to the degree of crystallinity, allophane, for example, has higher phosphate retention capacity than other more crystalline mineral forms (Takahashi and Dahlgren 2016; Nanzyo 2002). Differences in reactivity are related to several factors such as the chemical composition of the parent material, degree of weathering and leaching, pH, particle morphology, hydration state, and mineral crystallinity (Theng *et al*. 1982; Saunders 1959; Saunders 1965). In addition, PO_4^{3-} retention is related to the presence of organic matter in volcanic soils. The colloidal fraction in allophanic Andisols responsible for PO_4^{3-} retention is usually composed of allophane/imogolite and Al-humus complexes, whereas Al-humus complexes are the predominant component in PO_4^{3-} sorption in non-allophanic Andisols (Takahashi and Dahlgren 2016).

In general terms the phosphate retention capacity in volcanic soils is related to the reactivity of both mineral and organic particles. The reactivity depends on the degree of crystallization and size of the mineral particles where nanocrystalline or SRO fractions are more reactive, and crystalline fractions less reactive (e.g., allophane>imogolite>haloysite>gibbsite, ferrihydrite>goethite/hematite).

The degree of mineral crystallization is related to the degree of pedogenetic development of the soils. Although the literature on PO_4^{3-} retention in volcanic soils is extensive, the study of changes in mineral reactive surfaces and their association with PO_4^{3-} adsorption behavior along topographic sequences is a little explored topic. This is important because topography and climatic conditions, mainly humidity and temperature, are factors that play a very important role in the formation and development of soils (Jenny 1941).

Several pedogenetic studies along toposequences have found the presence of SRO minerals (including allophane and ferrihydrite) formed in the early stages of weathering of volcanic materials in humid areas with higher altitudes and lower temperatures. Furthermore, they evidenced that as weathering progresses and the altitude, humidity and temperature conditions of the environment change, such minerals transform to thermodynamically more stable and crystalline forms (For example, imogolite, haloysite, kaolinite, gibbsite, hematite, goethite, among others) (Tsai *et al*. 2010; Candra *et al*. 2019; Zehetner *et al*. 2003; Ranst *et al*. 2019; (Watanabe *et al*. 2023).

A positive correlation between organic carbon content and the retention of water and phosphate with increasing altitude has been reported (Candra *et al*. 2019; Tsai *et al*. 2010; Zehetner *et al*. 2003). This relationship is attributed to the presence of metastable materials such as allophane, ferrihydrite, and Al–humus complexes, which can adsorb and complex anions. At higher elevations, organic carbon accumulations are further promoted by the slow decomposition of organic matter under low temperatures (Shoji and Fujiwara 1984; Candra *et al*. 2019; Tsai *et al*. 2010; Zehetner *et al*. 2003). In these environments, organic carbon often accumulates in acidic conditions (pH in water <5), where organic acids serve as the main proton donors (Shoji and Fujiwara 1984). Under such conditions, Al–humus complexes predominate in volcanic soils, whereas the presence of allophane and imogolite is favored at higher pH values (>5) (Parfitt and Kimble 1989; Shoji and Fujiwara 1984; Tsai *et al*. 2010).

In Costa Rica previous studies have analyzed changes in the chemical and mineralogical properties of clay minerals in chrono- and topo-sequences with volcanic soils, mainly for mineralogical-pedogenetic and taxonomic purposes (Landaeta *et al*. 1978; Grieve *et al*. 1990; Nieuwenhuyse *et al*. 2000; Van Dooremolen *et al*. 1990; Martini and Mosquera 1972; Meijer and Buurman 2003; Alvarado *et al*. 2014; Kautz and Ryan 2003). The mineralogical-pedogenetic study, conducted by Nieuwenhuyse *et al*. (2000), identified mineralogical changes along a chronosequence of volcanic soils derived from andesitic lava in the Atlantic zone of Costa Rica. In this study, the age of the soil represents a predominant factor in the mineralogical evolution of the soils. Among the results, these authors found that in young soils (<2000 years) Al/Fe-humus complexes and nanocrystalline materials (allophane and ferrihydrite) are the predominant colloids, with minor amounts of gibbsite and kaolinitic minerals. Soils of intermediate age (<18 190 years) mineralogically were similar to the younger soils (presence of allophane and imogolite), with the distinction that they contain higher amounts of gibbsite and kaolinitic minerals in the Bw horizon mainly. And in the older soils (450 000 years), hydrated halloysite and goethite were obtained, while the predominant secondary mineral was gibbsite as well as significant amounts of kaolinitic minerals.

In addition, Nieuwenhuyse *et al*. (2000) explained that the chronosequence of volcanic soils showed a correlation of mineralogical evolution from less crystalline to more crystalline minerals as the age of the soils increases. Furthermore, such transformations are mediated by mineral desilification processes where allophane and imogolites are transformed to gibbsite, and metastable material forms are transformed into more stable forms such as ferrihydrite and Fe-humus complexes into goethite. Halloysite and kaolinitic minerals mainly occurred in drier

climates and, like gibbsite, their amount increased at greater depth. In the more superficial horizons, Al/Fe-humus complexes and nanocrystalline minerals (allophane, imogolite, ferrihydrite) were predominantly found. In areas with higher organic matter accumulation and low pH values, the presence of allophane was reduced due to the competition of humus and Si in solution for Al derived from the weathering of volcanic materials (Nieuwenhuyse *et al*. 2000).

Several investigations have been carried out in Costa Rica that include the study of phosphorus retention capacity in volcanic soils (Soto 1999; Alvarado *et al*. 2001; Henríquez 2005; Segura *et al*. 2005; Alvarado *et al*. 2009). In general, these soils have a high P retention capacity (>91%) associated with the presence of SRO Fe and Al minerals (formerly called "amorphous" such as allophane) and a high organic matter content. The P retention capacity can be obtained empirically by correlating the amount of extractable Al in ammonium oxalate (Alvarado and Buol 1985).

The reactive surface area given by SRO minerals is predominant in determining the P adsorption behavior in Andisols. It has been found that the total P content in Andisols of the Central Volcanic Cordillera of Costa Rica decreases with increasing altitude (Alvarado *et al*. 2001), which is related to the degree of crystallization of secondary minerals from less crystalline metastable minerals, such as allophane, imogolite and ferrihydrite, to more stable and crystalline minerals like haloysite, kaolinite, gibbsite, goethite, and hematite. These stable, crystalline minerals are less reactive with phosphate, resulting in an inverse pattern to available P where PO_4^{3-} retention increases with altitude (Tsai *et al*. 2010; Candra *et al*. 2019; Zehetner *et al*. 2003). Similarly, organic matter content, mainly Al/Fe-humus complexes, is better preserved at lower temperatures. It has been found that P retention by Al-Fe-humus complexes is usually stronger in non-allophanic Andisols than that resulting in allophanic Andisols with the presence of allophone and imogolite (Takahashi and Dahlgren 2016).

Despite the abundant information found in the literature on mineral composition and PO_4^{3-} retention in volcanic soils to date, no previous study has yet analyzed how changes in the total content and composition of SRO minerals, and RSA along an altitudinal gradient of soils derived from volcanic materials affect PO_4^{3-} adsorption behavior and P availability. The relationship between surface reactivity and PO_4^{3-} adsorption behavior in topographic sequences of soils derived from volcanic materials has also not been systematically analyzed. Therefore, the objective of this two Chapter project was to evaluate the changes in the content, composition, and surface reactivity of variable charge SRO minerals in two toposequences of volcanic soils with contrasting temperature and soil moisture regimes located on the southern flank of the Irazú

Volcano. It is expected that this information can contribute to a better understanding of the main chemical processes that influence P bioavailability in this type of soil. Therefore, this research will have broader implications beyond the region studied, as it will provide new insights into the relationship between changes in mineral composition, surface reactivity, and P availability in soils that have been formed or influenced by volcanic activity.

1.4. GENERAL OBJECTIVE

To determine the content and reactive surface area of variable charge minerals, including nanocrystalline aluminosilicates and Fe and Al (hydr)oxides, in the profiles of two topographic sequences of soils derived from volcanic materials, and their implications on phosphorus adsorption behavior.

1.5. SPECIFIC OBJECTIVES

1. To quantify the total content and relative composition (nanocrystalline vs. crystalline fractions) of variable charge minerals in soil profiles of two topographic sequences according to their altitudinal variation.

2. To estimate the changes in the reactive surface area of soils associated with the presence of variable charge minerals as a function of altitudinal changes of soil profile sites of two topographic sequences.

3. To analyze the adsorption behavior of phosphorus (in its chemical form of phosphate ion) in relation to the content and reactivity of variable charge minerals present in soils with contrasting chemical characteristics.

2. CHAPTER 1. ALTITUDINAL AND MOISTURE DRIVEN VARIATION IN SHORT-RANGE ORDER MINERAL CONTENT IN TWO SOIL TOPOSEQUENCES ON IRAZÚ VOLCANO, COSTA RICA

Cintya Solano Solano[1,*], , Manuel Camacho Umaña[2], Agustín F. Solano-Arguedas[3]. Juan Carlos Méndez Fernandez[2].

1 Facultad de Ciencias Agroalimentarias, Maestría en Ciencias Agrícolas and Recursos Naturales con énfasis en Suelos, Universidad de Costa Rica, San Pedro, Costa Rica.

2 Centro de Investigaciones Agronómicas (CIA) and Escuela de Agronomía, Universidad de Costa Rica, San Pedro, Costa Rica.

3 Unidad de Recursos Forestales (Reforesta), Instituto de Investigaciones en Ingeniería (INII), and Escuela de Química, Universidad de Costa Rica, San Pedro, Costa Rica.

ABSTRACT

Volcanic soil serves as a valuable resource for agriculture around the world. Their productivity is largely determined by the presence of minerals with variable charge, which play a key role in the high retention of oxy-anions like phosphate and the storage of organic carbon. In Costa Rica, studies on the variation in content and composition of variable charge minerals along an altitude gradient are limited. This study aimed to examine the variation in the content and composition of Short-Range-Order (SRO) minerals along altitudinal gradients and depth in two soil toposequences with contrasting conditions regarding soil moisture regimes. The area of study was located on the southern flank of the Irazú Volcano, where the two soil toposequences were defined along an altitudinal range from 1734 to 2853 m asl (East-South toposequence) and from 1724 to 3178 (West-South toposequence). Soil chemical extractions using ammonium oxalate (AO), dithionite-citrate (DC) and sodium pyrophosphate (Py) solutions were used to define operationally the content of Fe, Al, and Si present in soils as SRO and to analyze changes in weathering intensity along the altitudinal gradients. In the Eastern toposequence, characterized by a consistent udic regime, SRO content decreased with altitude, likely driven by enhanced weathering and stable humid conditions. By contrast, no clear altitudinal trend was observed in the Western toposequence, where a transition from udic to ustic regimes and lower precipitation likely promoted SRO transformation into more crystalline forms. Additionally, it was found that SRO-Fe content was less affected by variations in soil moisture regimes compared to SRO aluminosilicates. Additionally, a larger total carbon accumulation at lower elevations, particularly

in udic soils, was associated with reactive Al forms (Al_{ox}), indicating a key role for Al-SRO interactions in stabilizing organic matter under intense weathering. This study highlights the key role of soil moisture regime in modulating the content and persistence of short-range-order (SRO) aluminosilicates across volcanic soil toposequences. Moreover, our work contributes to improve the interpretations of nutrient dynamics, carbon cycling and soil development in volcanic landscapes and offers a scientific basis for guiding land use and sustainable management strategies in volcanic soil dominated regions.

Keywords: nanocrystalline minerals, soil moisture, toposequences, volcanic soils.

2.1. INTRODUCTION

Andisols are soils formed from volcanic parental materials, mainly pyroclastic deposits such as tephra (ash, lapilli, blocks and bombs), volcaniclastic sediments and lavas (Nanzyo & Kanno 2018, Neall 2000, Egli *et al*. 2008). Although these soils cover only 1% of the Earth's surface, they play a crucial agricultural and economic role, supporting 10% of the world's population (Neall 2000). In Costa Rica, Andisols cover ~14% of the surface territory (Alvarado *et al.* 2001), supporting agricultural activities of significant economic importance for the country, such as horticultural crops, coffee production, ornamental plant cultivation, and dairy farming (Bertsch *et al.* 2000).

From a mineralogical perspective, Andisols originate from the relatively rapid weathering of primary minerals like volcanic glass, quartz, pyroxenes, plagioclases, olivine, opaque minerals, hornblende, and biotite, which are present in tephra and lava (Nanzyo 2002), whereas a fraction of these minerals may remain unweathered within the coarser soil fractions, such as the sand fraction. As a result of the weathering processes, Al^{3+}, Fe^{3+}, Si^{4+} ions are released into solution to a large extent, creating an oversaturation condition of these ions with respect to secondary mineral phases. The weathering of mafic and intermediate volcanic materials favors the formation of clay minerals with poor degree of crystallinity, referred as short-range order (SRO) or nanocrystalline minerals (Schwertmann 1958, Parfitt & Wilson 1985, Churchman & Lowe 2012). Examples of these SRO minerals include aluminosilicates such as allophane, proto-imogolite and imogolite, as well as iron (hydr)oxides like ferrihydrite (Neall 2000, Nanzyo & Kanno 2018).

Short-range order (SRO) minerals are highly reactive due to their large surface area of amphoteric nature, as the surface charge varies with the protonation and deprotonation of exposed functional groups, thus resulting in minerals of variable charge (Wada *et al.* 1991, Qafoku *et al.* 2004). Surface charge is influenced by soil solution conditions, particularly pH and ionic strength. Hence, depending on the surrounding chemical environment, the interaction of SRO minerals with both

positive and negative charges enhance their adsorption capacity of ions and organic matter. The point of zero charge (PZC) of SRO minerals typically ranges from pH 7 to 9 (Qafoku *et al.* 2004), so under common soil pH levels, they tend to carry a net positive charge, allowing them to retain anions (Neall 2000).

Variations in environmental and climatic conditions (for instance, temperature and precipitation) modulate the pedogenetic conditions for Andisols development. These variations can affect both the chemical composition and stability of the SRO, promoting an improvement in the mineral crystallinity (Tsai *et al.* 2010, Candra *et al.* 2019, Schwertmann 1958, Ugolini & Dahlgren 2002) like in the alteration of ferrihydrite to hematite, or allophane/imogolite to gibbsite (Jongmans *et al.* 1995, Wada & Harward 1974). For this reason, in altitudinal gradients with variation in temperature and precipitation conditions, the mineralogical composition and the crystallinity of variable charge minerals are expected to differ. Consequently, poorly crystalline SRO minerals, which exhibit higher ion adsorption capacity due to their greater surface reactivity, may experience a decrease in surface reactivity when they transform into more crystalline phases (Ichinose *et al.* 2025).

The relationship between the changes in the mineralogical composition along soil toposequences and the variations in environmental factors such temperature, precipitation and moisture gradients, have been analyzed worldwide, like Northern Taiwan (Tsai *et al.* 2010), Galápagos islands (Candra *et al.* 2019), Andean Ecuador (Zehetner *et al.* 2003), and Cameroon (Watanabe *et al.* 2023). In general, these studies found that zones at higher altitude, with lower temperatures and higher precipitation/leaching, favor the formation of SRO minerals, while lower areas with drier conditions, promote the weathering of primary minerals and the formation of more crystalline phases.

In Costa Rica, Meijer and Buurman (2003) analyzed a perhumid soil catena on the Turrialba volcano, using soil extraction methods with ammonium oxalate (AO) to measure Al, Fe and Si present in SRO minerals, and X-ray Fluorecense minor elements determination. The study found that allophane was conducted by the weathering of fine-sand-sized pre-weathered volcanic ash under humid climatic conditions (high precipitation rate). Such conditions were uniquely present at altitudes between 600 and 1200 masl, with an annual average temperature of 20ºC. Whereas at lower altitudes, 85240 masl, allophane absence was reported due to higher environmental temperatures (~26ºC) and lower precipitation rate that inhibited its formation, resulting in a predominance of more crystalline Al phases like halloysite (Meijer & Burman 2003). However, this

study was focused on using trace elements as ‘‘tracers’’ to identify the weathering paths resulting in the formation of different amorphous or crystalline products in the soils.

Research on soil toposequences has been mostly focused on analyzing changes in pedogenetic processes and soil properties along a single altitudinal gradient (Tsai *et al.* 2010, Candra *et al.* 2019, Zehetner *et al.* 2003, Watanabe *et al.* 2023), without exploring variations in local environmental factors (For instance, changes in soil moisture regime) across multiple toposequences within the same study area. The southern flank of the Irazú volcano offers a unique alternative to study toposequences with contrasting soil moisture regimes. While the eastern area of the flank is dominated by a single moisture regime (Udic), the western area exhibits a transition from udic to ustic regimes along the altitudinal gradient.

Therefore, the aim of this research was to analyze and compare the changes in the mineralogical composition, particularly SRO minerals with variable charge surfaces, as a function of the altitudinal variation and the contrasting soil moisture regimes in two toposequences of the southern flank of Irazú volcano. We hypothesize that the content of SRO minerals decreases with altitude in both toposequences, due to more intense weathering conditions promoted by higher mean annual temperatures at lower altitude in the southern flank. Also, we hypothesize that the moisture regime of each toposequence modulates the altitudinal effect on the soil mineralogy.

To test these hypotheses, soil chemical extractions using ammonium oxalate (AO), sodium pyrophosphate (Py), and dithionite-citrate (DC) are proposed to define the content of Fe, Al, and Si present in soils as SRO and to analyze changes in weathering intensity along the altitudinal gradients. The information provided by this study will be crucial to improve the understanding of pedogenetic processes occurring on volcanic soils related to environmental changes and their implications for biogeochemical cycling of elements and nutrient availability, carbon storage capacity, and land use management.

2.2. MATERIAL AND METHODS

2.2.1. Soil sampling

Sampling locations were selected based on existing information on the physicochemical properties of a series of soil profiles previously characterized along two altitudinal transects allocated in the Irazú Volcano, Cartago, Costa Rica. The study area is characterized by having annual average precipitation ranges from 3000 – 4000 mm at the highest altitudes and at the eastern part of the flank, to precipitations bellow 1500 mm at the lowest parts (**Figure S1.1**). The mean annual temperature ranges between 8 ºC (at highest altitude) to 20 ºC at lowest altitudes

(**Figure S1.2**). The two soil toposequences were defined at the southern flank of Irazú volcano, and hereinafter they will be referred to as West-South (WS) and East-South (ES) toposequence (Figure.1). General characteristics of the sampling sites from both sequences are shown in **Table 1.1**. The Western sequence was previously characterized as part of a joint project of the United States Department of Agriculture (USDA), the University of Costa Rica (UCR) and the Costa Rican Association of Soil Sciences (ACCS), while the information on the eastern sequence was obtained from the soil profile database compiled by the Natural Resources Laboratory of the CIA-UCR. One of the main characteristics distinguishing the two soil toposequences are soil moisture regimes and soil orders. The WS toposequence exhibits a mix of moisture regimes: the highest elevation profiles have a Udic regime, while the lower profiles show an Ustic regime. In contrast, the ES toposequence has a uniform Udic moisture regime throughout the altitudinal profile. Additionally, the western sequence contains soils of various orders including Entisol, Andisols, and Alfisol whereas all soils in the eastern sequence are classified as Andisols.

Soil samples were collected between February and July 2022. At each sampling site, a soil pit was dug, and a sample was collected from each soil horizon identified in the field. The horizon distinction was primarily based on physical characteristics such as color, texture, and density. In total, 34 soil samples were collected in eight soil profiles (four profiles in each sequence) within an altitude range from 1724 to 3178 m asl (**Figure 1.1**). The sampling depths varied according to the specific conditions of each site and ranged from 0.70 m to 2.40 m (see **Table 1.1**).

Samples were air-dried for approximately seven days at 25-30 °C and then sieved using a No. 10 sieve with a 2 mm mesh size. Moisture content of the air-dried soil samples was determined by oven-drying approximately 50 g of each sample at 105 °C for 24 hours. The ratio of air-dried to oven-dried mass (AD/OD) was calculated and used to correct the results of chemical analyses, allowing them to be expressed on an oven-dried mass basis.

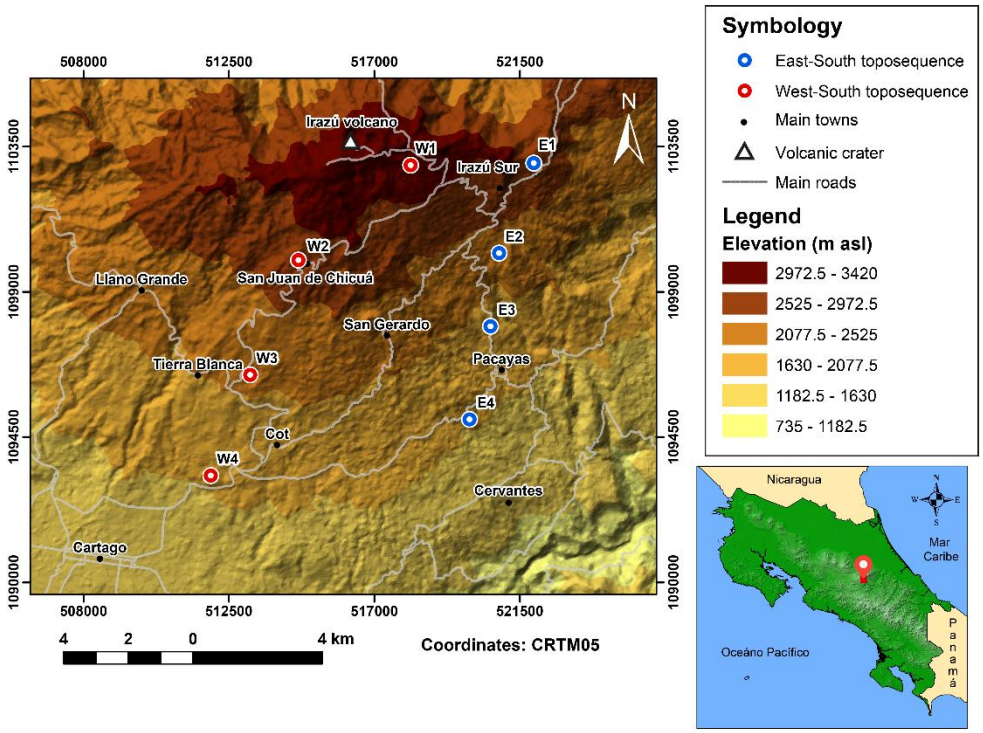

Figure 1. 1 Location of the soil sequences in the study area along the altitudinal profile in the southern flank of Irazú volcano, Costa Rica. East-South toposequence (blue dots) and West-South toposequences (red dots).

Table 1. 1 General characteristics of the sample sites including the sample depth, elevation, annual average precipitation and temperature, soil order and moisture regime from two soil sequences located at the southern flank of Irazú volcano.

Profile	Depth (cm)	Altitude (masl)	Mean anual temperature (ºC)	Menan anual precipitation (mm)	Soil order [a]	Moisture regime
West-South toposequence						
W1	0-80	3178	8 - 10	2000 – 3000	Entisol	Udic
W2	0-240	2777	10 – 12	1500 – 2000	Andisol	Udic
W3	0-120	2150	14 – 16	< - 1500	Andisol	Ustic
W4	0-70	1724	16 – 18	< - 1500	Alfisol	Ustic
East-South toposequence						
E1	0-96	2853	12 – 14	2000 – 3000	Andisol	Udic
E2	0-110	2355	14 – 16	2000 – 3000	Andisol	Udic
E3	0-120	1983	16 – 18	2000 – 3000	Andisol	Udic
E4	0-120	1734	16 – 18	2000 – 3000	Andisol	Udic

[a] According to the Soil Taxonomy (Soil Survey Staff 2022)

In addition to the samples collected from the two toposequences described above, existing data from ammonium oxalate extractions of soil samples (n = 66) collected in the area between the two toposequences, were used in this study to compliment the analysis of moisture regime effects on SRO mineral content (**Figure S1.3**).

2.2.2. Soil physical and chemical characterization

2.2.2.1. Particle size distribution analysis (PSDA)

The analysis of the particle size distribution was performed using the Hydrometer method (Soil Survey Staff 2014a). First, 40 g (or 60 for coarser textures) of soil was placed into 250 ml plastic beaker with 100 ml of a solution composed of sodium hexametaphosphate (~0.059 M), and sodium carbonate (~0.075 M), 100 ml of distilled water, and further dispersed through a horizontal shaker (120 oscillation minute^{-1}) overnight (12 h). The sample was quantitative transferred to a 1 L graduated sedimentation cylinder, and thoroughly mixed with a plunger. Measurements of the density of soil particles suspended in the solution (g L^{-1}) were taken using the Bouyoucos scale densimeter (ASTM-152H) at 0.5, 1, 5, 10, 30, 60, 90, 120, 360, and 1440 minutes. Data were processed using an Excel data sheet developed by the Stillwater, OK Soil Survey Office and Modified by NSSC and Ricky Lambert, Nacogdoches, TX. Soil texture was classified according to the USDA texture triangle (Soil Survey Staff 1999).

2.2.2.2. pH measurement

The pH of the soil samples was measured in 1:2.5 (v/v) soil/solution extractions using ultra-pure water (pH-H_2O) and in 1 M KCl (pH-KCl). In both cases, the soil suspension was shaken for 10 minutes, and then left to settle for 2 minutes before pH was measured with a Metler-Toledo pH-meter with glass membrane electrode. Additionally, the pH of the soil samples was measured in a 1:10 (m/v) soil/solution extraction using 0.01 M $CaCl_2$ (pH-$CaCl_2$). Samples were shaken for 2 hours before the pH was determined. Lastly, the pH of the samples was analyzed in a solution of 0.01 M NaF (pH-NaF) at a 1:50 (m/v) soil/solution extraction. The samples were shaken for 2 minutes, and the pH was measured.

2.2.2.3. Total carbon content

The soil samples (previously dried at 50°C and sieved through a 2 mm sieve) were analyzed for total carbon (C) content by dry combustion, using an automated C/N analyzer (Elementar, Vario MACRO cube).

2.2.3. Soil chemical extractions

The content of the variable charge minerals, particularly the SRO minerals, was assessed by performing different soil extraction procedures. These methods rely on the use of extractants to

break chemical bonds and solubilize target substances, such as Fe and Al (hydr)oxides, and metal-organic associations of Al and Fe (Rennert 2019). These extraction methodologies have been widely used in soil analysis as standard procedures for soil classification purposes (Rennert 2019), as well as for characterizing the reactive fraction of SRO minerals in various soil types (Mendez *et al.* 2022, Gustafsson *et al.* 1999). In this research, three different chemical extractions were used: acid ammonium oxalate (AO), dithionite citrate (DC) and sodium pyrophosphate (Py), in order to obtain an operationally defined estimation of the content of Fe and Al present in target substances SRO aluminosilicates (i.e. allophanic materials) and Fe (hydr)oxides (i.e. ferrihydrite), as well as Al associations with soil organic matter (SOM).

2.2.3.1. Acid ammonium oxalate (AO) extractions

A solution of 0.2 M acid ammonium oxalate (AO) (pH 3) was used to extract Fe, Al, and Si primarily associated with SRO minerals (Schwertmann 1964), hereafter referred to as Fe_{ox}, Al_{ox}, and Si_{ox}, respectively. This procedure was performed for all the samples including the two toposequences and the additional soils from the data set. The extractions followed the procedure described by Soil Survey Staff (2014b), with modifications proposed by Van Reeuwijk (1993), using a 1:100 soil-to-solution ratio (SSR) for soils with high concentrations of extractable Fe_{ox} and Al_{ox}. Additionally, AO may dissolve Al species complexed with SOM (Al -organic complexes), which could significantly contribute to the total Al_{ox} content, particularly in Andisols with high SOM content. The extractions of Fe, Al and Si in AO were analyzed by Inductively Coupled Plasma Optical Emission Spectrometry (ICP-OES) using a Perkin Elmer spectrometer.

2.2.3.2. Sodium pyrophosphate

A solution of 0.1 M sodium pyrophosphate (pH=10) was used to extract forms of Al associated with SOM, hereafter referred as Al_{py}. The extractions followed the procedure described by Van Reeuwijk (1993) using a 1:100 SSR. The elemental analysis of Al_{py} was conducted by ICP-OES.

2.2.3.3. Dithionite-citrate (DC) extractions

A solution of (0.57 M sodium citrate) dithionite citrate (DC) was used to extract Fe present in pedogenic Fe-(hydr)oxide minerals, including both the SRO and crystalline Fe-(hydr)oxide phases (Fe_{dc}). The extractions were performed following the procedure described by Mera and Jackson (1960), using approximately 1:100 SSR. The elemental analysis of Fe_{dc} was carried out by ICP-OES.

2.2.3. Data analysis

The data obtained from the different soil extractions were analyzed using dispersion graphs of key variables (Al_{ox}, Si_{ox}, Fe_{ox}, and the Fe_{ox}/Fe_{dc} ratio) as a function of altitude and depth, in order to identify trends within each toposequence. Additional dispersion graphs were created to visualize the relationships between Al_{ox}, Fe_{ox}, and carbon content with altitude, while boxplots were used to assess differences in these variables based on the soil moisture regime. Statistical descriptors such as quantiles, mean values, standard deviations, and maximum values were employed to characterize the data, and t-tests (*p value* < *0.001*, 95% IC: Confidence Interval) were conducted to determine significant differences in the content of Al_{ox}, Fe_{ox} and C related to soil moisture regimes. Furthermore, Pearson correlation analyses were used to identify relationships among Al_{ox}, Fe_{ox}, C content, and altitude within the context of each moisture regime. Additionally, the data obtained from the different extractions were used to calculate various molar ratios for analyzing differences in pedogenic conditions between along and across the toposequences. For example, the Al_{py}/Al_{ox} ratio was calculated to determine the relative contribution of Al present as Al-organic complexes to the total amount of Al_{ox}. Moreover, the Fe_{ox}/Fe_{dc} ratio was calculated to determine the fraction of Fe present as SRO in relation to the total content of pedogenic Fe oxides. This ratio provides an estimation of the degree of crystallinity of the Fe (hydr)oxides and it can be related to comparing the degree of weathering among soils (Schwertmann 1958). The $((Al_{ox}-Al_{py})/Si_{ox})$ ratio was calculated to estimate the Al/Si molar ratio of SRO aluminosilicate minerals (Parfitt 1990, Dahlgren 1994, Vacca *et al.* 2003).

2.3. RESULTS

2.3.1. General soil characteristics

The particle size distribution evidenced a Sandy Loam (SaLo) or Loamy Sand (LoSa) texture for most of the soils (**Figures S1.4 and S1.5**). As an exception, soil samples from W4 profile (lowest altitude at the WS toposequence) contained a higher content of clay (32-43% vs 2-17% for the rest of profiles), and their texture was classified as a clay-loam or clayed (**Tables S1.1 and S1.2**).

In general, the soil samples from both toposequences had slightly acid to acidic pH values, with similar values of pH-H_2O for soils from the WS toposequence (5.96 ± 0.47) , and the ES toposequence (5.78 ± 0.42) (Tables S1-S2). The results of the pH-KCl in the WS toposequence are on average generally lower (4.90 ± 0.35) than the values of the ES toposequence (5.27 ± 0.37 on average), whereas the pH-$CaCl_2$ values are relatively similar for the WS toposequence (on average 5.10 ± 0.49), and the ES toposequence (5.22 ± 0.37) (**Tables S1.1 and S1.2**).

The comparison of pH measurement methods showed an average ΔpH (pH-KCl – pH-H_2O) of -1.06 ± 0.21 in soils from the WS toposequence and -0.51 ± 0.23 in those from the ES toposequence (**Tables S1.1 and S1.2**). This difference was statistically significant (t = 6.94, df = 31.97, p < 0.001). Topsoils from the WS toposequence exhibited an increase in the ΔpH (pH-KCl – pH-H_2O) as altitude decreases, whereas in ES toposequences this trend was not evident. Additionally, the average ΔpH (pH-$CaCl_2$ – pH-H_2O) was -0.85 ± 0.15 in the WS toposequence and -0.56 ± 0.16 in the ES toposequence (**Tables S1.1 and S1.2**), this difference was statistically significant (t = 5.32, df = 31.99, p < 0.001). Moreover, the pH-NaF results varied between 9.38 – 10.88 (10.14 ± 0.57 on average) for soils from the WS toposequence, and 10.05 – 11.15 (10.74 ± 0.26 on average) for soils from the ES toposequence (**Tables S1.1 and S1.2**).

The soils of the WS toposequence exhibited (Al_{ox}-Al_{py})/Si_{ox} ratios ranging from 0.58 to 1.80 (**Table S1.3**), while the soils of the ES toposequence showed (Al_{ox}-Al_{py})/Si_{ox} molar ratios between 1.84 and 2.62, with most of the soil samples presenting values higher than 2 (**Table S1.4**). When comparing both sequences, the WS toposequence generally showed lower (Al_{ox}-Al_{py})/Si_{ox} ratios (1.36 ± 0.29) than the ES toposequence (2.34 ± 0.23), like the SRO aluminosilicates in soil samples from the WS toposequence that were richer in Si. The ratios Al_{py}/Al_{ox} of soils from both toposequences were generally below 0.5, except for the soils W4 (1.64 - 3.49), and the first two horizons of the soil W1 with 0.84 and 1.03, respectively. The rest of the soils from the WS toposequence have Al_{py}/Al_{ox} ratios between 0.08 – 0.41, and soils of the ES toposequence have ratios between 0.05 – 0.35 (**Tables S1.3 and S1.4**).

2.3.2. Changes in SRO mineral content as a function of altitude and depth

When establishing as a reference the sampling depth of ~50 cm, the soils from the ES toposequence contained higher Al_{ox} and Si_{ox} content compared to those from the WS toposequence, regardless of the altitude (**Figure 1.2 and 1.3**). In the ES toposequence, there was a clear inverse trend between the Al_{ox} and Si_{ox} and the altitude (**Figure 1,3**), whereas this pattern was not observed in the soils from the WS toposequence (**Figure 1.2**). Additionally, in the soils from the ES toposequence, Al_{ox} and Si_{ox} content increased with sampling depth, while this pattern was not observed in the soils from the WS toposequence.

In both toposequences, the topsoil samples showed a trend of increasing Fe_{ox} content with decreasing altitude (**Figures 1.2 C and 1.3 C**). Fe_{ox} content along with the sampling depth differed between soil profiles from the two toposequences. From the WS toposequence, soils W1 and W2 (located at the highest altitudes and characterized by Udic moisture regime) toposequence showed an increase in Fe_{ox} content with depth, while W3 and W4 (both located at the lowest

altitude and characterized by Ustic moisture regime) exhibited the opposite trend. In contrast, soils from the ES toposequence, the Fe_{ox} content in the E1 and E3 soil profiles remained relatively constant, whereas in the E2 and E4 profiles, it increased after approximately 40 cm depth.

The Fe_{ox}/Fe_{dc} ratio showed a relationship with altitude in the soil samples from the WS toposequence: the higher the altitude of the soil profile, the greater the value of this ratio (**Figure 1.2 D**). This trend was less clear in the soil samples from the ES toposequence (**Figure 1.3 D**),where only the E1 profile (highest altitude) presented Fe_{ox}/Fe_{dc} ratios that were higher than for the other soil profiles in this toposequence. In relation to depth, the Fe_{ox}/Fe_{dc} ratios in the W4 and W3 profiles (at lower altitudes and under ustic regime) of the WS toposequence decreased with sampling depth, whereas the W2 and W1 profiles exhibited the opposite trend (**Figure 1.2 D**). In the ES toposequence, the Fe_{ox}/Fe_{dc} ratios in profiles E2, E3, and E4 remained relatively consistent across sampling depths, while in the E1 profile this ratio decreased with depth, particularly at sampling depths > 40 cm (**Figure 1.3 D**).

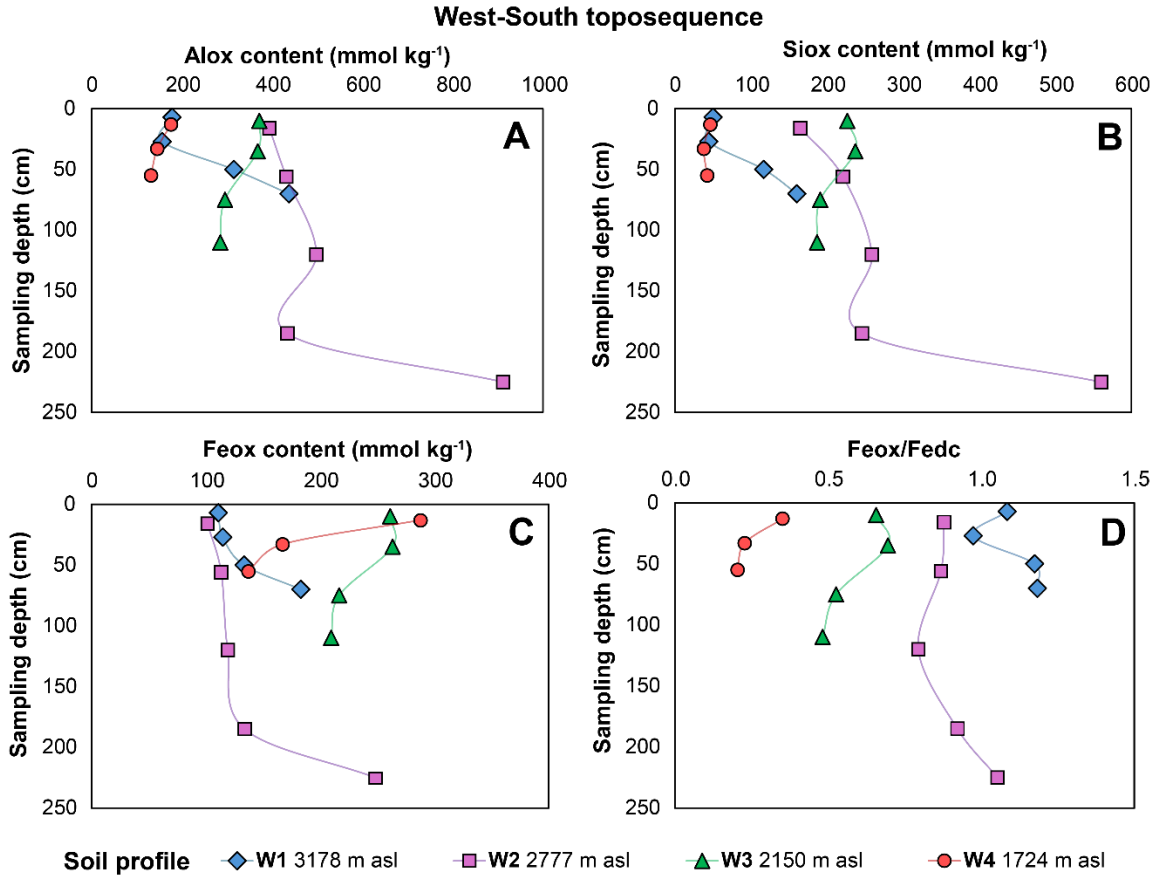

Figure 1. 2. Content of Alox (A), Siox (B), and Feox (C), all extracted with a 0.2 M ammonium oxalate solution, and Feox/Fedc ratio that indicates the fraction of Feox in relation to the total content of pedogenic Fe (hydr)oxides (D), plotted against sampling depth.

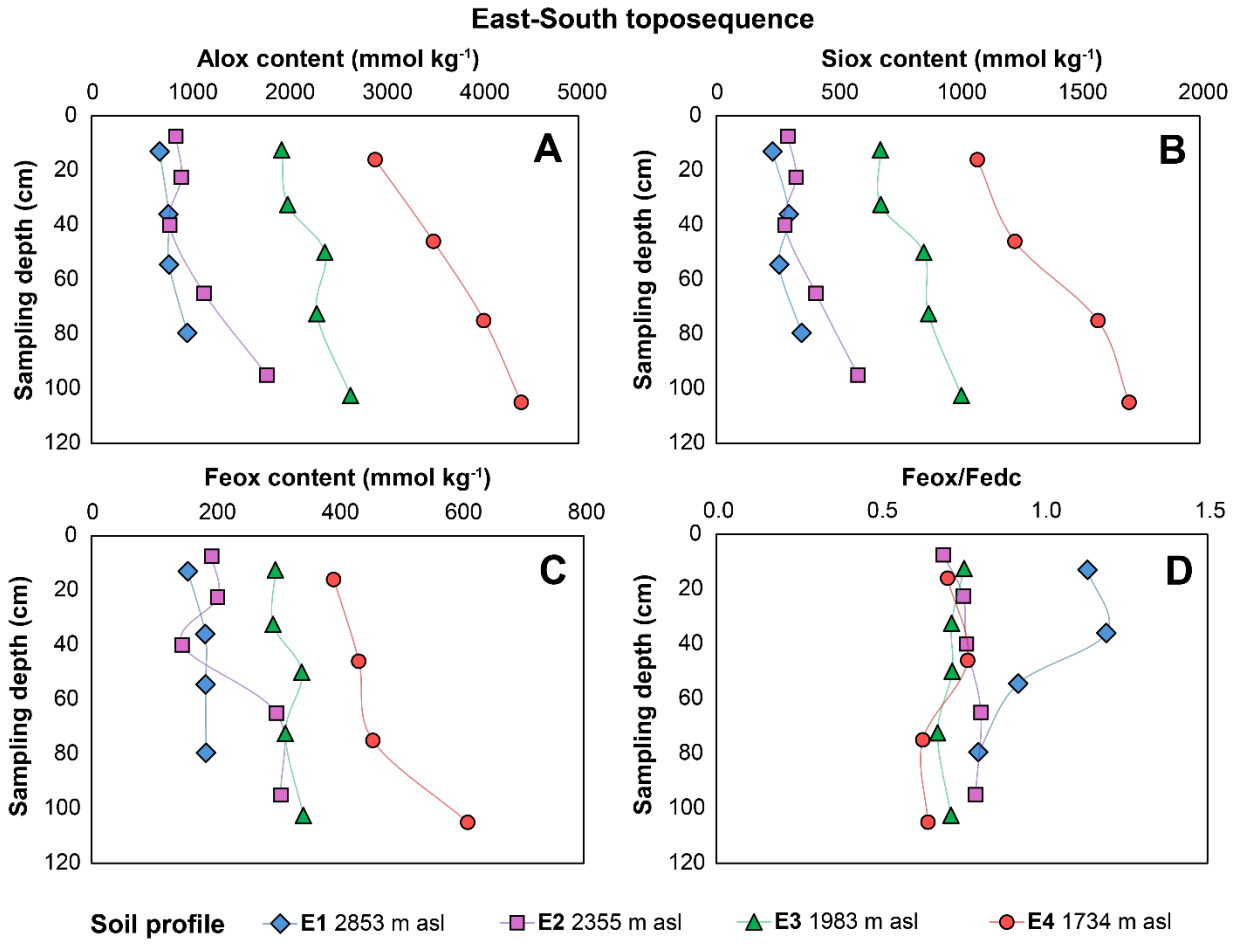

Figure 1. 3. Content of Alox (A), Siox (B), and Feox (C), extracted with a 0.2 M ammonium oxalate solution, along with the Feox/Fedc ratio (D) that indicates the fraction of Feox in relation to the total content of pedogenic Fe (hydr)oxides, plotted against sampling.

In general, the Al_{ox} content was higher than Fe_{ox} content in the soils, as reflected in the Al_{ox}/Fe_{ox} ratios (**Figure 1.4**). In general the ratios Al_{ox}/Fe_{ox} are lower in the WS toposequence (2.2 ± 1.2) compared with the ES toposequence (6.1 ± 1.5), with soils at the lower altitude (E3 and E4) having higher proportions of Al_{ox} compared to Fe_{ox} content.

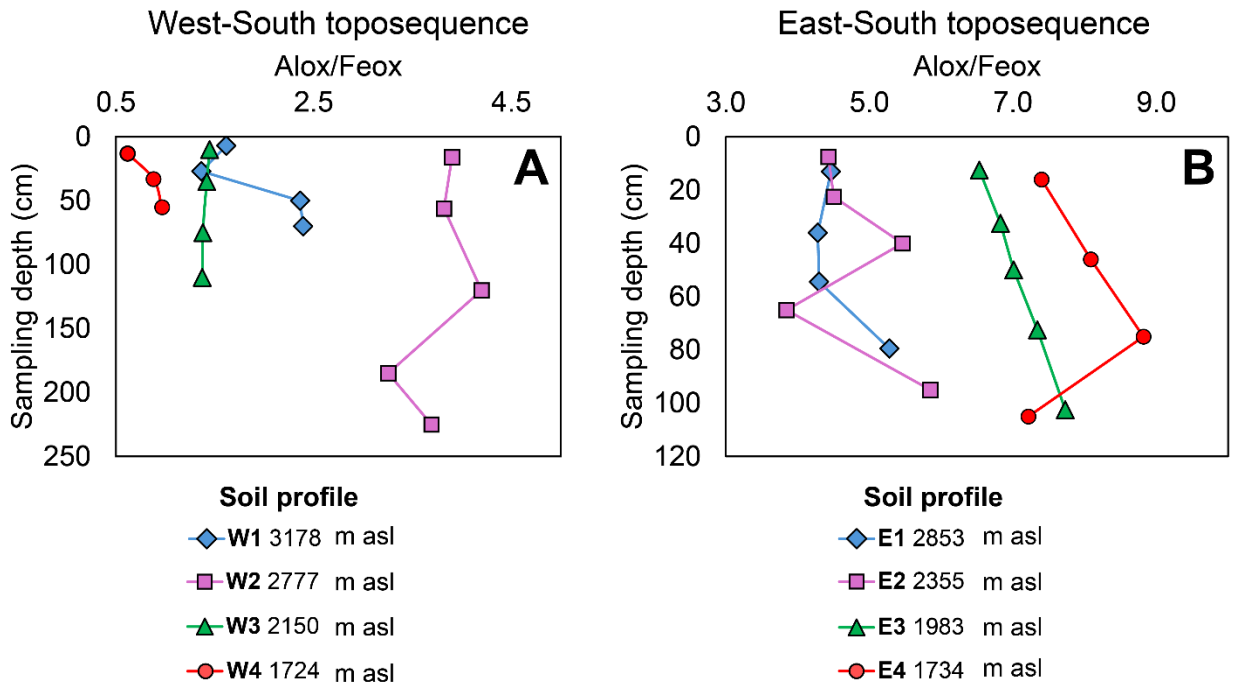

Figure 1. 4. Content of Alox/Feox ratio and its variation by sampling depth in soil profiles from the Western toposequence (A) and the Eastern toposequence (B) on the southern flank of the Irazú Volcano, Costa Rica.

2.3.3. Changes in SRO content related to moisture regime

The potential role of moisture regime on the content of SRO minerals was assessed also considering a complementary data set (n = 66) with information about Al_{ox}, Fe_{ox} and total C content from soils located in the study area at the southern flank of Irazú volcano. A summary of descriptive statistical parameters for these variables is shown in **Table 1.3**.

Soils under two distinct moisture regimes: Udic and Ustic, evidenced differences in Al_{ox} and C content (**Figure** 1.**5**). Soils samples collected from Udic moisture regime had a significantly higher Al_{ox} content (1027.38 ± 722.65) mmol kg^{-1} compared to soils under Ustic moisture regime (426.06 ± 258.04) mmol kg^{-1} (t = 5.47, df = 68.84, $p < 0.001$). In contrast, Fe_{ox} content showed no significant variation between both moisture regimes, with Udic soils averaging 236.25 ± 104.99 mmol kg^{-1} and Ustic soils 245.74 ± 71.63 mmol kg^{-1}, indicating that soil moisture did not influence Fe_{ox} accumulation in these volcanic soils (t = -0.43, df = 32.65, $p = 0.670$). Soils under Udic moisture regime had a significantly higher total C content (3.78 ± 2.06) % compared to soils under Ustic moisture regime (2.36 ± 1.54) %, suggesting that soil moisture also influences carbon accumulation (t = 3.09, df = 29.66, $p < 0.05$).

Table 1. 2. Descriptive statistical parameters of the Alox and Feox content extracted with a 0.2 M ammonium oxalate solution and the total carbon content (C) in soil samples derived from volcanic materials in the south flank of the Irazú Volcano, classified according to the dominant moisture regime: udic and ustic. The data are for samples taken from both the topsoil (from 0 to ~20 cm) and subsoil horizon (from ~ 20 to 40 cm) in total 82 samples from 41 different sampling locations. The analysis includes the samples from the main dataset of soil profiles and the additional data set specified in the section of methodology.

Variables assessed	N° samples	Min.	1st. Quartile	Median	3rd. Quartile	Mean	Max.	SD
Udic regime								
Al_{ox} (mmol/kg)	66	23.91	503.02	847.93	1390.85	1027.38	3378.21	722.65
Fe_{ox} (mmol/kg)	66	50.39	164.30	214.39	302.25	236.25	483.48	104.99
C (%)	66	0.32	2.59	3.55	4.38	3.78	12.07	2.06
Ustic regime								
Al_{ox} (mmol/kg)	16	145.30	331.70	359.90	412.10	426.06	1160.5	258.04
Fe_{ox} (mmol/kg)	16	107.40	209.50	257.90	285.10	245.74	366.00	71.63
C (%)	16	0.46	1.59	2.14	2.57	2.36	7.08	1.54

SD: standard deviation.

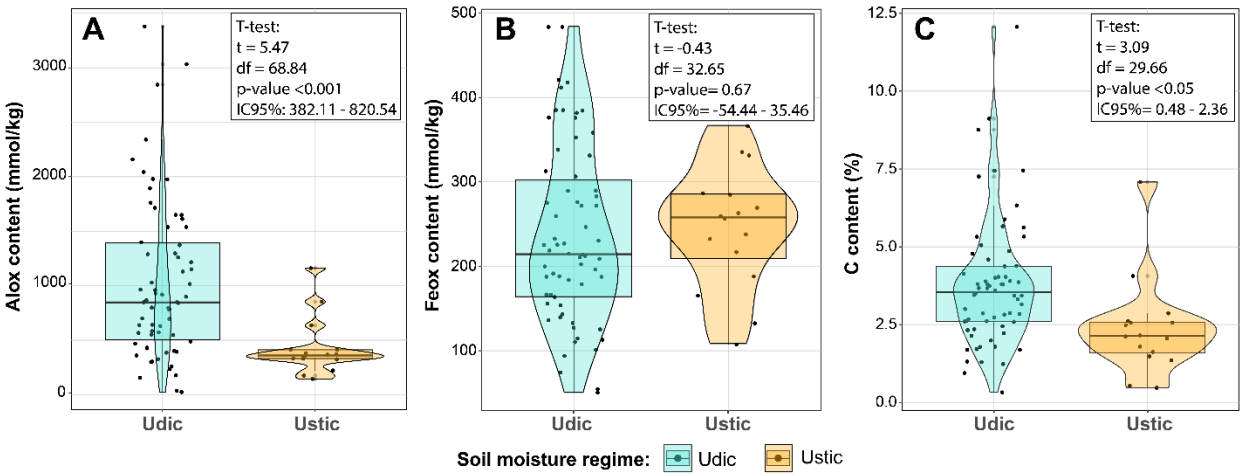

Figure 1. 5. Content of Alox (A), Feox (B), and total C content (C) per moisture regime, in both the topsoils and subsoils including data from the toposequences defined in this study and from a complementary dataset for soil samples located at the southern flank of the Irazú volcano, Costa Rica. The boxplot is represented as the square shape, the violin plot as the curve shape, and the data as small dot points whose concentration value is given in the Y axis. In each panel, the

results of a t-test are given, which were applied to find significant differences between the ustic and udic moisture regimes.

Moisture regime (Udic vs Ustic) was a key factor to influence the content of Al_{ox} and consequently, the content of total C. In addition, further analysis with topsoil samples showed that the moisture regime modulates the relationship between the Al_{ox} content and altitude (**Figure 1.6 A**). In soils under Udic moisture regime, Al_{ox} and altitude exhibited a significant negative correlation (Pearson's r = -0.76, $p < 0.01$), whereas in Ustic soils, no significant correlation was found (r = -0.32, $p \geq 0.10$). In contrast, the relationship between Fe_{ox} content and altitude was not influenced by moisture regime, as both Udic and Ustic soils showed similar correlation values (r = -0.67, $p < 0.01$ and r = -0.62, $p < 0.05$, respectively). A negative relationship between total C content and altitude was observed for soils under Udic regime (r=-0.54, $p < 0.01$), predominantly with altitudes close or below 2000 m asl (**Figure 1.6 C**). In contrast, no such trend was observed in soils under Ustic moisture regime (r = -0.29, $p \geq 0.10$). Additionally, a significant positive correlation was found between Al_{ox} content and C in both Udic (r = 0.42, $p < 0.01$) and Ustic soils (r = 0.66, $p < 0.01$), with a stronger relationship observed in Ustic soils.

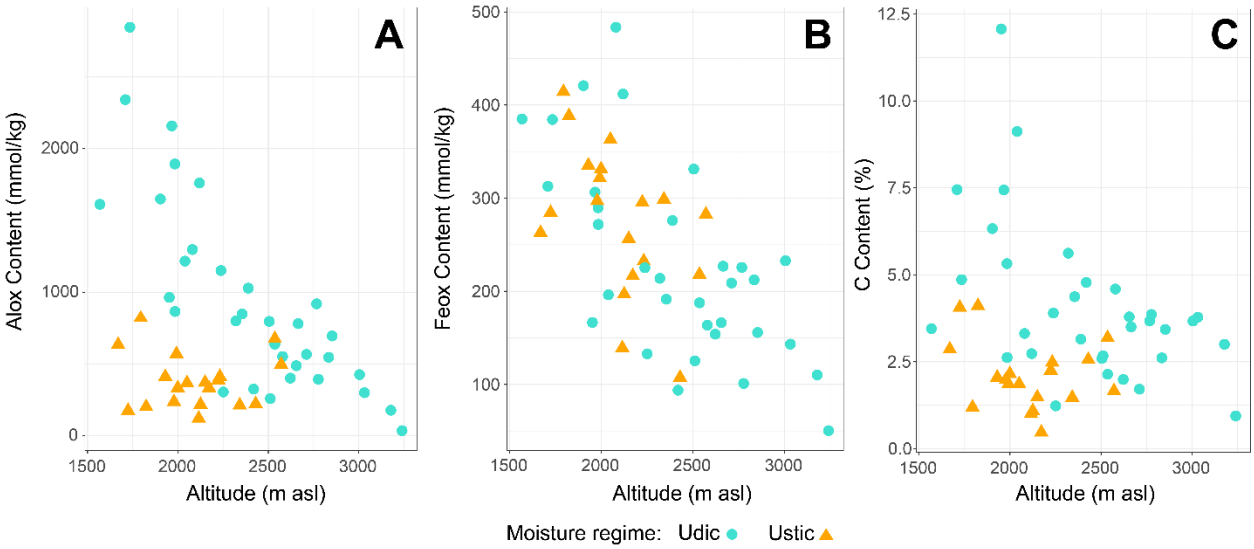

Figure 1. 6. Content of Alox (A) and the Feox (B), extracted with a 0.2 M ammonium oxalate solution, and C content (C) plotted against the altitude in m asl in the topsoils from the West-South and East-South toposequences located at the southern flank of the Irazú Volcano, Costa Rica and the topsoils from the complementary data mentioned in the materials and methods.

Table 1. 3. Pearson correlation coefficients between Alox, Feox, total C content and Altitude in dataset (n =82) topsoil and subsoil samples from Udic and Ustic moisture regimes.

	Variable	Al_{ox}[a]	Fe_{ox}[b]	C[c]	Altitude
Udic	Al_{ox}	1	0.77***	0.42***	-0.76***
	Fe_{ox}		1	0.18	-0.67***
	C			1	-0.54***
	Altitude				1
Ustic	Al_{ox}	1	0.43*	0.66***	-0.32
	Fe_{ox}		1	0.21	-0.62**
	C			1	-0.29
	Altitude				1

Asterisks are equivalent to significance. (*) = 90 % confidence. (**) = 95% confidence. (***) = 99% confidence. No asterisks equivalent to statistically insignificant.
a = aluminum (Al) extracted with ammonium oxalate.
b = iron (Fe) extracted with ammonium oxalate.
c = total carbon content.

2.4. DISCUSSION

2.4.1. Variation in chemical and mineralogical properties in relation to altitude and moisture regime

The difference between pH measured in water and in electrolyte solutions such as KCl or $CaCl_2$ is commonly used to indicate the presence of variable charge minerals in soils, particularly when pH-KCl or pH-$CaCl_2$ is lower than pH-H_2O (Gavriloaiei 2012). Lower pH values in electrolytic solutions suggest a net negative surface charge on reactive soil particles, such as short-range order (SRO) minerals or more crystalline oxides. In both soil toposequences, the trend of pH-KCl/$CaCl_2$ < pH-H_2O indicated the presence of variable charge minerals (**Tables S1.1 and S1.2**). However, the magnitude of ΔpH values revealed a higher prevalence of variable charge components in soils from the ES toposequence compared to the WS one. Additionally, topsoils from the WS toposequences exhibited an inverse trend delta pH (pH-KCl) with altitude which may indicate an increase in the variable charge components in soils at lower altitudes, such trend is less evident in the ES toposequence (**Tables S1.1 and S1.2**).

The presence of variable charge components in these volcanic soils, is further supported by the pH-NaF values, which serve as indicators of active Al–OH groups on the soil exchange complex (Fieldes and Perrot 1966; Zehetner *et al.* 2003), suggesting the presence of SRO aluminosilicates or Al–humus complexes (Parfitt 1990). The high pH-NaF values (> 9.5) observed in both toposequences confirmed the presence of SRO minerals, with consistently higher values in the

Eastern toposequence. The latter implies more Al–OH functional groups, likely associated with SRO aluminosilicates, in the ES soils compared to the WS toposequence.

The Al_{py}/Al_{ox} ratio has been used to estimate the fraction Al_{ox} that corresponds to the organically complexed Al (Al_{ox} comprises both SRO and organic complexed Al), with values higher than 0.5 indicating the dominance of Al-organic complexes over the Al present in SRO minerals (Candra *et al*. 2019). Some studies have raised concerns about the selectivity of the sodium pyrophosphate extractions, because this method can partially solubilize Al hydroxides when present in soils, besides the Al-organic associations (Rennert 2019, Farmer *et al.* 1983, Kaiser & Zech 1996, Kleber *et al*. 2004). Despite these concerns, if this ratio is consistently calculated for a set of soils, it can serve as an indication of the dominance of different pedogenetic processes, for instance formation of metal-organic complexes vs formation of SRO aluminosilicates, resulting from differences in climate or topography (Watanabe *et al.* 2023).

In this context, the Al_{py}/Al_{ox} ratio <0.5 obtained for most soils suggested that the Al_{ox} was present mainly as SRO and not as Al-organic associations. The lack of predominance of Al associated with SOM in these soils might be conditioned by the pH of soils. According to Shoji and Fujiwara (1984) Al associated with SOM tends to be predominant a pH-H_2O < 5. However, there were two exceptions, the soil profile W4 and the soil W1 that had proportionally higher Al_{py} content than the Al_{ox} content, despite their pH-H2O were also below 5. For the W4 soil the results of the Al_{py}/Al_{ox} ratio may indicate an increased solubilization of various inorganic Al forms, such as hydroxides, and some Al in organic associations. In the case of W1 soil, its conditions of high altitude, lower temperature, and limited pedogenic development suggest favorable conditions for the presence of active Al (Al_{ox}) interacting or complexed with soil organic matter (SOM). This observation aligns with findings by Watanabe *et al.* (2023), who reported that volcanic soils in cooler environments, such as those in Cameroon, exhibited higher contents of Al_{ox} and Al_{py} strongly correlated with total carbon.

The $(Al_{ox} - Al_{py})/Si_{ox}$ ratio is commonly used to identify differences in the composition of SRO aluminosilicates based on molarity variations in Al and Si, particularly in minerals such as allophane and imogolite (Parfitt and Wilson 1985). The molar Al/Si ratio of these materials depends on the composition of the soil solution from which they precipitate, and lower dissolved Si concentrations favor the formation of allophane over imogolite (Delmelle *et al.* 2015). The results indicated compositional differences between the two soil toposequences. Soil samples from the ES toposequence, all under Udic moisture regime, exhibited $(Al_{ox}-Al_{py})/Si_{ox}$ ratios higher than 1.50, which are characteristic of Al-rich allophanes and proto-imogolite (Wada 1978). The

formation of Al-rich soils may be attributed to Si leaching under higher precipitation, associated with an Udic moisture regime. According to Parfitt and Kimble (1989) Al-rich allophanes are commonly found in Udic moisture regimes and are less frequent in drier environments, such as those with Ustic moisture regime (Wada 1978).

On the other hand, soils from the WS toposequence showed a $(Al_{ox}-Al_{py})/Si_{ox}$ ratio generally lower than 1.50, indicating the formation of SRO minerals richer in Si compared to those found in the soils from the ES toposequence. In drier conditions, the higher Si concentrations in solution favor the formation of halloysite, an aluminosilicate with higher degree of crystallinity than allophane and with a molar ratio Al/Si = 1 (Delmelle *et al.* 2015, Parfitt 2009). Thus, the Al/Si ratios found for the Western toposequence might result from the mixture of different materials (allophane / halloysite) with varied chemical composition and degree of crystallinity.

In this regard, Alvarado *et al.* (2001) propose that in general terms a mixture of allophane / halloysite is expected to be found at medium position of the foot slopes of the volcanoes in the Central Ridge of Costa Rica, whereas allophane would dominate at the higher altitudes.

Similarly, Parfitt *et al.* (1983) reported that Si-rich allophanes dominate at the highest altitude (with higher rainfall), whereas halloysite dominates at the lowest altitude (will lower rainfall) in a sequence of volcanic soils from New Zealand. According to the present data, this trend is valid only in the WS toposequence where a transition from Udic to Ustic regime occurs, whereas under constant Udic conditions Al rich allophane would be dominant along the whole altitudinal gradient. These differences in composition of the SRO aluminosilicates affect the soil ability to interact specifically with ions, such as phosphate. It has been reported that halloysitic soils have lower phosphate retention capacity than allophanic soils (Theng *et al.* 1982). These implications will be further discussed in Chapter 2 of this thesis.

The similar altitudinal patterns of Al_{ox} and Si_{ox} content (**Figures 1.2 and 1.3**, panels A and B) in both sequences suggested that these soils are predominantly composed of SRO aluminosilicates. Differences in SRO content between the sequences appear to be driven by the soil moisture regime likely via leaching processes (under higher precipitation). Greater humidity has been shown to promote the formation of SRO aluminosilicates like allophane (Parfitt 1990; Lyu et al. 2018; Candra et al. 2019, Watanabe et al. 2023), whereas drier conditions and higher temperatures favor their transformation into more stable crystalline forms (Zehetner *et al.* 2003, Watanabe *et al.* 2023). The Eastern toposequence, which consistently receives higher precipitation and maintains a udic moisture regime across elevations (**Figure S1.1**), contrasts

with the Western toposequence, where precipitation is lower and moisture regimes vary from udic at high elevations to ustic at lower elevations.

The inverse relationship between SRO aluminosilicates and altitude observed only for soil samples from the ES toposequence could be a key result. This trend is likely driven by higher mean temperatures at lower altitudes (**Figure S1.2**), which accelerate the weathering of primary minerals and promote the formation of SRO aluminosilicates (Nanzyo 2002, Parfitt & Kimble 1989). However, this result contrasts with previous studies in toposequences of volcanic soils, which have reported a decrease in SRO minerals, such as allophanes, when decreasing the altitude (Nizeyimana *et al.* 1997, Zehetner *et al.* 2003, Tsai *et al.* 2010, Candra *et al.* 2019, Van Ranst *et al.* 2019). These earlier studies have also documented an increase in more crystalline Al secondary minerals such as halloysite, gibbsite, and kaolinite at lower altitudes (Zehetner *et al.* 2003; Tsai *et al.* 2010, Candra *et al.* 2019, Watanabe *et al.* 2023). Despite the regional differences in environmental conditions, one consistent observation across studies, including the present one, is the greater abundance of SRO aluminosilicates in more humid zones. However, it is important to note that the presence of more crystalline Al minerals was not specifically assessed in this study and therefore cannot be ruled out.

In contrast, this pattern of increasing SRO aluminosilicates at decreasing altitude was not observed in the Western toposequence. The combination of environmental factors such as variation in precipitation rate, moisture regime and mean temperature along this toposequence difficulted the presence of consistent trends. In this sequence, the drier conditions (ustic regime) and higher temperatures of the profile at the lowest altitudes could have promoted the transformation of SRO into more stable mineral forms. This trend was also observed when analyzing the complementary dataset presented in **Figure 1.6**. Soils under a udic moisture regime showed an increase in Al_{ox} content as altitude decreased, likely associated with the presence of SRO aluminosilicates. However, soils under ustic moisture regime did not exhibit this pattern (**Figure 1.6**).

Additionally, the Fe_{ox}/Fe_{dc} ratio, which has been commonly used as a weathering index (Schwertmann 1958, Vacca *et al.* 2003), also evidenced the role of moisture in the weathering and crystallization of the SRO minerals. Lower Fe_{ox}/Fe_{dc} ratios indicated a higher proportion of crystalline iron oxides relative to poor crystalline forms, whereas higher ratios suggested the opposite. In the WS toposequence, a more evident trend was observed, with an increasing proportion of well-crystalline iron oxides relative to less crystalline forms. In contrast, this pattern was less evident in the Eastern toposequence. These results suggest that the transformation of

SRO iron minerals into more crystalline forms is limited under consistent humid conditions. Watanabe *et al.* (2023) reported similar results where high humidity and leaching rate promoted the formation and persistence of SRO minerals (e.g., allophane, imogolite, ferrihydrite) by accelerating weathering while inhibiting crystallization. In comparison, soils under an Ustic moisture regime (W3 and W4) exhibited lower Fe_{ox}/Fe_{dc} ratios, indicating a greater proportion of crystalline iron minerals with decreasing altitude.

The iron extracted with AO (Fe_{ox}) has been used to determine the extraction of amorphous iron compounds or SRO Fe (hydro)oxide minerals, such as ferrihydrite (Pansu and Gautheyrou 2006). In the ES toposequence, the Fe_{ox} content in topsoils, commonly associated with SRO Fe minerals, inversely increased with altitude. Whereas, in the WS toposequence such pattern was not clear. However, unlike SRO aluminosilicates, the differences in Fe_{ox} content between soils from both toposequences were smaller compared with Al_{ox} (**Tables S1.3 and S1.4**).

This trend was further confirmed by the complementary data set comparing soils with Udic and Ustic soil moisture (**Figure 1.5**). Therefore, two possible hypotheses could explain the Fe_{ox} content behavior. First, SRO iron minerals were not as sensitive to changes in the soil moisture regimes (Udic and Ustic) as SRO aluminosilicates in these soils. Alternatively, the extraction may have dissolved other non-target iron species like more crystalline iron oxides (Schwertmann & Taylor 1972, Taylor & Schwertmann 1974, Walker 1983, Childs & Wilson 1983, Reyes & Torrent 1997, Poulton & Canfield 2005, Acebal *et al.* 2000, Mansfeldt *et al.* 2012, Rennert *et al.* 2021), iron from allophanes in allophanic soils (Rennert *et al.* 2021), and iron from organic associations (e.g. McKeague & Day 1966, Parfitt & Henmi 1982, Farmer *et al.* 1983).

Overall, these results showed the key role of moisture regime in modulating the content of SRO in volcanic soils, affecting their reactivity and ion adsorption capacity. These topics will be further discussed in detail in Chapter 2.

2.4.2. Trends along the depth

In general, soils under udic moisture regime exhibited an increase in SRO aluminosilicates (Al_{ox} and Si_{ox}) and SRO-Fe minerals (Fe_{ox}), with depth, whereas Ustic soils showed the opposite trend. Similar findings were reported by Tsai *et al.* (2010) in a toposequence study in northern Taiwan across a broader elevation range (140 – 1090 m asl), comparing Perudic and Udic regimes. They found that allophane content increased with depth in the more humid (Perudic) soils, whereas soils under lower moisture conditions (udic, below 500 masl) showed reduced allophane formation. Clay data obtained from the particle size distribution analysis (**Tables S1.1 and S1.2**)

does not indicate significant clay illuviation into deeper horizons. This suggests that the formation of secondary minerals SRO may occur *in situ*, likely facilitated by the downward transport of dissolved Al^{3+}, Fe^{3+}, and H_4SiO_4. This process can be favored by the higher average precipitation in Udic soil moisture regimes (**Figure S1.1**), which may enhance element mobility and subsequent mineral precipitation under supersaturation conditions in deeper horizons. The relative constat Al_{ox}/Fe_{ox} found along the profile of soils under Udic conditions (**Figure 1.4**) supported this hypothesis of downward transport of dissolved Al and Fe species.

2.4.3. Implications of changes in SRO content for carbon stabilization in soils

Moisture availability in soils have been positively correlated with organic carbon (OC) content (Tsai *et al.* 2010, Candra *et al.* 2019, Van Ranst *et al.* 2019). Our results showed an increase in total C at lower elevations, predominantly in Udic soils below 2500 m asl (r = -0.54, $p < 0.01$). The total C content in soils under an Udic regime showed a moderate correlation with Al_{ox} (r = 0.42, $p < 0.01$), but a rather weaker correlation with Fe_{ox} (r = 0.18, $p > 0.10$). Similarly, the total C showed a significant correlation with Al_{ox} in Ustic soils (r = 0.66, $p < 0.01$), and weaker with Fe_{ox} (r = 0.21, $p > 0.10$) suggesting a preferential interaction of C to Al compounds, either Al-humus complexes or SRO aluminosilicates, over Fe compounds. This preference might be related to a higher affinity of C for Al compounds (Watanabe *et al.* 2023) or to the significantly higher content of reactive Al species compared to Fe species in these volcanic soils. Hall and Thompson (2022), reported a similar stronger correlation between Al_{ox} and soil organic carbon compared to Fe_{ox}.

The complexation of soil carbon with SRO minerals or its specific adsorption onto these phases, may explain the larger total C content at lower altitudes. These associations help to prevent organic matter decomposition (Powers and Schlesinger 2002, Kleber *et al.* 2005, Prado *et al*. 2007, Takahashi and Dahlgren 2016, Candra *et al.* 2019) promoting its stabilization at lower elevations where the weathering rates and subsequent formation of SRO minerals are more intense. Similarly happened in Ustic soils, where the correlation between total C and Al_{ox} may suggest a stabilization of the organic matter that prevents its decomposition in stronger weathering conditions, thus evidencing the relevance of these pedogenetic processes to the biogeochemical cycling of C and other nutrients.

2.5. CONCLUSION

The initial hypothesis of increasing content of SRO minerals as altitude decreases was only fulfilled for the ES toposequence, while no such trend was observed in the WS toposequence. The major difference between both toposequences were the different in soil moisture regimes, while ES toposequence has a constant Udic soil moisture regime along the topographic gradient,

the WS toposequence has a transition between Udic to Ustic moisture regimes as altitude decreases. Therefore, in general the results showed that soil moisture regime is a factor that modulated the content of SRO minerals and their trends along the altitude, with Udic moisture regimes enhancing the formation and preservation of SRO minerals. In contrast, drier conditions and higher temperatures, typical of Ustic regimes, favor the transformation of these amorphous minerals into more crystalline forms. Differences were also observed with depth, as only the ES profiles exhibited a consistent increase in SRO mineral content with depth.

These findings highlight the important role of soil moisture regimes in controlling the formation and stability of SRO minerals along volcanic toposequences. Since SRO minerals strongly influence nutrient dynamics and soil reactivity, understanding their distribution under different climatic conditions is essential for establishing good land-use practices. Future research should integrate long-term monitoring of soil moisture, mineral transformations, and nutrient availability across different climatic settings to better quantify the mechanisms driving SRO mineral persistence or transformation.

2.6. ACKNOWLEDGEMENTS

We would like to thank Professor Thilo Rennert of the Department of Soil Chemistry and Pedology of the University of Hohenheim for his contribution in terms of technical consultations and bibliography, which was of great help for the discussion of the results.

2.7. REFERENCES

Acebal, SG; Mijovilovich, A; Rueda, EH; Aguirre, ME; Saragovi, C. 2000. Iron-oxide mineralogy of a Mollisol from Argentina: A study by selective-dissolution techniques, X-ray diffraction, and Mössbauer spectroscopy. Clays and Clay Minerals 48: 322–330. doi:10.1346/CCMN.2000.0480303

Alvarado Hernández, A; Bertsch HF; Bornemisza Steiner, E. 2001. Suelos derivados de cenizas volcánicas (andisoles) de Costa Rica. 1. ed. San José, C.R, ACCS, Asociación Costarricense de la Ciencia del Suelo. 111 p.

Bertsch, F; Alvarado, A; Henríquez, C; Mata, R. 2000. Properties, geographic, distribution, and management of major soil orders of Costa Rica. In Hall, Ch. A. S. ed. Quantifying sustainable development: the future of tropical economies. San Diego, California, USA, Academic Press. p. 265-294.

Campbell, AS; Schwertmann, U. 1985. Evaluation of selective extractants in soil chemistry and mineralogy by differential X-ray diffraction. Clay Minerals 20: 515–519. doi:10.1180/claymin.1985.020.4.07

Candra, IN; Gerzabek, MH; Ottner, F; Tintner, J; Wriessnig, K; Zehetner, F. 2019. Weathering and soil formation in rhyolitic tephra along a moisture gradient on Alcedo Volcano, Galápagos. Geoderma 343: 215–225. https://doi.org/10.1016/J.GEODERMA.2019.01.051

Childs, CW; Wilson, AD. 1983. Iron oxide minerals in soils of the Ha'apai group, Kingdom of Tonga. Australian Journal of Soil Research 21: 489–503. doi:10.1071/SR9830489

Churchman, J; Lowe, D. 2012. Alteration, formation, and occurrence of minerals in soils. s.l., s.e., vol.1. p. pp.33.29-33.48.

Dahlgren, RA. 1994. Quantification of Allophane and Imogolite, In: J. E. Amonette and L. W. Zelazny, Eds., Quantitative Methods in Soil Mineralogy, Soil Sciences Society of America, 1994, pp. 430-451.

Delmelle, P; Opfergelt, S; Cornelis, J-T; Ping, C-L. 2015. Chapter 72 - Volcanic Soils (en línea). In Sigurdsson, H (ed.). Amsterdam, Academic Press. p. 1253-1264 DOI: https://doi.org/10.1016/B978-0-12-385938-9.00072-9.

Egli, M; Nater, M; Mirabella, A; Raimondi, S; Plötze, M; Alioth, L. 2008. Clay minerals, oxyhydroxide formation, element leaching and humus development in volcanic soils. Geoderma 143(1):101-114. DOI: https://doi.org/10.1016/j.geoderma.2007.10.020.

Evans, LJ; Wilson, WG. 1985. Extractable Fe, Al, Si and C in B horizons of Podzolic and Brunizolic soils from Ontario. Canadian Journal of Soil Science 65: 489–496. doi:10.4141/cjss85-052

Farmer, VC; Russell, JD; Smith, BFL. 1983. Extraction of inorganic forms of translocated Al, Fe and Si from a podzol Bs horizon. Journal of Soil Science 34: 571–576. doi:10.1111/j.1365-2389.1983.tb01056.x

Fieldes, M; Perrott, KW. 1966. The nature of allophane in soils. part 3, Rapid field and laboratory test for allophane. Wellington, N.Z., Govt. Printer, (New Zealand Soil Bureau publication). 623 p.

Filimonova, S; Kaufhold, S; Wagner, FE; Häusler, W; Kögel-Knabner, I. 2016. The role of allophane nano-structure and Fe oxide speciation for hosting soil organic matter in an allophanic Andosol. Geochimica et Cosmochimica Acta 180:284-302. DOI: https://doi.org/10.1016/j.gca.2016.02.033.

Gavriloaiei, T. 2012. The Influence of Electrolyte Solutions on Soil pH Measurements. Revista de Chimie 63:396-400.

Gustafsson, JP; Bhattacharya, P; Karltun, E. 1999. Mineralogy of poorly crystalline aluminium phases in the B horizon of Podzols in southern Sweden. Applied Geochemistry 14(6):707-718. DOI: https://doi.org/10.1016/S0883-2927(99)00002-5.

Hall, SJ; Thompson, A. 2022. What do relationships between extractable metals and soil organic carbon concentrations mean?. Soil Sci. Soc. Am. J. 86:195–208. DOI: 10.1002/saj2.20343

Ichinose, Y; Matsui ,Kayo; Fukumasu ,Jumpei; Matsuura ,Shoji; Takata ,Yusuke; and Wagai, R. 2025. How do reactive aluminum and iron phases control soil organic carbon and phosphate adsorption capacity in agricultural topsoils across Japan? Soil Science and Plant Nutrition 71(1):38-52. DOI: https://doi.org/10.1080/00380768.2024.2410322.

Jongmans, AG; Verburg, P; Nieuwenhuyse, A; van Oort, F. 1995. Allophane, imogolite, and gibbsite in coatings in a Costa Rican Andisol. Geoderma 64(3):327-342. DOI: https://doi.org/10.1016/0016-7061(94)00015-3.

Kaiser, K; Zech, W. 1996. Defects in estimation of aluminum in humus complexes of podzolic soils by pyrophosphate extraction. Soil Science 161: 452–458. doi:10.1097/00010694-199607000-00005

Kleber, M; Mikutta, C; Jahn, R. 2004. Andosols in Germany – pedogenesis and properties. Catena 56: 67–83. doi:10.1016/j.catena.2003.10.015

Kleber, M; Mikutta, R; Torn, MS; Jahn, R. 2005. Poorly crystalline mineral phases protect organic matter in acid subsoil horizons. European Journal of Soil Science, vol. 56, issue 6, pp. 717-725. Doi: 10.1111/j.1365-2389.2005.00706.x

Lyu, H; Watanabe, T; Kilasara, M; Funakawa, S. 2018. Effects of climate on distribution of soil secondary minerals in volcanic regions of Tanzania. Catena 166: 209-219. https://doi.org/10.1016/j.catena.2018.04.005

Mansfeldt, T; Schuth, S; Hausler, W; Wagner, FE; Kaufhold, S; Overesch, M. 2012. Iron oxide mineralogy and stable iron isotope composition in a Gleysol with petrogleyic properties. J. Soils Sediments 12: 97–114.

McKeague, JA; Day, JH. 1966. Dithionite- and oxalateextractable Fe and Al as aids in differentiating various classes of soils. Canadian Journal of Soil Science 46(1): 13–22. https://doi.org/10. 4141/cjss66-003

Mehra, OP; Jackson, ML. 1960. Iron oxide removal from soils and clays by a dithionite–citrate system buffered with sodium bicarbonate, in: Clays and Clay Minerals. Pergamon, pp. 317–327. https://doi.org/10.1016/b978-0-08-009235-5.50026-7

Meijer, EL; Buurman, P. 2003. Chemical trends in a perhumid soil catena on the Turrialba volcano (Costa Rica). Geoderma 117(3-4):185-201. DOI: https://doi.org/10.1016/S0016-7061(03)00122-8.

Mendez, JC; Van Eynde, E; Hiemstra, T; Comans, RNJ. 2022. Surface reactivity of the natural metal (hydr)oxides in weathered tropical soils. Geoderma 406:115517. DOI: https://doi.org/10.1016/j.geoderma.2021.115517.

Nanzyo, M. 2002. Unique Properties of Volcanic Ash Soils. Global Environmental Research, Vol. 6, 2002, pp. 99-112. https://www.researchgate.net/publication/228797761_Unique_properties_of_volcanic_ash_soils

Nanzyo, M; Kanno, H. 2018. Non-crystalline Inorganic Constituents of Soil (en línea). In Nanzyo, M; Kanno, H (eds.). Singapore, Springer. p. 59-95 DOI: https://doi.org/10.1007/978-981-13-1214-4_4.

Neall, V. 2000. Volcanic Soils (online). Consulted at 17 abr. 2024. Disponible en https://www.academia.edu/25598856/Volcanic_Soils.

Nizeyimana, E; Bicki, TJ; Agbu, PA. 1997. An assessment of colloidal constituents and clay mineralogy of soils derived from volcanic materials along a toposequence in Rwanda. Soil Sci. 162: 361-371.

Pansu, M; Gautheyrou, J. 2006. Handbook of Soil Analysis. Springer, Berlin.

Parfitt, LR; Kimble, MJ. 1989. Conditions for Formation of Allophane in Soils. Soil Sci. Soc. Am. J. 53: 971-977. https://doi.org/10.2136/sssaj1989.03615995005300030057x

Parfitt, R; Childs, C. 1988. Estimation of forms of Fe and Al - a review, and analysis of contrasting soils by dissolution and Mossbauer methods. Australian Journal of Soil Research 26: 121–144. https:// doi.org/10.1071/SR9880121

Parfitt, RL. 1990. Allophane in New Zealand - a review. Soil Research 28: 343-360.

Parfitt, RL. 2009. Allophane and imogolite: role in soil biogeochemical processes. Clay Minerals 44(1):135-155. doi:10.1180/claymin.2009.044.1.135

Parfitt, RL; Henmi, T. 1982. Comparison of an oxalate-extraction method and an infrared spectroscopic method for determining allophane in soil clays. Soil Science and Plant Nutrition 28: 183–190. doi:10.1080/00380768.1982.10432435

Parfitt, RL; Kimble, JM. 1989. Conditions for Formation of Allophane in Soils. Soil Science Society of America Journal 53(3):971-977. DOI: https://doi.org/10.2136/sssaj1989.03615995005300030057x.

Parfitt, RL; Russell, M; Orbell, GE. 1983. Weathering sequence of soils from volcanic ash involving allophane and halloysite, New Zealand. Geoderma 29(1):41-57. DOI: https://doi.org/10.1016/0016-7061(83)90029-0.

Parfitt, RL; Wilson, AD. 1985. Estimation of allophane and halloysite in three sequences of volcanic soils, New Zealand. Catena Supp. 7:1-8.

Poulton, SW; Canfield, DE. 2005. Development of a sequential extraction procedure for iron: implications for iron partitioning in continentally derived particulates. Chemical Geology 214: 209–221. doi:10.1016/j.chemgeo.2004.09.003

Powers, JS; Schlesinger, WH. 2002.Relationships among soil carbon distributions and biophysical factors at nested spatial scales in rain forests of northeastern Costa Rica. Geoderma 109 (3–4): 165-190.

Prado, B; Duwig, C; Hidalgo, C; Gómez, D; Yee, H; Prat, C; Esteves, M; Etchevers, JD. 2007. Characterization, functioning and classification of two volcanic soil profiles under different land uses in Central Mexico. Geoderma 139(3-4). p.300. doi:10.1016/j.geoderma.2007.02.008

Qafoku, N; Van Ranst, E; Noble, A; Baert, G. 2004. Variable Charge Soils: Their Mineralogy, Chemistry and Management. Advances in Agronomy 84:159-215. DOI: https://doi.org/10.1016/S0065-2113(04)84004-5.

Regelink, IC; Voegelin, A; Weng, L; Koopmans, GF; Comans, RNJ. 2014. Characterization of colloidal Fe from soils using field-flow fractionation and Fe K-edge X-ray absorption spectroscopy. Environmental Science & Technology 48: 4307–4316. doi:10.1021/es405330x

Rennert, T. 2019. Wet-chemical extractions to characterise pedogenic Al and Fe species – a critical review. Soil Res. 57(1): 1–16. https://doi.org/10.1071/SR18299.

Rennert, T; Dietel, J; Heilek, S; Dohrmann, R; Mansfeldt, T. 2021. Assessing poorly crystalline and mineral-organic species by extracting Al, Fe, Mn, and Si using (citrate-) ascorbate and oxalate. Geoderma 397: 115095. https://doi.org/10.1016/j. geoderma.2021.115095.

Reyes, I; Torrent, J. 1997. Citrate-ascorbate as a highly selective extractant for poorly crystalline iron oxides. Soil Science Society of America Journal 61: 1647–1654. doi:10.2136/sssaj1997.03615995006100060015x

Schwertmann, U. 1958. The Effect of Pedogenic Environments on Iron Oxide Minerals. In: Stewart, B.A. (eds) Advances in Soil Science. Advances in Soil Science, vol 1. Springer, New York, NY. https://doi.org/10.1007/978-1-4612-5046-3_5

Schwertmann, U. 1964. Differenzierung der Eisenoxide des Bodens durch Extraktion mit Ammoniumoxalat-Lösung. Zeitschrift für Pflanzenernährung, Düngung, Bodenkd. 105: 194–202. https://doi.org/10.1002/jpln.3591050303

Schwertmann, U; Taylor, RM. 1972. The transformation of lepidocrocite to goethite. Clays and Clay Minerals 20: 151–158. doi:10.1346/CCMN.1972.0200306

Shoji, S, Fujiwara, Y. 1984. Active Aluminum and Iron in the Humus Horizons of Andosols from Northeastern Japan: Their Forms, Properties, and Significance in Clay Weathering. Soil Science, 137(4): 216-226

Soil Survey Staff. 2022. Keys to Soil Taxonomy, 13th ed. USDA-Natural Resources Conservation Service.

Soil Survey Staff. 2014a. Kellogg Soil Survey Field and Laboratory Methods Manual. U.S. Department of Agriculture, Natural Resources Conservation Service, Soil Survey Investigations Report No. 51, Version 5.0, Washington, USA.

Soil Survey Staff. 2014b. Kellogg Soil Survey Laboratory Methods Manual. U.S. Department of Agriculture, Natural Resources Conservation Service, Soil Survey Investigations Report No. 42, Version 5.0, Washington, USA.

Soil Survey Staff. 1999. Soil taxonomy: A basic system of soil classification for making and interpreting soil surveys. 2 ed. Washington, DC, US, United States Department of Agriculture, Natural Resources Conservation Service. 869 p.

Takahashi, T; Dahlgren, RA. 2016. Nature, properties and function of aluminum–humus complexes in volcanic soils. Geoderma 263: 110–121. https://doi.org/10.1016/j.geoderma.2015.08.032

Taylor, RM; Schwertmann, U. 1974. Maghemite in soils and its origin. I. Properties and observations on soil maghemites. Clay Minerals 10: 289–298. doi:10.1180/claymin.1974.010.4.07

Theng, BKG; Russell, M; Churchman, GJ; Parfitt, RL. 1982. Surface Properties of Allophane, Halloysite, and Imogolite. Clays and Clay Minerals 30(2):143-149. DOI: https://doi.org/10.1346/CCMN.1982.0300209.

Tsai, CC; Chen ZS; Kao CI; Ottner F; Kao SJ; Zehetner, F. 2010. Pedogenic development of volcanic ash soils along a climosequence in Northern Taiwan. Geoderma 156: 48–59. https://doi.org/10.1016/j.geoderma.2010.01.007

Ugolini, F; Dahlgren, R. 2002. Soil development in volcanic ash. Global Environmental Research Engl. Ed. 6.

Vacca, A; Adamo, P; Pigna, M; Violante, P. 2003. Genesis of Tephra-derived Soils from the Roccamonfina Volcano, South Central Italy. Soil Science Society of America Journal 67:198–207. SSSAJ. 67. 10.2136/sssaj2003.0198.

Van Ranst, E; Mees, F; De Grave, E; Ye, L; Cornelis, J-T; Delvaux, B. 2019. Impact of andosolization on pedogenic Fe oxides in ferrallitic soils. Geoderma 347:244-251. DOI: https://doi.org/10.1016/j.geoderma.2019.04.013.

Van Reeuwijk, LP. 1993. n. International Soil Reference and Information Centre (ISRIC). Wageningen. Netherlands.

Wada, K. 1978. Chapter 4 Allophane and imogolite (en línea). In Sudo, T; Shimoda, S (eds.). s.l., Elsevier, vol.26, (Clays and Clay Minerals of Japan). p. 147-187 DOI: https://doi.org/10.1016/S0070-4571(08)70685-X.

Wada, K; Harward, ME. 1974. Amorphous Clay Constituents of Soils (en línea). In Brady, NC (ed.). s.l., Academic Press, vol.26. p. 211-260 DOI: https://doi.org/10.1016/S0065-2113(08)60872-X.

Wada, SI; Kawabata, K; Kawabata, K. 1991. Ion adsorption on variable charge materials and thermodynamics of ion exchange. Soil Science and Plant Nutrition 37(2):191-200. DOI: https://doi.org/10.1080/00380768.1991.10415029.

Walker, AL. 1983. The effects of magnetite on oxalate- and dithioniteextractable iron. Soil Science Society of America Journal 47: 1022–1026. doi:10.2136/sssaj1983.03615995004700050036x

Watanabe, T; Ueda, S; Nakao, A; Ze, AM; Dahlgren, RA; Funakawa, S. 2023. Disentangling the pedogenic factors controlling active Al and Fe concentrations in soils of the Cameroon volcanic line. Geoderma 430:116289. DOI: https://doi.org/10.1016/j.geoderma.2022.116289.

Zehetner, F; Miller, PW; West, TL. 2003. Pedogenesis of Volcanic Ash Soils in Andean Ecuador. Soil Science Society of America Journal. 67(6):1797-1809. https://doi.org/10.2136/sssaj2003.1797

2.8. SUPPLEMENTARY INFORMATION

Table S1. 1. Physicochemical Properties of soil profiles from the West-South toposequence: pH values in different solutions (H_2O, KCl, $CaCl_2$, NaF) and Particle Size Distribution (sand, silt, clay content).

West-South toposequence												
Sample ID	**Horizon**	**Depth (cm)**	**pH-H_2O**	**pH-$CaCl_2$**	**pH-KCl**	**pH-NaF**	**C %**	**sand %**	**silt %**	**Clay %**	**ΔpH1**	**ΔpH2**
3178 m asl												
W1-1	Ap	0-14	5.29	4.59	4.51	10.66	3	72	26	2	-0.78	-0.7
W1-2	AC	14-40	5.37	4.41	4.39	10.69	2.87	71	27	2	-0.98	-0.96
W1-3	C1	40-60	5.48	4.61	4.67	10.98	1.56	76	22	2	-0.81	-0.87
W1-4	C2	60-80	5.5	4.84	4.81	10.88	2.52	69	29	2	-0.69	-0.66
2777 m asl												
W2-1	Ap	0-32	6.28	5.2	5.13	10.5	3.86	67	31	2	-1.15	-1.08
W2-2	A2	32-80	5.76	4.74	4.75	10.82	2.22	71	27	2	-1.01	-1.02
W2-3	A3	80-160	5.52	4.64	4.62	10.5	2.27	71	27	2	-0.9	-0.88
W2-4	A4	160-210	5.92	5.22	5.01	10.2	2.18	68	28	4	-0.91	-0.7
W2-5	Bw	210-240+	5.96	5.27	5.12	10.26	1.7	69	28	3	-0.84	-0.69
2150 m asl												
W3-1	Ap	0-20	6.08	5.35	4.88	9.54	1.48	49	34	17	-1.2	-0.73
W3-2	Ad	20-50	6.43	5.72	5.26	9.58	1.35	49	34	17	-1.17	-0.71
W3-3	AB	50-100	6.86	6.04	5.57	9.58	1.2	47	36	17	-1.29	-0.82
W3-4	Bw	100-120+	6.91	6.13	5.63	9.61	0.82	49	37	14	-1.28	-0.78
1724 m asl												
W4-1	Ap	0-26	6	4.85	4.71	9.38	4.06	33	35	32	-1.29	-1.15
W4-2	AB	26-40	5.89	4.97	4.63	9.48	1.62	24	33	43	-1.26	-0.92
W4-3	Bt	40-70+	6.03	5.07	4.63	9.53	0.88	27	30	43	-1.4	-0.96

ΔpH1: pH (KCl) - pH (H_2O).
ΔpH2: pH ($CaCl_2$) - pH (H_2O).

Table S1. 2. Physicochemical properties of soil profiles from the East-South toposequence: pH values in different solutions (H_2O, KCl, $CaCl_2$, NaF) and Particle Size Distribution (sand, silt, clay content).

East-South toposequence												
Sample ID	**Horizon**	**Depth (cm)**	**pH-H_2O**	**pH-$CaCl_2$**	**pH-KCl**	**pH-NaF**	**C %**	**sand %**	**silt %**	**Clay %**	**ΔpH1**	**ΔpH2**
2853 m asl												
E1-1	Ap	0-26	5.55	4.99	4.99	11.14	3.43	69	29	2	-0.56	-0.56

E1-2	A2	26-46	4.83	4.75	4.99	11.01	2.35	73	25	2	0.16	-0.08
E1-3	AB	46-63	5.19	4.8	4.99	11.15	2.81	75	23	2	-0.2	-0.39
E1-4	Bw	63-96+	5.42	5.12	5.25	10.05	2.87	78	20	2	-0.17	-0.3
					2355 m asl							
E2-1	Ap	0-15	5.56	4.89	4.81	10.71	4.37	69	29	2	-0.75	-0.67
E2-2	A2	15-30	5.44	4.8	4.77	10.6	4.13	70	27	3	-0.67	-0.64
E2-3	Bwg	30-50	5.29	4.58	4.62	10.7	4.59	70	28	2	-0.67	-0.71
E2-4	Bw2	50-80	5.8	5.06	5.08	10.92	3.43	76	22	2	-0.72	-0.74
E2-5	Bw3	80-110+	5.89	5.21	5.32	11.13	4.65	84	14	2	-0.57	-0.68
					1893 m asl							
E3-1	Ap	0-25	5.79	5.2	5.17	10.85	5.32	50	44	6	-0.62	-0.59
E3-2	A2	25-40	5.9	5.18	5.13	10.72	5.33	50	45	5	-0.77	-0.72
E3-3	Bw	40-60	5.95	5.48	5.57	10.71	3.77	82	16	2	-0.38	-0.47
E3-4	Bw2	60-85	6.11	5.67	5.73	10.61	3.25	80	18	2	-0.38	-0.44
E3-5	Bw3	85-120+	6.24	5.7	5.79	10.75	3	84	14	2	-0.45	-0.54
					1734 m asl							
E4-1	Ap	0-32	6.18	5.53	5.45	10.69	4.86	61	34	5	-0.73	-0.65
E4-2	AB	32-60	6.24	5.66	5.69	10.63	3.74	84	13	3	-0.55	-0.58
E4-3	Bw	60-90	6.32	5.66	5.75	10.53	2.36	88	10	2	-0.57	-0.66
E4-4	Bw2	90-120+	6.38	5.75	5.81	10.46	2.47	86	9	5	-0.57	-0.63

ΔpH1: pH (KCl) - pH (H_2O).
ΔpH2: pH ($CaCl_2$) - pH (H_2O).

Table S1. 3. Contents and ratios of aluminum (Al), iron (Fe), and silicon (Si) Extracted with ammonium oxalate (ox), Pyrophosphate (py), and Dithionite-Citrate (dc) in Soil Profiles from the West-South toposequence.

West-South toposequence										
Sample ID	**Depth (cm)**	**mmol/kg of soil**						**Al_{py} / Al_{ox}**	**(Al_{ox} - Al_{py}) / Si_{ox}**	**Fe_{ox}/Fe_{dc}**
		Al_{py}	**Al_{ox}**	**Fe_{ox}**	**Si_{ox}**	**Fe_{dc}**	**Al_{dc}**			
					3178 m asl					
W1-1	0-14	150	179	110.8	50.5	102.1	115.4	0.84	0.58	1.09
W1-2	14-40	160.8	156.6	114.8	44.7	117.8	132.2	1.03	ND*	0.97
W1-3	40-60	128.9	315.2	133.4	117	113.5	135.6	0.41	1.59	1.17
W1-4	60-80	149.2	437.9	183	160.5	154.6	167.6	0.34	1.8	1.18
					2777 m asl					
W2-1	0-32	148.4	395.4	101.4	164.9	115.3	129.4	0.38	1.5	0.88
W2-2	32-80	114.6	433.1	113.4	221	130.5	144.2	0.26	1.44	0.87
W2-3	80-160	108.5	500.1	119.1	259.1	149.8	163	0.22	1.51	0.8
W2-4	160-210	81	435.9	133.9	245.9	145.2	125.8	0.19	1.44	0.92
W2-5	210-240+	74.3	918	248.6	560.3	236	211.6	0.08	1.51	1.05
					2150 m asl					
W3-1	0-20	83.4	378.6	261.4	226.7	397.5	145.3	0.22	1.3	0.66
W3-2	20-50	69.9	373.7	263.5	237.2	378.5	139	0.19	1.28	0.7
W3-3	50-100	76.2	299.1	216.8	191.2	411.4	147.6	0.25	1.17	0.53

W3-4	100-120+	57	288	209.6	187.1	434.3	145.7	0.2	1.23	0.48
					1724 m asl					
W4-1	0-26	290.7	177.8	288	46.2	818.9	191	1.64	ND*	0.35
W4-2	26-40	332	146.7	166.8	38.3	731.2	166.6	2.26	ND*	0.23
W4-3	40-70+	462.3	132.6	137.3	42.7	669.4	146.8	3.49	ND*	0.21

Chemical soil extractions: Pyrophosphate (py), ammonium oxalate (ox), dithionite-citrate (dc). Al_{py}: aluminum extracted with pyrophosphate. Al_{ox}: aluminum extracted with ammonium oxalate. Fe_{ox}: iron extracted with ammonium oxalate. Si_{ox}: silicon extracted with ammonium oxalate. Fe_{dc}: extracted iron with dithionite-citrate. ND*: negative values where the content of Alpy is higher than the content of Alox.

Table S1. 4. Contents and ratios of aluminum (Al), iron (Fe), and silicon (Si) Extracted with ammonium oxalate (ox), Pyrophosphate (py), and Dithionite-Citrate (dc) in soil profiles from the East-South toposequence.

East-South toposequence										
Sample ID	**Depth (cm)**	**mmol/kg of soil**						**Al_{py} / Al_{ox}**	**(Al_{ox} - Al_{py}) / Si_{ox}**	**Fe_{ox}/Fe_{dc}**
		Al_{py}	**Al_{ox}**	**Fe_{ox}**	**Si_{ox}**	**Fe_{dc}**	**Al_{dc}**			
					2853 m asl					
E1-1	0-26	183	698.8	156.5	233.6	138	188.7	0.26	2.21	1.13
E1-2	26-46	127.1	790.4	184.6	300.9	155	211.8	0.16	2.2	1.19
E1-3	46-63	178.1	796.9	185.4	260.9	201.1	284.5	0.22	2.37	0.92
E1-4	63-96+	147.7	981.9	186	353.7	232.5	298.3	0.15	2.36	0.8
					2355 m asl					
E2-1	0-15	264.1	864.9	195.3	297.1	281.5	320	0.31	2.02	0.69
E2-2	15-30	294.5	922.2	204.8	330.3	271.6	343.2	0.32	1.9	0.75
E2-3	30-50	278.6	802.8	147	284.2	192.4	269.7	0.35	1.84	0.76
E2-4	50-80	260.2	1155.9	300.6	412.9	371.9	421.2	0.23	2.17	0.81
E2-5	80-110+	272.6	1801.2	307.9	586.7	388.8	604.8	0.15	2.61	0.79
					1893 m asl					
E3-1	0-25	324.5	1952.3	298.8	679.4	394.7	512.9	0.17	2.4	0.76
E3-2	25-40	295.4	2014.7	295.1	681	410.5	526.6	0.15	2.52	0.72
E3-3	40-60	235.3	2396.9	341.8	859	474.1	600.6	0.1	2.52	0.72
E3-4	60-85	193.7	2313.2	315	878.9	466	602.1	0.08	2.41	0.68
E3-5	85-120+	NA	2660.9	344.2	1014.9	480.4	647.7	ND	2.62	0.72
					1734 m asl					
E4-1	0-32	247.2	2913.7	393.7	1080.8	557.5	575.2	0.08	2.47	0.71
E4-2	32-60	274.4	3512	434.4	1236.1	565.7	741.6	0.08	2.62	0.77
E4-3	60-90	254.9	4032.5	457.2	1579.6	724.7	851.3	0.06	2.39	0.63
E4-4	90-120+	221.8	4413.3	611.6	1708.8	946.3	1218.8	0.05	2.45	0.65

Chemical soil extractions: Pyrophosphate (py), ammonium oxalate (ox), dithionite-citrate (dc). Al_{py}: aluminum extracted with pyrophosphate. Al_{ox}: aluminum extracted with ammonium oxalate. Fe_{ox}: iron extracted with ammonium oxalate. Si_{ox}: silicon extracted with ammonium oxalate. Fe_{dc}: extracted iron with dithionite-citrate. ND*: negative values where the content of Al_{py} is higher than the content of Al_{ox}.

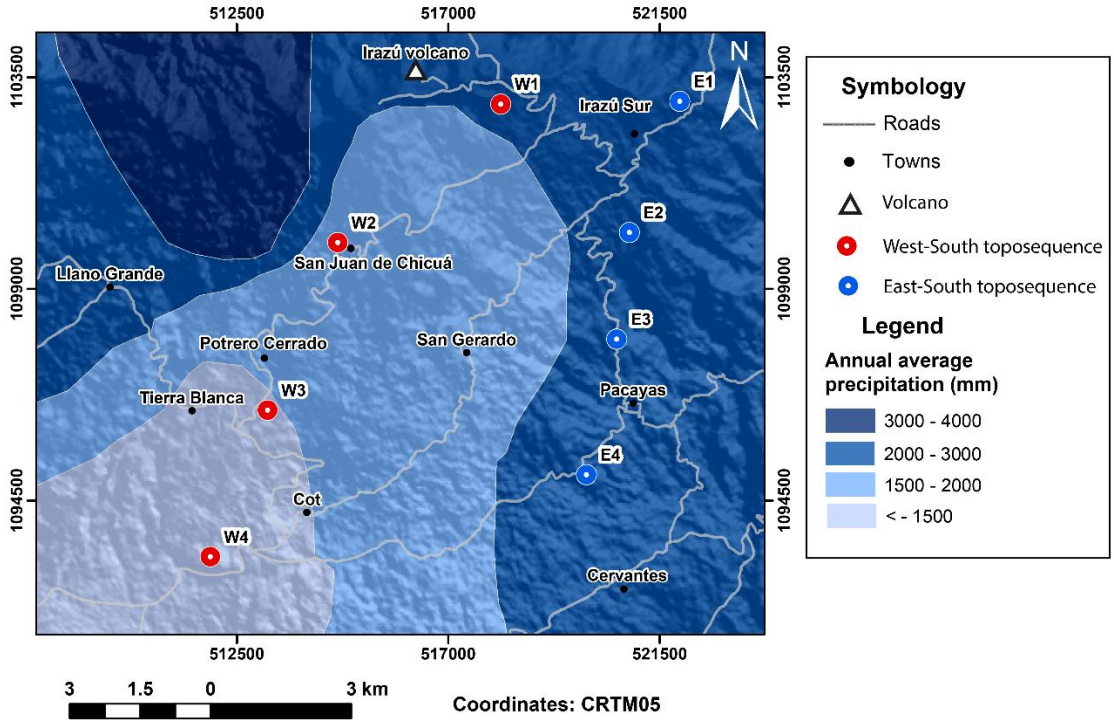

Figure S1. 1. Annual average precipitation (mm) in the study area, southern flank of the Irazú volcano, Costa Rica.

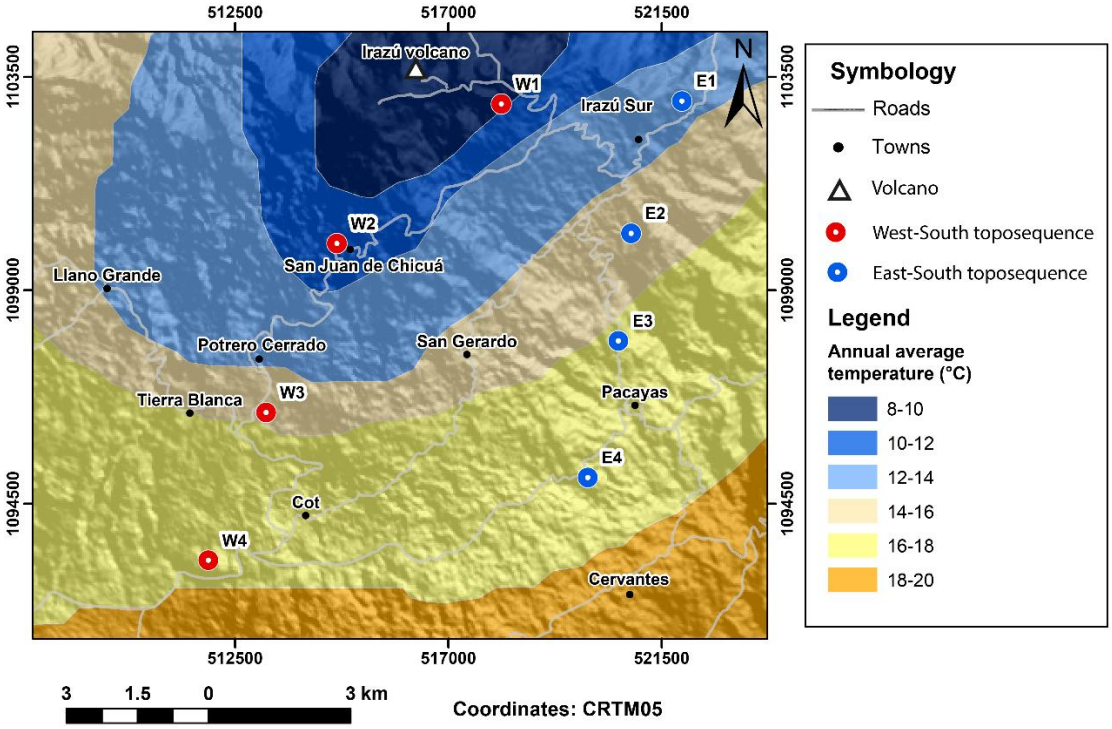

Figure S1. 2. Annual average temperature (ºC) in the study area, southern flank of the Irazú volcano, Costa Rica.

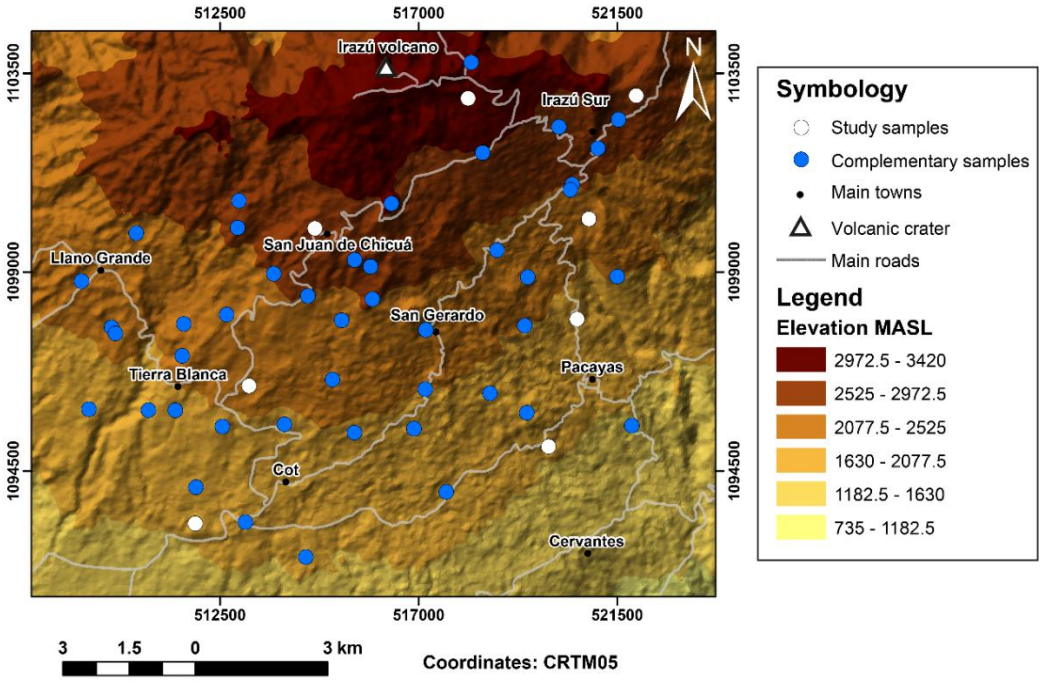

Figure S1. 3. Sample site location map of the West-South and East-South toposequences, and the complementary data located at the southern flank of the Irazú volcano, Costa Rica.

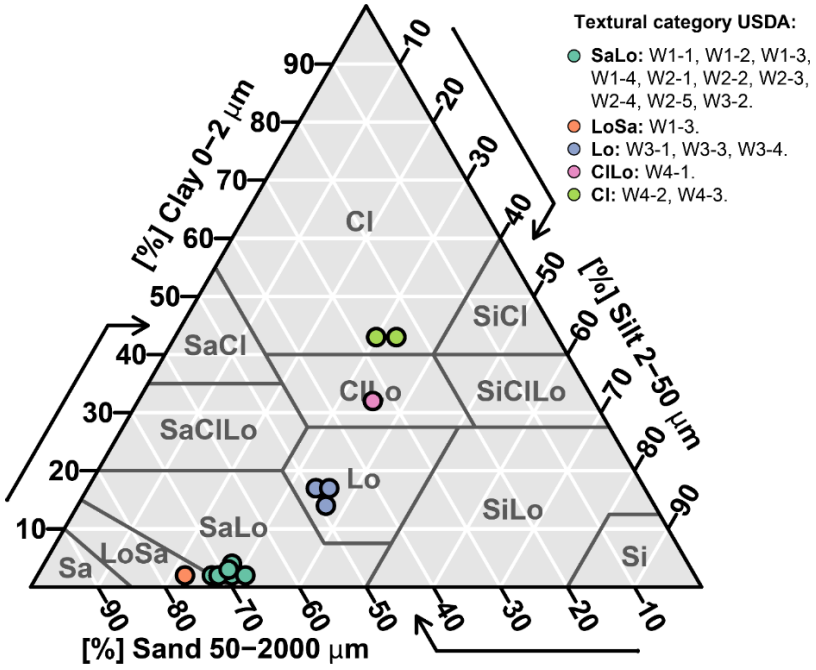

Figure S1. 4. Texture triangle according to the USDA classification system, from samples of the West-South toposequence (WS), located on the southern flank of the Irazú volcano, Costa Rica. The following abbreviatures correspond to the textures **SaLo**: Sandy Loam, **LoSa**: Loamy Sand, **Lo**: Loam, **ClLo**: Clay Loam, and **Cl**: Clay.

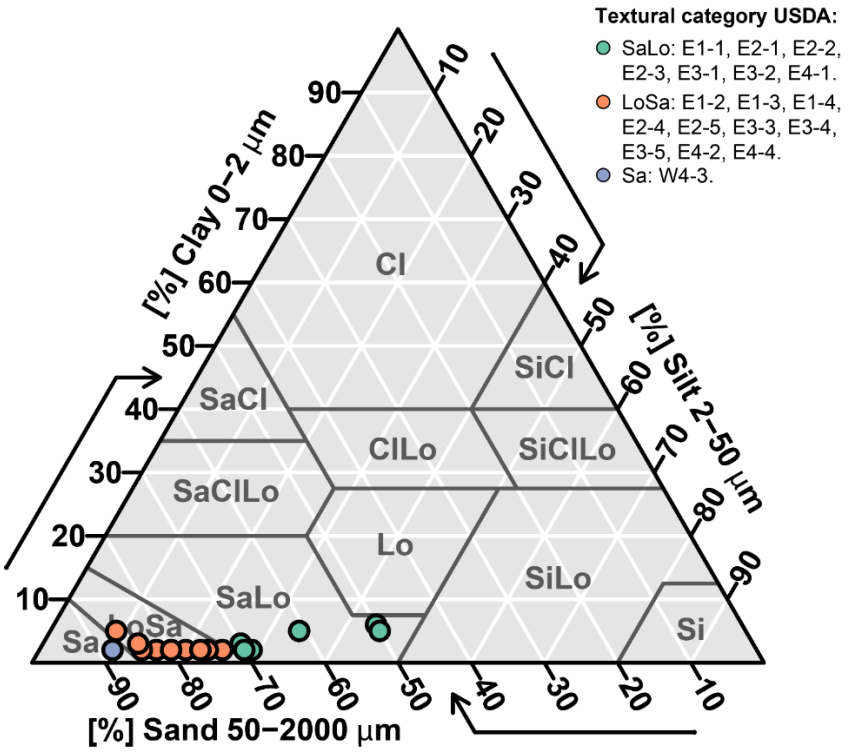

Figure S1. 5. Texture triangle according to the USDA classification system, from samples of the East-South toposequence (ES), located on the southern flank of the Irazú volcano, Costa Rica. The following abbreviatures correspond to the textures SaLo: Sandy Loam, **LoSa**: Loamy Sand, and **Sa**: Sand.

3. CHAPTER 2. PHOSPHORUS ADSORPTION ALONG TWO TOPOSEQUENCES OF TROPICAL VOLCANIC SOILS IN COSTA RICA: INFLUENCE OF SHORT-RANGE ORDER MINERAL REACTIVITY

Cintya Solano Solano[1], Manuel E. Camacho-Umaña[2], Agustín Solano Arguedas[3], Juan Carlos Méndez Fernandez[2]

1 Facultad de Ciencias Agroalimentarias, Maestría en Ciencias Agrícolas y Recursos Naturales con énfasis en Suelos, Universidad de Costa Rica, San Pedro, Costa Rica.

2 Centro de Investigaciones Agronómicas (CIA), Universidad de Costa Rica, San Pedro, Costa Rica.

3 Unidad de Recursos Forestales (Reforesta), Instituto de Investigaciones en Ingeniería (INII) and Escuela de Química, Universidad de Costa Rica, San Pedro, Costa Rica.

ABSTRACT

Phosphorus (P) availability in volcanic soils is strongly influenced by short-range order (SRO) minerals, but how changes in their reactivity along altitudinal gradients affect P adsorption remains largely unexplored. This study aims to analyze how the reactivity and content of SRO minerals affect both the P adsorption and P availability along two volcanic soil toposequences with contrasting moisture regimes on the southern flank of Irazú Volcano, Costa Rica. Soil samples from different horizons were collected along an East-South (ES) toposequence (1734–2853 m asl) with consistent Udic regime, and a West-South (WS) toposequence (1724–3178 m asl) that transitions from Udic to Ustic regime when decreasing altitude. Soil extractions (ammonium oxalate, dithionite-citrate, and sodium pyrophosphate) were performed to quantify Fe, Al, and Si associated with different mineral phases, aiming to define P pools. The reactive surface area (RSA) of soils was assessed by implementing a method that uses soil phosphate as probe ion, followed by interpretation with Surface Complexation Model (SCM). Phosphorus retention was evaluated through batch adsorption experiments followed by data interpretation using a Langmuir approach. Results revealed that soils from the ES toposequence exhibited higher RSA and total oxalate-extractable phosphorus (P_{ox}) than soils from the WS sequence. Phosphorus sorption capacity (Q_{max}) was also higher in soils from the ES toposequence and increased with altitude, which is related with enhanced weathering under a consistent Udic regime. In contrast, the WS toposequence showed no clear trend in P sorption capacity along the altitudinal gradient, likely due to a shift from Udic to Ustic moisture regimes that promoted the transformation of SRO

minerals into more crystalline forms. The P-Olsen fraction remained low in all soils (<10% of P_{ox}), suggesting that sorption onto SRO minerals strongly limits P availability in these soils. Overall, these findings underscore the importance of changing mineral reactivity along altitudinal gradients of volcanic soils in terms of P cycling and availability. Understanding the sorption capacity of these soils has important implications for site-specific nutrient management practices aimed at improving P-use efficiency. In particular, estimating the sorption capacity can guide the adjustment of fertilizer application rates to exceed sorption thresholds, thereby enhancing plant-available P in volcanic agroecosystems.

Keywords: volcanic toposequences, surface reactivity, phosphorus, sorption.

3.1. INTRODUCTION

Volcanic soils, commonly classified as Andisols, develop from pyroclastic deposits or tephra, such as ash, lapilli, blocks, and bombs (Nanzyo 2002). Additionally, Andisols can be formed from scoria deposits, epiclastic volcanic materials and lava flows (Neall 2006). These volcanic soils are characterized by an abundance of nanocrystalline or short-range order (SRO) minerals with variable charge surfaces, which constitute the main components of the reactive colloidal fractions. These SRO minerals include aluminosilicates such as allophane, imogolite, proto-imogololite, as well as Fe (hydr)oxide minerals like ferrihydrite (Neall 2006, Nanzyo and Kanno 2018, Cornell and Schwertmann 2003, Nanzyo 2002).

Due to their nanometric particle size and their relative abundance in Andisols, the SRO minerals are responsible for the high reactivity of these soils towards inorganic anions such as phosphate and soil organic carbon (SOC). Both the ultra-small particle size and high content of SRO define the reactive surface area (RSA) of soils, which can be defined as the overall surface area of the SRO minerals in field samples that effectively participate in adsorption processes (Hiemstra *et al*. 2010). Key physicochemical processes, such as adsorption, occur on the solid-solution interface of these reactive surfaces, which play a critical role on regulating the mobility and availability of soil nutrients, particularly phosphorus (P) in its anionic form as phosphate (Qafoku *et al*. 2004).

In Andisols, one of the main challenges related to soil fertility is the low availability of P, which is caused by the high adsorption capacity and affinity between the reactive SRO minerals and phosphate. The adsorption of phosphate on SRO minerals occurs primarily through ligand exchange reactions, also referred to as specific adsorption or chemisorption (Goldberg y Sposito 1985). In this process, phosphate might form mono or bidentate complexes by replacing surface hydroxyl (-OH) groups on the mineral surfaces with the -O ligands of phosphate molecule (PO_4^{3-})(Zheng *et al.* 2012; Elzinga and Sparks 2007; Zhong *et al.* 2007). This high adsorption

mechanism significantly limits the availability of phosphate in volcanic soils, leading to the frequent application of high quantities of phosphate fertilizers (Nanzyo 2002).

Understanding the relationship between SRO content, its surface reactivity, and P adsorption is essential for accurately assessing P cycling and availability in soils derived from volcanic parent materials. While several studies have analyzed changes in mineralogical composition along different soil topo- and chronosequences (Tsai *et al.* 2010, Candra *et al.* 2019, Zehetner *et al.* 2003, Watanabe *et al.* 2023), only a limited number of studies have systematically explored how these changes in mineral composition influence P adsorption and availability (Van Ranst *et al.* 2004, Rechberger *et al.* 2021, Chiu *et al.* 2021, Neto *et al.* 2004).

For instance, Van Ranst *et al*. (2004) analyzed how variations in parent ash materials influenced the surface reactivity of highland Andisols along an east-to-west sequence in Java Island, Indonesia. They found that the SRO minerals and active aluminum (Al) and iron (Fe) compounds were positively correlated with P adsorption in these soils. Rechberger *et al*. (2021) evaluated the phosphate adsorption–desorption behavior along a chronosequence of volcanic topsoils from the Galápagos Islands and found that both the SRO minerals as well as Fe and Al bound to organic matter were the major soil factors that positively correlated with phosphate adsorption. The results of Rechberger *et al*. (2021) also showed that increasing precipitation favored the formation of SRO minerals, leading to a steep increase in phosphorus sorption capacity (PSC) from arid lowlands to very humid highlands.

Chiu *et al*. (2021) studied the effects of lateritization on the speciation and retention of soil P along a topo- and chronosequence on Green Island, Taiwan, and found that P adsorption was positively correlated with the content of Al and Fe extracted with ammonium oxalate. Similarly, Neto *et al*. (2004) investigated P adsorption in soils developed from mafic and ultramafic volcanic rocks in the Alto Paranaíba region of Minas Gerais, Brazil, and established relationships between P adsorption and specific surface area and soil mineralogy. In these highly weathered soils, the well-crystallized metal (hydr)oxides such as goethite and gibbsite play a dominant role in P adsorption (Neto *et al*. 2004).

The studies, previously mentioned, have investigated how the content and type of reactive minerals affect the phosphorus adsorption in soils. However, no study has specifically explored the interactions between phosphorus adsorption, mineralogy, and RSA by comparing two toposequences of volcanic soils within the same study region but under different climatic conditions. Therefore, this study aims to analyze how the changes in RSA and the content of SRO

minerals influence P adsorption capacity and P availability along two soil toposequences with different moisture regimes on the southern flank of Irazú Volcano, Costa Rica.

A novel aspect of this project is the implementation of an advanced surface complexation model (SCM) to derive the RSA of soils formed from volcanic materials. Another novel aspect of this study is the comparison of the P sorption capacity of two toposequences with similar conditions regarding parent materials but contrasting climatic factors like the soil moisture regime (Udic vs Ustic/Udic transition). This study will contribute to a deeper understanding of the key chemical and mineralogical factors that influence P bioavailability in Andisols. Consequently, the findings of this research will have broader implications beyond the region studied, offering new insights into the relationship between mineral composition, surface reactivity, and phosphate availability in soils formed or influenced by volcanic activity.

3.2. MATERIALS AND METHODS

3.2.1. Soil sampling

Sampling locations were selected along two altitudinal transects based on existing information on the physicochemical properties of a series of soil profiles, previously described and characterized in the first Chapter of this thesis. Two toposequences, within an altitude range from 1724 to 3178 m asl, were sampled at the southern flank of Irazú volcano, defined as the West-South (WS) and East-South (ES) toposequences (**Figure S2.1**). General characteristics of the sampling sites from both toposequences are shown in **Table S2.1**. In total, 34 soil samples were collected in the eight soil profiles (four profiles in each toposequence). Both toposequences differed in climatic conditions, particularly moisture regime. The ES toposequence had a consistent Udic moisture regime along the altitudinal gradient, while the WS toposequence presented a transition from Udic to Ustic conditions with decreasing altitude.

3.2.2. Soil chemical extractions

Data on the content of mineral fraction that is reactive towards phosphate (i.e. the SRO minerals) were taken from the first chapter of the thesis and were used to support the interpretation of the results related to P pools and adsorption in the studied soils. The dataset comprises concentrations of Fe, Al, and Si extracted with a 0.2 M ammonium oxalate solution (Fe_{ox}, Al_{ox}, Si_{ox}), Al extracted with 0.1 M sodium pyrophosphate solution (Al_{py}), and Fe extracted with dithionite-citrate solution (Fe_{dc}). The results are shown in **Tables S2.2** and **S2.3**.

3.2.3. Determination of reactive surface area (RSA)

The RSA (in $m^2\ g^{-1}$ of soil) was evaluated applying a methodology originally proposed by Hiemstra *et al.* (2010), incorporating modifications by Mendez *et al.* (2020), which uses the native soil phosphate as a probe ion. The method is based on experimentally measuring the competitive interaction between phosphate and carbonate anions onto reactive surface groups of variably charged minerals. The resulting data was interpreted using a surface complexation model (SCM), allowing the estimation of the effective RSA of all the mineral phases that determine the equilibrium solid-solution partitioning of phosphate in soils.

Briefly, air-dried soil samples were equilibrated with a 0.5 M $NaHCO_3$ solution (pH 8.5) at five solution-to-solid ratios (SSR) ranging from 10 to 200 L kg^{-1}. Consequently, a desorption curve is obtained representing the changes in concentration of extracted PO_4^{3-} as a function of the SSR. The ubiquitous presence of soil organic matter (SOM) might affect the adsorption interaction between PO_4^{3-} and carbonate during the equilibration, due to the competition of SOM functional groups with PO_4^{3-} for binding sites on the soil surface. Thus, to remove dissolved organic matter released during $NaHCO_3$ extractions, activated carbon (AC) (0.40 g g^{-1} soil) was added to soil suspensions (Hiemstra *et al.* 2010). The AC may contain small amounts of $PO_4^{3-,}$ therefore, it was pre-cleaned with ammonium oxalate and $NaHCO_3$ solutions, as described by Koopmans *et al.* (2020).

The samples were equilibrated for 15 days under constant agitation. After equilibration, the final pH of each soil suspension was measured, the samples were centrifuged at 3000 *g* for 10 min and the supernatant was filtered through a 0.45 µm cellulose acetate membrane filter. Then, phosphate concentration in the filtrate was measured colorimetrically with a molybdenum blue method (Murphy and Riley 1962) using a Flow Injection Analyzer (FIA) (Model, Brand, City, Country).

The RSA of soils were estimated by interpreting experimental phosphate desorption data measured in $NaHCO_3$ soil extracts with the Charge-Distribution Multisite Ion Complexation Model (CD-MUSIC). For the modeling approach, adsorption parameters previously derived in model systems using ferrihydrite as a reference material were used (Mendez and Hiemstra 2020). Therefore, ferrihydrite was used as a proxy to describe the general reactivity of variable charge minerals in soils. In the calculations, phosphate concentrations predicted by the modeling were fitted to experimental phosphate concentrations measured in 0.5 M $NaHCO_3$ extraction solutions at different SSRs, defining RSA and the amount of PO_4^{3-} reversibly adsorbed to the reactive

mineral surfaces (R-PO_4^{3-}) as the only adjustable parameters. The underlying calculations for deriving RSA and R-PO_4^{3-} with the CD-MUSIC model is explained in detail in Mendez *et al.* (2020).

The model calculations were performed using the program ECOSAT (version 4.9) (Keizer and van Riemsdijk 1998) in combination with the program FIT (version 2.581) (Kinniburgh 1993) for the optimization of RSA and R-PO_4 values. T-tests (*p value* < *0.001*, 95% IC: Confidence Interval) were conducted to determine significant differences in the content of RSA between both toposequences.

3.2.4. Phosphorus extractions

Phosphorous fractions were operationally defined by applying different soil extraction procedures. First, total P (P_{ox}) and inorganic phosphate ($PO_4^{3-}{}_{(ox)}$) extractable with a 0.2 M ammonium acid oxalate solution (pH = 3) were measured using ICP-OES (Perkin Elmer) and a Flow Injection Analyzer (FIA), respectively (8500 Series 2, QuikChem, Colorado, USA). These P_{ox} and $PO_4^{3-}{}_{(ox)}$ fractions are proxies for the total P and inorganic phosphate adsorbed on the reactive surfaces of SRO minerals, respectively. The fraction of organic P (P_{org}) associated with this mineral fraction was calculated from the difference between P_{ox} minus $PO_4^{3-}{}_{(ox)}$. In addition, Olsen extractions (0.5 M NaHCO3, pH = 8.5) (Olsen 1954) were performed on samples from the upper two soil horizons to quantify potentially bioavailable P (P-Olsen). This fraction comprises readily soluble phosphate and non-specific fraction of phosphate that can be easily desorbed from the soil surfaces. The phosphorus retention capacity (PRC) was measured using the method described by Blakemore *et al*. 1987 for the upper two horizons of the soil profiles to determine the ability of soil to retain P.

3.2.5. Adsorption isotherms of phosphate (PO_4^{3-})

The adsorption isotherms of PO_4^{3-} were performed on the topsoil samples from each profile to compare PO_4^{3-} adsorption behavior in relation to changes in the content and reactivity of SRO minerals along the altitudinal position in the soil toposequences.

Adsorption isotherms were determined by equilibrating soil samples for 48 h with a phosphate-containing solution at SSR of 10 L kg^{-1}. Each adsorption isotherm consisted of six concentration points for the WS toposequence and seven for the ES toposequence. The number of points for the WS toposequence was limited to six due to abrupt changes in the apparent PO_4^{3-} adsorption observed at higher concentrations, which may indicate a shift to a different process, such as precipitation. The concentration range of added PO_4^{3-} was according to the content of SRO minerals of each sample (first Chapter of this thesis). The concentrations of added PO_4^{3-} varied from 0 to 750 mg L^{-1} (24.2 mmol L^{-1}) for soils from the WS sequence (W1-1, W2-1, W3-1, W4-1)

and for the topsoil (E1-1) at the highest altitude of the ES sequence from 0 to 1000 mg L^{-1} (32.2 mmol L^{-1}). For the rest of soils from the ES sequence (E2-1, E3-1, E4-1) the PO_4^{3-} concentration varied from 0 to 1500 mg L^{-1} (48.4 mmol L^{-1}). The adsorption isotherms were performed at a fixed pH (5.30 ± 0.30) and ionic strength (I = 0.05 M), using $NaNO_3$ as the background electrolyte solution. These adsorption isotherms were performed in duplicates (**Figures S2.2 and S2.3**), and the data shown in the results section corresponds to the average values from the duplicates.

Furthermore, additional adsorption isotherms were performed using 0.01 M $Ca(NO_3)_2$ as the background electrolyte solution together with $NaNO_3$ to reach a final ionic strength value of 0.05 M. The objective was to analyze the effect of adding a divalent electrolyte cation such as Ca^{2+} on the PO_4^{3-} adsorption. These additional adsorption isotherms were conducted in four soil samples with contrasting adsorption capacity. These samples were selected (W1-1, W2-1, E1-1 and E3-1) based on the results of the isotherms performed with only $NaNO_3$. The pH range for these isotherms was between 5.40 ± 0.15.

After the equilibration period, the samples were centrifuged for 15 min to separate the solid and liquid phases. The supernatant was filtered through a 0.25 µm cellulose acetate filter and analyzed for PO_4^{3-} in an FIA (8500 Series 2, QuikChem, Colorado, USA), applying a molybdenum blue colorimetric method (Murphy and Riley 1962). The amount of added PO_4^{3-} adsorbed to the solid phase were calculated as the difference of the total added and the PO_4^{3-} remaining in solution after equilibration, corrected by the PO_4^{3-} concentration measured in the control sample with no PO_4^{3-} added. Thus, the adsorption data represents the fraction of added PO_4^{3-} that was retained on the soil surfaces, i.e. an excess PO_4^{3-} adsorption compared to the natural soil condition.

The results of PO_4^{3-} adsorption isotherms were interpreted using the Langmuir equation (Langmuir 1918). Substituting the experimental data of PO_4^{3-} adsorption (Q_{ads}, in mmol kg^{-1}) and equilibrium PO_4^{3-} concentration (C_i, in mmol L^{-1}) into a linearized form of the equation 1, the maximum adsorption capacity (Q_{max}, in mmol kg^{-1}) and the Langmuir adsorption constant (K_L) were fitted for each adsorption isotherm.

$$[Qads] = [Qmax] * \frac{K[C_i]}{1 + K_L[C_i]} \quad (1)$$

3.3. RESULTS

3.3.1. Estimation of the RSA in soils from two volcanic toposequences from Costa Rica

The comparison of the RSA between the two soil toposequences (**Figure 2.1**) revealed significant differences, where soils from the ES toposequence exhibited a significantly higher mean RSA

(31.34 ± 7.04) m^2 g^{-1} compared to those from the WS toposequence (14.60 ± 6.90) m^2 g^{-1} (t = 5.87, df = 21.12, *p* < *0.001*) (**Table S2.3**).

In the WS toposequence, there is not a clear relationship between the RSA values and altitude (**Figure 2.1 A**). Only for soil profile W4 (located at a lower altitude) a higher RSA was measured compared to the other samples located at higher altitudes in this sequence. In contrast, topsoils from the ES toposequence (**Figure 2.1 B**) show an increase in RSA with decreasing altitude in profiles E1, E2, and E3. For the profile E4 very low results were obtained which made it impossible to estimate the RSA during the modeling. In this case the modeling approach that uses only ferrihydrite as proxy had a limitation for the estimation of the RSA, probably due to a poor quality of the experimental data of the $NaHCO_3$ extractions.

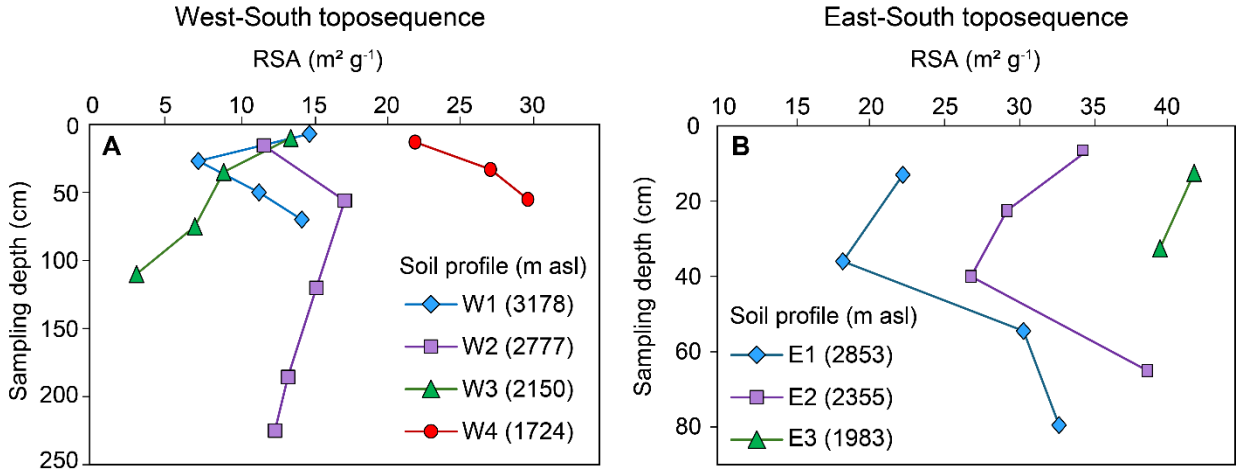

Figure 2. 1. Relationship between the reactive surface area (RSA) and sampling depth (cm), from soil samples from A) the West-South (WS) and B) East-South (ES) toposequences located at the southern flank of the Irazú Volcano, Costa Rica. For samples from profile E4, it was not possible to adjust the values of RSA with the experimental results.

In relation to changes in RSA as a function of depth, the RSA values showed a trend to increase below 40 cm in profiles W1, E1, and E2 (**Figure 2.1**). In contrast, profiles W2 (after 50 cm), W3, and E3 exhibited a decrease in RSA with depth (**Figure 2.1**). Only the profile W4 showed a consistent increase in RSA throughout the entire soil profile.

3.3.2. Phosphorus fractions in soils from two volcanic toposequences from Costa Rica

Soils from the WS toposequence exhibited P_{ox} contents ranging from 0 to 19 mmol kg^{-1}, whereas soils from the ES sequence showed generally higher P_{ox} values, ranging from 6 to 57 mmol kg^{-1}. The comparison of the P_{ox} content between the two toposequences showed significant differences, where the soils from the ES toposequence exhibited a higher mean P_{ox} (23.41 ± 15.12) mmol kg^{-1} compared to those from the WS toposequence (11.17 ± 5.58) mmol kg^{-1} (t =

3.145, df = 22.225, *p < 0.01,* IC:95%). Available phosphorus determined by the Olsen extraction ranged from 2 to 54 (23 ± 20) mg kg^{-1} in soils from the WS toposequence, whereas in the ES the values varied between 1 and 46 (23 ± 15) mg kg^{-1}. There were not statistically significant differences in the P-Olsen content between both toposequences (t = -0.03, df = 12.97, *p = 0.98*). Regarding the phosphorus retention capacity (PRC) the results showed a statistically significant difference in PRC values between toposequences (t = 6.83, df = 13.915, *p < 0.00001*). The soils from ES toposequence exhibited higher PRC (91.70 ± 8.80) % compared to those from the WS toposequence (60.76 ± 8.14) %.

A linear relationship was observed between the total phosphorus (P_{ox}) and the inorganic phosphate ($PO_{4,ox}^{3-}$) fractions, both extractable by ammonium oxalate solution (**Figure 2.2**). Points closer to the red dotted 1:1 line indicated that the P_{ox} extracted by the oxalate solution is predominantly present as inorganic phosphate ($PO_{4,ox}^{3-}$). Samples from the WS toposequence (**Figure 2.2 A**) exhibited greater dispersion around the 1:1 line in comparison with the samples from the ES toposequence, indicating a larger variability in the relative contribution of $PO_{4,ox}^{3-}$ to P_{ox} in the soils from the WS sequence. The few values located slightly above the 1:1 line resulted from the intrinsic variability of the soil samples or due to the uncertainty of the AO extraction method.

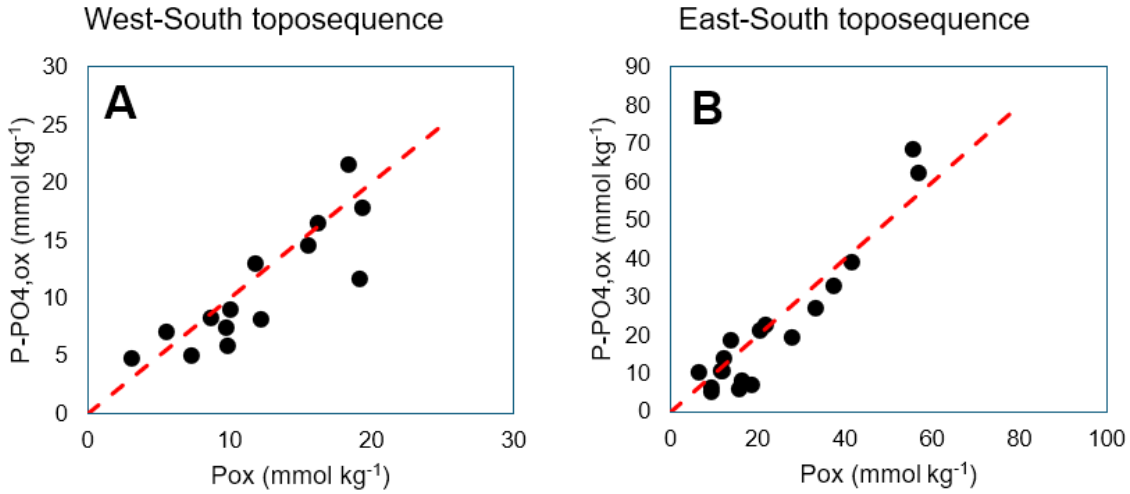

Figure 2. 2. Relationship between total phosphorus (P_{ox}) and inorganic phosphorus present as phosphate ($PO_{4,ox}^{3-}$), both extracted with a 0.2 M ammonium oxalate solution, in soils from toposequences located at the southern flank of the Irazú Volcano, Costa Rica. Panel A is for soil samples from the West-South (WS) toposequence, and panel B for soils samples from the East-South (ES) toposequence. Doted lines represent 1:1 ratio.

The trends in P_{ox} content with respect to sampling depth and altitude along the toposequences are presented in **Figure 2.3**. In general, higher P_{ox} concentrations were found in the topsoil layers of the soil profiles, except for profile W2, which shows an increase in P_{ox} content in the deepest horizon. The rest of the soil profiles typically show a decreasing trend in P_{ox} content with depth. To account for the differences on the amount of reactive minerals between samples, the P_{ox} content can be normalized to the molar sum of [Fe_{ox} + Al_{ox}]. When this is done, a marked decrease in the P_{ox} / [Fe_{ox} + Al_{ox}] ratio was observed down to 50 cm depth. Below this depth, this ratio remained relatively constant with increasing depth in all soil profiles (**Figure S2.4**).

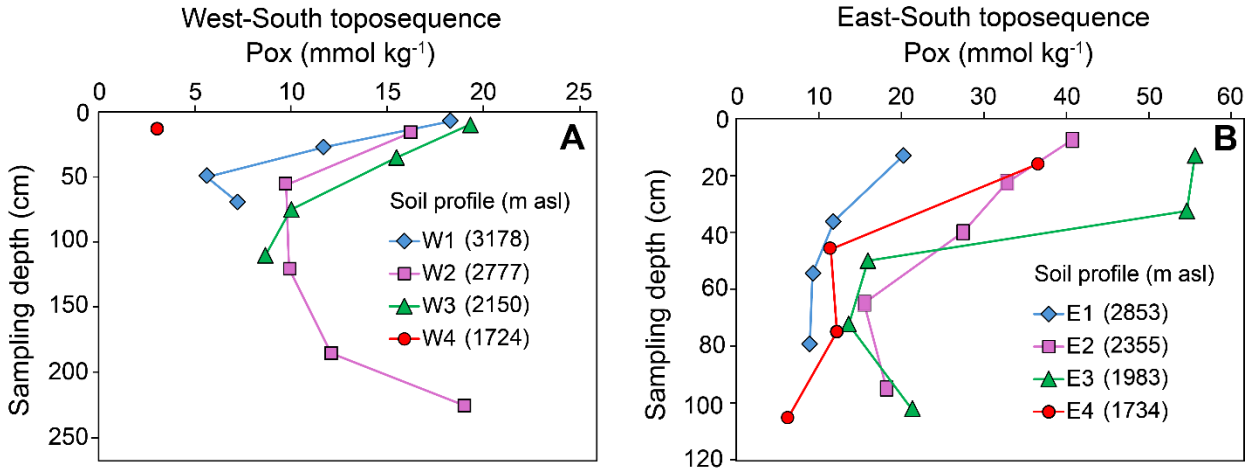

Figure 2. 3. Content of Pox extracted with a 0.2 M ammonium oxalate solution, plotted against sampling depth in soil profiles from the West-South (WS) toposequence (A) and the East-South (ES) toposequence (B) on the southern flank of the Irazú Volcano, Costa Rica.

The results show that the content of available phosphorus (P-Olsen) in the topsoils and subsurface samples represented only a small fraction (< 10 %) of the total amount of P associated with the surfaces of the SRO minerals (P_{ox}) (**Figure 2.4**). Additionally, the results indicated a decrease in the ratio P-Olsen/P_{ox} ratio in the subsoil horizons compared to the corresponding topsoil samples. When comparing sequences, soils from the ES toposequence exhibited a lower P-Olsen/P_{ox} ratio, compared to soils from the WS toposequence (**Figure 2.4**). For the ES toposequence, there is a trend of decreasing this ratio when the altitude decreases (**Figure 2.4 B**). The P-Olsen/P_{ox} ratio is inversely related to the PRC (**Figure 2.5**) of the analyzed soil samples, suggesting that P availability in these soils was more strongly influenced by the adsorption to SRO minerals, rather than by the total P content.

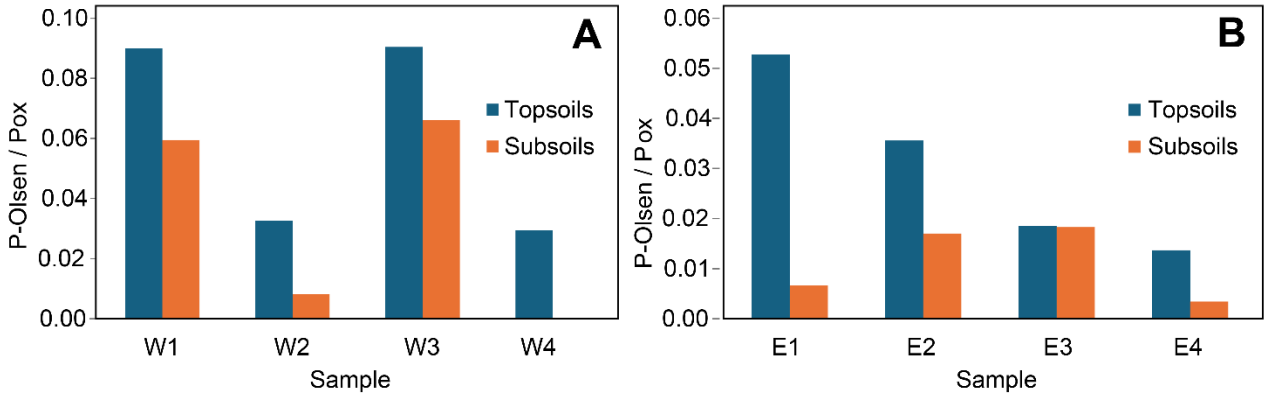

Figure 2. 4. Fraction of available phosphorus (P-Olsen) relative to the total phosphorus (Pox), extracted by a 0.2 M ammonium oxalate solution, in topsoil and subsoil samples from the West-South (A) and East-South (B) toposequences on the southern flank of Irazú Volcano, Costa Rica.

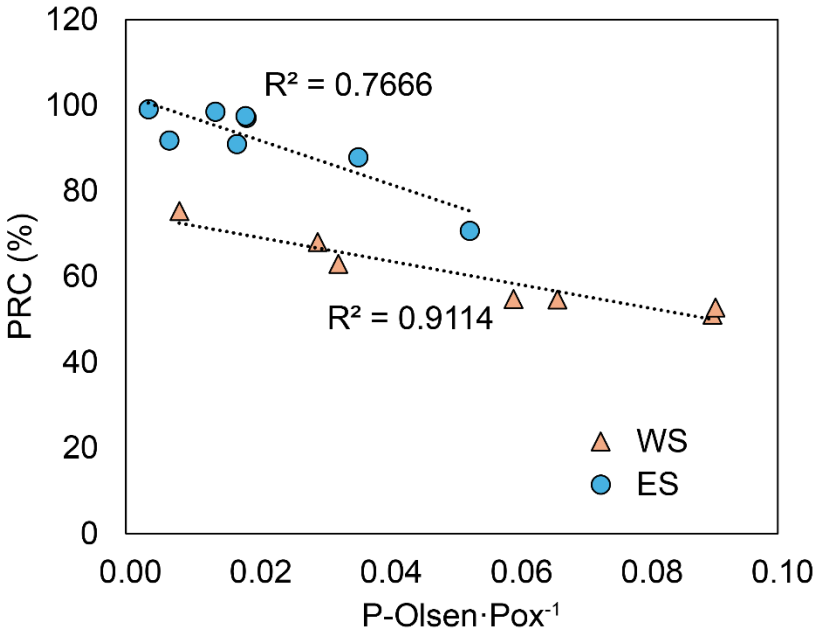

Figure 2. 5. Relationship between the ratio of P-Olsen/Pox and phosphorus retention capacity (PRC), measured according to Blakemore et al. (1987), for soil samples from the West-South (WS) and the East-South (ES) toposequences on the southern flank of the Irazú Volcano, Costa Rica.

3.3.3. Phosphate adsorption isotherms in soils from two volcanic toposequences from Costa Rica

The results of the adsorption experiments revealed important differences in P adsorption between the topsoil samples from both toposequences. Expressed in a soil mass basis (mmol PO_4^{3-} kg^{-1}

soil), soils from the ES toposequence exhibited higher PO_4^{3-} sorption capacities than those from the WS toposequence (**Figure 2.6**). This difference was evident when comparing the data of both toposequences presented in **Figure 2.6** and further supported by the Q_{max} values fitted with the Langmuir equation (**Table 2.1**).

Additionally, **Figure 2.6** shows that only in the ES toposequence a clear trend is observed in which the adsorption of PO_4^{3-} increases with decreasing altitude, E1 > E2 > E3 > E4 (**Figure 2.6 B**). In contrast, this trend was not observed for the soils from the WS toposequence (**Figure 2.6 A**).

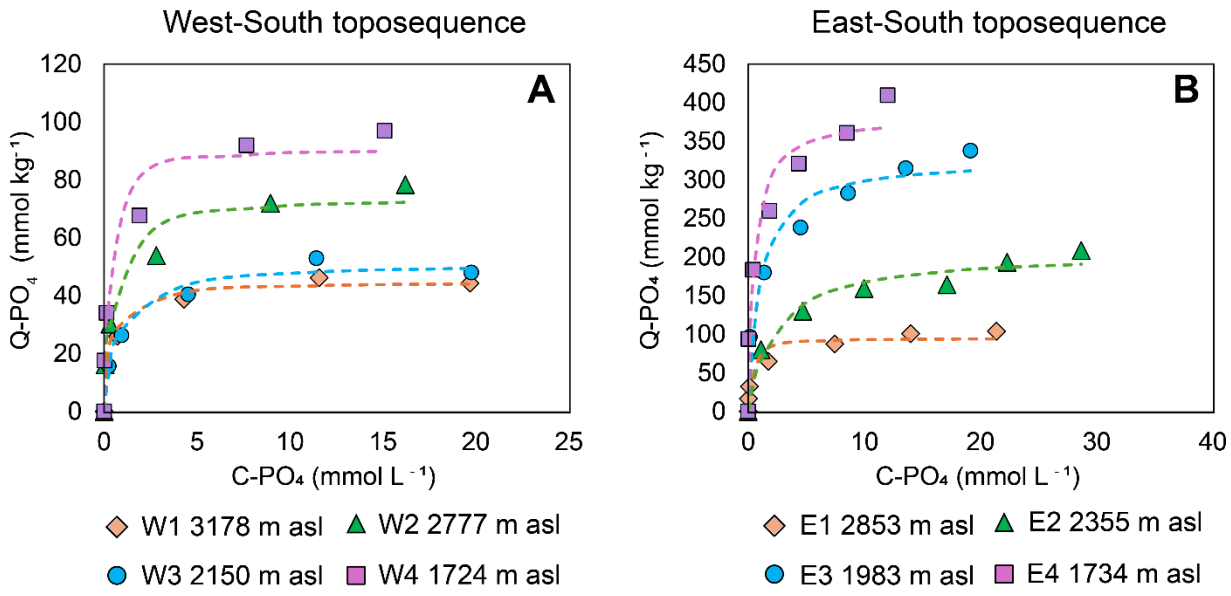

Figure 2. 6. Phosphate (PO_4^{3-}) adsorption isotherms for topsoils samples collected from the West-South (WS) (A) and East-South (ES) (B) toposequences on the southern flank of Irazú volcano, Costa Rica. Altitude in masl is provided for each sample below the graphs. The isotherms were conducted with a solution-solid ratio (SSR) of 10 L kg^{-1}, a background electrolyte solution of 0.05 M NaNO3 and a pH of 5.30 ± 0.30. Symbols are for experimental data and the dotted lines represent the modeled values obtained with the Langmuir equation (Eq. 1), adjusting the values of maximum adsorption capacity (Q_{max}) and the Langmuir affinity constant (K_L).

Table 2. 1. Maximum adsorption capacity (Qmax) and affinity constant (KL), with the corresponding standard errors (SE) values, fitted with the Langmuir equation for the adsorption isotherms of phosphate determined in the topsoil samples from the West- South (WS) and East-South (ES) toposequences on the southern flank of Irazú volcano, Costa Rica. Statistical parameters including Root Mean Square Error (**RMSE**), Mean Squared Error (**MSE**), Mean Absolute Error (**MAE**) and Chi-squared statistic (**Chi-sq**) for the fitted model are also provided.

Sample	Q_{max}	SE	K_L	SE	RMSE	MSE	MAE	Chi-sq
W1	49.09	2.93	1.82	0.64	5.83	34.03	3.84	14.22

W2	80.63	4.70	1.52	0.54	8.34	69.55	6.26	49.72
W3	61.13	6.17	0.74	0.36	9.64	92.93	6.10	28.47
W4	98.09	5.52	2.99	1.19	10.83	117.37	7.56	71.24
E1	95.27	5.13	3.65	1.60	11.30	127.60	8.90	76.19
E2	206.23	8.27	0.43	0.09	12.51	156.46	10.66	17.11
E3	327.42	16.21	1.02	0.29	27.21	740.61	20.15	NaN*
E4	384.71	21.04	1.94	0.60	36.56	1336.89	28.71	448.12

NaN*: Not a Number, indicates undefined or invalid numerical result.

In the **Figure 2.7** it was observed the data of PO_4^{3-} adsorption normalized to the molar content of [Fe_{ox}+Al_{ox}], which is a proxy for the amount of Fe and Al present in soils as SRO minerals. In the WS toposequence, soils W2 and W1 presented higher PO_4^{3-} adsorption per mol of [Fe_{ox} + Al_{ox}] compared to the soil W3. In contrast, the soils from the ES toposequence exhibited more consistent PO_4^{3-} sorption capacity across sites, with less variation in P adsorption per mol [Fe_{ox} + Al_{ox}] than soils from the WS toposequence.

For soil W4, PO_4^{3-} adsorption was normalized using the dithionite-citrate (DC)-extractable Fe content rather than the ammonium oxalate extractable Fe. This choice was motivated due to the advanced weathering stage of the soil, in which most pedogenic Fe (hydr)oxides have been transformed into crystalline Fe (hydr)oxides (see Chapter 1).

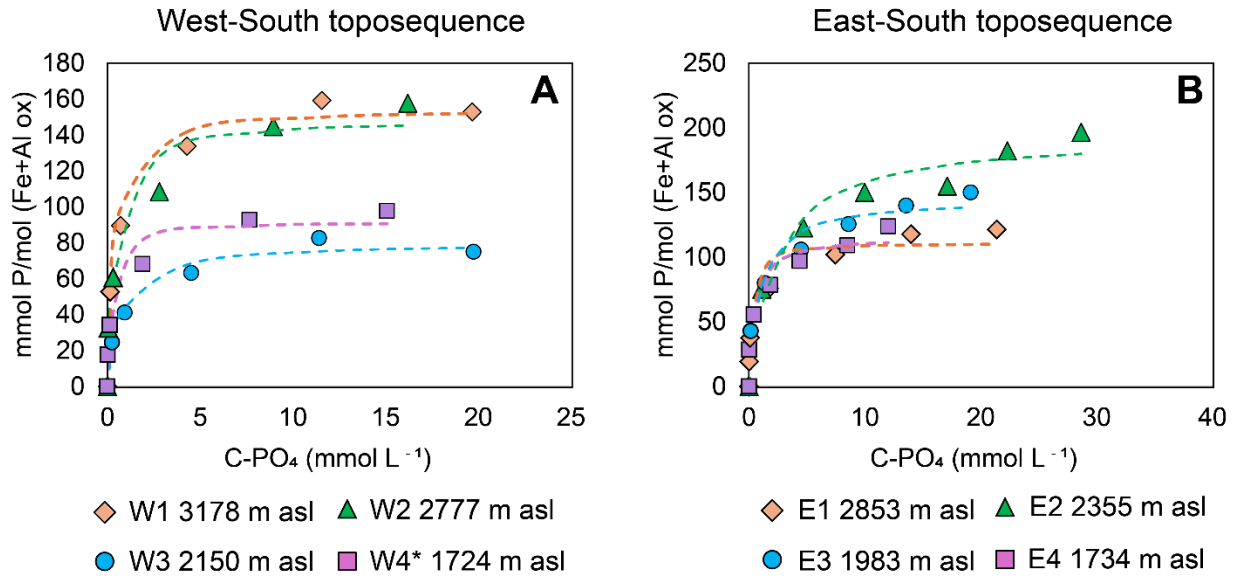

Figure 2. 7. Adsorption isotherms of mmol P per mmol Fe + Al (Fe and Al extracted using a 0.2 M ammonium oxalate solution, with the exception of the soil W4 which Fe was extracted with Dithionite Citrate solution), plotted against PO_4^{3-} in equilibrium of topsoils of West-South (WS) (**A**) and East-South (ES) (**B**) toposequences on the southern flank of Irazú volcano, Costa Rica. Symbols are for experimental data and the dotted lines represent the modeled values obtained with the Langmuir equation (Eq. 1), adjusting the values of maximum adsorption capacity (Qmax) and the Langmuir affinity constant (K_L). *Soil W4= mmolP/mol (Fe_{dc}+Al_{ox}).

3.3.4. Effect of Ca^{2+} on PO_4^{3-} adsorption

The **Figure 2.8** presented the PO_4^{3-} adsorption isotherms of selected soil samples measured with and without the addition of $Ca(NO_3)_2$ to the electrolyte solution. The corresponding Langmuir model parameters (Q_{max} and K_L) are shown in **Table 2.2**. Overall, the results indicated that the presence of Ca^{2+} consistently enhanced PO_4^{3-} sorption capacity in all tested samples. Relatively, the observed effect of Ca^{2+} on enhancing PO_4^{3-} adsorption was more pronounced in soils W1, W2 and E1 compared to the soil E3 (**Table 2.2**).

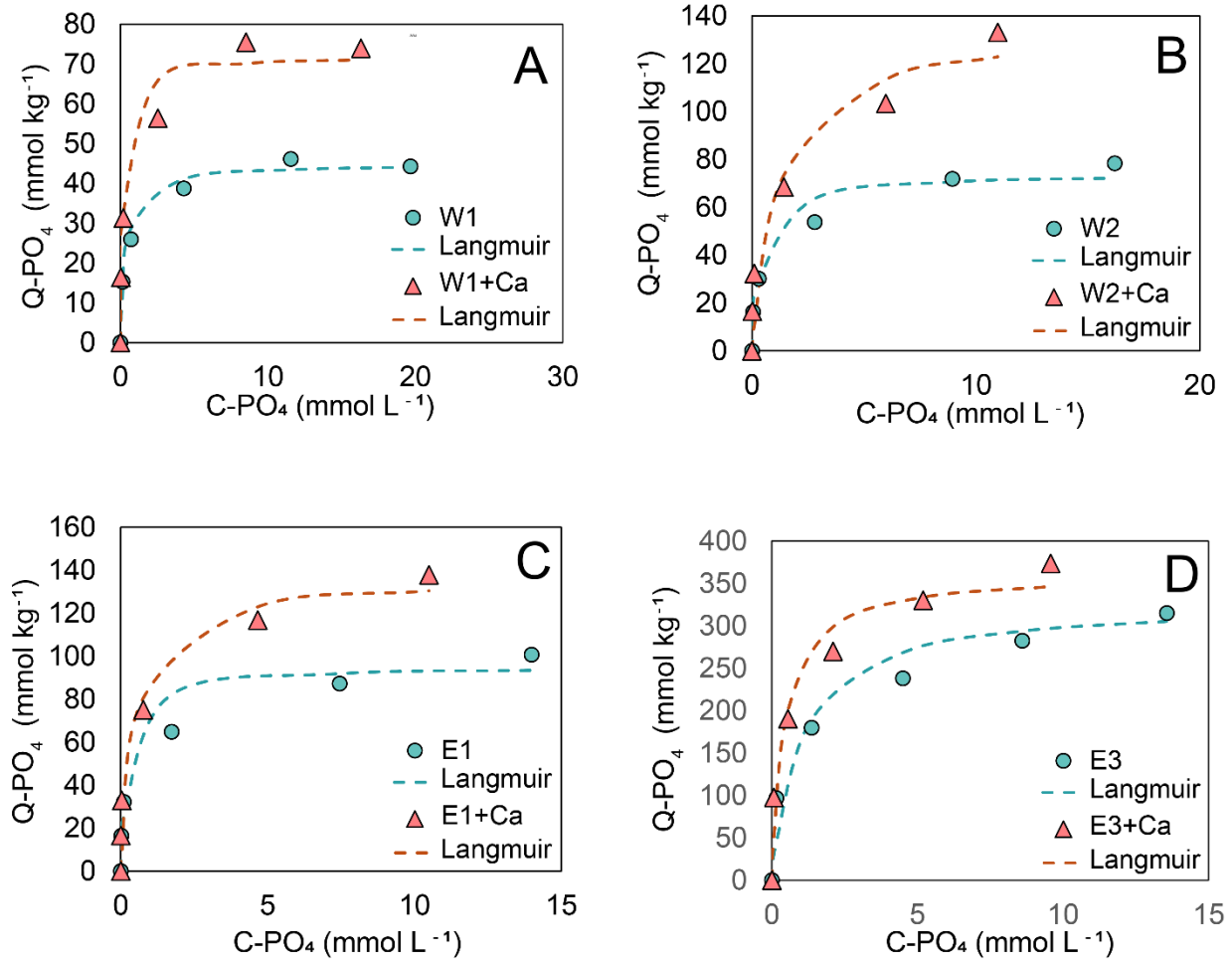

Figure 2. 8. Phosphate (PO_4^{3-}) adsorption isotherms of selected topsoils with and without the addition of $Ca(NO_3)_2$ 0.01 M as a background electrolyte solution together with NaNO3 0.05 M, and a fixed pH ranged of 5.40 ± 0.15 , from the West-South (W1 **A** and W2 **B**) and the East-South (E1 **C** and E3 **D**) toposequences, located on the southern flank of Irazú volcano, Costa Rica. The soils were selected based on contrasting adsorption capacities. Symbols are for experimental data and the dotted lines represent the modeled values obtained with the Langmuir equation (Eq. 1).

Table 2. 2. Maximum adsorption capacity (Qmax) and affinity constant (KL), with the corresponding standard errors (SE) values, fitted with the Langmuir equation for the adsorption isotherms of phosphate (PO_4^{3-}) with and without the addition of Ca, determined in the topsoils W1 and W2 from the West-South (WS) and E1 and E3 from the East-South (ES) toposequences, located at the southern flank of Irazú volcano, Costa Rica. Statistical parameters including Root Mean Square Error (**RMSE**), Mean Squared Error (**MSE**), Mean Absolute Error (**MAE**) and Chi-squared statistic (**Chi-sq**) for the fitted model are also provided.

Sample	Q_{max}	SE	K_L	SE	RMSE	MSE	MAE	Chi-sq	ΔQmax (%) due to Ca addition
W1	49.09	2.93	1.82	0.64	5.83	34.03	3.84	14.22	66.57
W1+Ca	81.77	5.45	4.13	1.71	6.68	44.66	5.29	14.49	
W2	80.63	4.70	1.52	0.54	8.34	69.55	6.26	49.72	92.79
W2+Ca	155.45	22.38	0.81	0.51	14.07	198.04	11.69	191.27	
E1	95.27	5.13	3.65	1.60	11.30	127.60	8.90	76.19	64.42
E1+Ca	156.64	17.48	1.85	1.09	14.49	209.91	11.23	314.71	
E3	327.42	16.21	1.02	0.29	27.21	740.61	20.15	NaN	6.46
E3+Ca	348.58	26.36	2.22	0.87	25.07	628.26	19.01	52.69	

ΔQ_{max} (%) values of the adsorption isotherms with and without Ca, calculated as: (Q_{max} isotherm +Ca – Q_{max} isotherm without Ca)/ Q_{max} isotherm without Ca. NaN*: Not a Number, indicates undefined or invalid numerical result.

3.4. DISCUSSION

3.4.1. RSA, PO_4^{3-} sorption capacity and P availability

The higher content of P_{OX}, RSA (**Tables S2.2 and S2.3**), and PO_4^{3-} sorption capacity (see Q_{max} values in **Table 2.1**) for soils from the ES toposequence, compared to the WS toposequence, can be related to the higher content of SRO aluminosilicates which provide greater abundance of PO_4^{3-} sorption sites in these soils. As previously described in Chapter 1, SRO minerals are highly reactive towards oxyanions such as phosphate and are abundant in volcanic soils (Takahashi and Dahlgren 2016; Nanzyo 2002; Strawn 2015; Mwende Muindi 2019). Phosphate adsorption in these soils occurs primarily via inner-sphere complexation, where phosphate forms strong chemical bonds with surface functional groups on SRO minerals, limiting its bioavailability (Qafoku and Sumner 2000; Selim 2018), further supported by the low proportion of available phosphorus (P-Olsen), which rarely exceeded 10% of total P_{ox} (**Figure 2.4**) and it was inversely correlated with the PRC (**Figure 2.5**).

Additionally, the higher content of P_{ox} found in surface horizons, compared with deeper horizons, of soils from both toposequences (**Figure 2.2**) suggests an influence from land use practices, particularly P fertilization (Alvarado-Hernandez *et al*. 2008). Moreover, P_{ox} normalized to the molar content of $[Fe+Al]_{ox}$ decreased from the surface to about 50 cm depth (**Figure S2.4)**, also

suggests that the higher P_{ox} levels in the topsoil are not due to greater amounts of reactive minerals but are more likely linked to external P inputs.

Differences in the content of SRO minerals, particularly SRO aluminosilicates, which influence PO_4^{3-} adsorption in both toposequences, are driven by their contrasting soil moisture regimes (Udic vs. Ustic), as discussed in Chapter 1. Volcanic soils developed under consistently humid conditions (i.e. Udic moisture regime) tend to favor the formation and preservation of SRO minerals (Watanabe *et al*. 2023; Candra *et al*. 2019; Tsai *et al*. 2010; Dinter *et al*. 2020), whereas drier conditions (i.e. Ustic moisture regimes) promote the transformation of SRO minerals into more crystalline mineral phases (Zehetner *et al*. 2003; Watanabe *et al*. 2023).

In the ES toposequence, the consistent Udic moisture regime promotes the weathering of the primary minerals, and the persistence of SRO minerals formed *in-situ*. Additionally, increasing mean temperatures might further enhance SRO formation under constant Udic conditions, reflected by the increase in SRO content with decreasing altitude in the ES toposequence. Thus, higher RSA of soils (**Figure 2.1**) and greater PO_4^{3-} adsorption capacity (**Figure 2.6 B; Table 2.1**).

In contrast, the WS toposequence experiences a transition from Udic to Ustic conditions along its slope. This transition favors the transformation of SRO minerals into more crystalline and less reactive phases, reducing their capacity to adsorb PO_4^{3-} (Gérard 2016; Strauss *et al*. 2005; Qin *et al*. 2018; Stoner *et al*. 2012). As a result, the increasing trends in PO_4^{3-} adsorption and RSA observed in the ES toposequence are not present in the WS toposequence (**Figure 2.6 A; Table 2.1**).

Similar patterns have been reported in other volcanic toposequences, where high PO_4^{3-} adsorption capacity is related with elevated levels of active Al associated with SRO aluminosilicates (Van Ranst *et al*. 2004; Hashimoto *et al*. 2012). For example, Van Ranst *et al*. (2004) reported that on Java Island, Indonesia, soils exhibiting higher PO_4^{3-} adsorption capacity were associated with a Udic soil moisture regime and elevated allophane content, particularly at elevations between 1250 and 1600 m asl. Likewise, Hashimoto *et al*. (2021) reported that Andisols in Japan presented a higher PO_4^{3-} sorption capacity when the oxalate-extractable Al and allophane content were also higher.

3.4.2. Phosphate sorption isotherms normalized by the sum of Fe and Al extracted with oxalate

When PO_4^{3-} adsorption data are normalized to the molar sum of Fe and Al extracted with oxalate $[Fe+Al]_{ox}$ (**Figure 2.7 B**), the differences in adsorption capacity between soils from the ES

toposequences largely disappear compared to when the adsorption is expressed on a soil mass basis (**Figure 2.6**). This suggests that the increase of adsorption capacity at lower altitudes is driven by enhanced weathering and formation of SRO minerals, and changes in their intrinsic adsorption properties like particle size and surface site density. The consistent Udic moisture regime and uniform parent material along the toposequence likely contribute to maintaining relatively similar reactive properties of the SRO minerals, such as particle size, surface site density, and intrinsic affinity for phosphate.

In contrast to the ES toposequence, normalization of PO_4^{3-} adsorption data to $[Fe+Al]_{ox}$ in soils from the WS toposequence (**Figure 2.7 A**) reveals that differences in adsorption capacity persist, showing an inverse trend compared to the corresponding adsorption data expressed on a soil mass basis (**Figure 2.6 A**). The notably lower PO_4^{3-} adsorption capacity per unit of Fe and Al in soils under an Ustic regime suggests the presence of reactive minerals with larger particle sizes and, consequently, lower reactive surface areas (RSA), likely reflecting the transformation of SRO minerals into more crystalline and less reactive forms (Wang *et al*. 2013; McLaughlin *et al*. 1981; Amadou *et al*. 2022). This observation is particularly evidenced in the soil W4, where more crystalline Fe phases (Fe_{dc}) appear to significantly contribute to PO_4^{3-} adsorption. In this case, nanocrystalline Fe oxides are likely to have transformed into more crystalline forms (Wang *et al*. 2018; Neto *et al*. 2004; Rechberger *et al*. 2021). Interestingly, WS soils formed under Udic conditions exhibited adsorption behavior like those of the ES toposequence, highlighting the critical role of soil moisture in sustaining SRO minerals with comparable PO_4^{3-} sorption properties.

3.4.3. Effect of the addition of Ca in PO_4^{3-} sorption capacity

The results showed a general increase in PO_4^{3-} sorption capacity upon Ca^{2+} addition (**Figure 2.8**), likely due to cooperative adsorption mechanisms in which Ca^{2+} facilitates PO_4^{3-} binding through electrostatic interactions and the formation of ternary surface complexes (Mendez and Hiemstra 2020). A similar synergistic effect has also been reported in volcanic soils from the Galápagos Islands, specifically in younger topsoils with high exchangeable Ca^{2+} levels >100 $cmol_c\ kg^{-1}$ (Rechberger *et al*. 2021). However, this effect appears to be modulated by the reactivity of SRO minerals in the soils. Samples with lower sorption capacity (W1, W2 and E1), lower content of SRO aluminosilicates, and a lower RSA, presented a higher relative increase in PO_4^{3-} adsorption following Ca^{2+} addition compared to soils with high mineral reactivity (i.e. E4).

This can be related to the fact that soils with larger surface reactivity already have a high PO_4^{3-} adsorption capacity and a relatively low PO_4^{3-} adsorption density, leaving more surface sites available for PO_4^{3-} adsorption, limiting the incremental effect of Ca^{2+}. Conversely, soils with lower

SRO content and RSA are more responsive to the formation of ternary complexes when Ca^{2+} is added, which enhance phosphate binding despite their initially lower reactivity (Mendez and Hiemstra 2020).

3.4.4. Implications

From a practical perspective, these findings have important implications for soil management. Even within a single soil type, such as Andisols, heterogeneity can exist. Factors like altitude and soil moisture regime significantly influence the formation of SRO minerals, which consequently affect their content, composition, and RSA. These variations ultimately modulate the sorption capacity and availability of phosphate (PO_4^{3-}) in the soils. In addition, mineralogical differences can also shape the impact of other agricultural management practices such as liming, which is commonly applied to volcanic soils in the study area. It was evidenced that the addition of Ca^{2+} can enhance the PO_4^{3-} sorption in these soils. However, further investigations in land use management in the field should be carried out to understand better the impact of agricultural practices on P behavior in the agricultural systems of the region.

3.5. CONCLUSION

This study showed that differences in PO_4^{3-} adsorption among soil toposequences are mainly controlled by the abundance and surface reactivity of short-range order (SRO) minerals. These are influenced by soil moisture regimes, together with altitude and temperature, which regulate weathering intensity. Higher humidity promotes the formation of SRO aluminosilicates, and under humid (Udic) conditions, both adsorption capacity and reactive surface area increased with decreasing altitude, reflecting greater SRO mineral accumulation along the gradient.

The study revealed that P availability, reflected by the P-Olsen/Pox ratio, is generally low in these volcanic soils due to strong PO_4^{3-} sorption onto reactive SRO minerals rather than total P content. Additionally, Ca^{2+} can enhance PO_4^{3-} retention via cooperative adsorption mechanisms, though its effect is limited in soils with already high sorption capacity, such as the E3 topsoil from the ES toposequence.

In general, the results underscore the importance of considering both mineralogical properties and environmental factors, such as altitude and moisture regime, when managing P behavior in volcanic soils. Despite soils presented similar taxonomical classifications within these two toposequences, they exhibit marked differences in P behavior due to contrasting mineral contents driven by the soil moisture regime and weathering intensities. These differences could influence

the response of soils to fertilization and liming practices, pointing to the need for site-specific nutrient management strategies.

3.6. REFERENCES

Alvarado-Hernandez, A; McHugh, A; Laura, R; Brenes, L; Pujol, R. 2008. Indicadores para estimar la sostenibilidad agrícola de la cuenca media del río Reventado, Cartago, Costa Rica. Agronomía Costarricense 32. DOI: https://doi.org/10.15517/rac.v32i2.6758.

Amadou, I; Faucon, M-P; Houben, D. 2022. Role of soil minerals on organic phosphorus availability and phosphorus uptake by plants. Geoderma 428:116125. DOI: https://doi.org/10.1016/j.geoderma.2022.116125.

Blakemore, L.C., Searle, P.L. and Daly, B.K. (1987) Methods for chemical analysis of soils. N. Z. Soil Bureau Scientific Report 80, Soil Bureau, Lower Hutt, 38-41. - References - Scientific Research Publishing. 2025. Consulted at 24 jul. 2025. Disponible en https://www.scirp.org/reference/referencespapers?referenceid=921823.

Candra, IN; Gerzabek, MH; Ottner, F; Tintner, J; Wriessnig, K; Zehetner, F. 2019. Weathering and soil formation in rhyolitic tephra along a moisture gradient on Alcedo Volcano, Galápagos. Geoderma 343:215-225. DOI: https://doi.org/10.1016/j.geoderma.2019.01.051.

Chiu, C-Y; Baillie, I; Jien, S-H; Hallett, L; Hallett, S. 2021. Sequestration of P fractions in the soils of an incipient ferralisation chronosequence on a humid tropical volcanic island. Botanical Studies 62(1):20. DOI: https://doi.org/10.1186/s40529-021-00326-5.

Cornell, RM; Schwertmann, U. 2003. The Iron Oxides: Structure, Properties, Reactions, Occurrences and Uses. s.l., John Wiley & Sons. 714 p.

Dinter, TC; Gerzabek, MH; Puschenreiter, M; Strobel, BW; Strahlhofer, M; Couenberg, PM; Zehetner, F. 2020. Changes in topsoil characteristics with climate and island age in the agricultural zones of the Galápagos. Geoderma 376:114534. DOI: https://doi.org/10.1016/j.geoderma.2020.114534.

Elzinga, EJ; Sparks, DL. 2007. Phosphate adsorption onto hematite: an in situ ATR-FTIR investigation of the effects of pH and loading level on the mode of phosphate surface complexation. Journal of Colloid and Interface Science 308(1):53-70. DOI: https://doi.org/10.1016/j.jcis.2006.12.061.

Fallas-Corrales, RA; Mendez, JC; Meeussen, JCL. 2025. Boron Adsorption and Interaction With Phosphate in a Volcanic Soil From the Humid Tropic (online). Journal of Plant Nutrition and Soil Science n/a(n/a). DOI: https://doi.org/10.1002/jpln.70012.

Gérard, F. 2016. Clay minerals, iron/aluminum oxides, and their contribution to phosphate sorption in soils — A myth revisited. Geoderma 262:213-226. DOI: https://doi.org/10.1016/j.geoderma.2015.08.036.

Goldberg, S; Sposito, G. 1985. On the mechanism of specific phosphate adsorption by hydroxylated mineral surfaces: A review. Communications in Soil Science and Plant Analysis 16(8):801-821. DOI: https://doi.org/10.1080/00103628509367646.

Hashimoto, Y; Kang, J; Matsuyama, N; Saigusa, M. 2012. Path Analysis of Phosphorus Retention Capacity in Allophanic and Non-allophanic Andisols. Soil Science Society of America Journal 76(2):441-448. DOI: https://doi.org/10.2136/sssaj2011.0196.

Hiemstra, T; Antelo, J; Rahnemaie, R; Riemsdijk, WH van. 2010. Nanoparticles in natural systems I: The effective reactive surface area of the natural oxide fraction in field samples. Geochimica et Cosmochimica Acta 74(1):41-58. DOI: https://doi.org/10.1016/j.gca.2009.10.018.

Jahinge, THL; Payne, MK; Unruh, DK; Jayasinghe, AS; Yu, P; Forbes, TZ. 2023. Characterization of Water Structure and Phase Behavior within Metal–Organic Nanotubes. Langmuir 39(51):18899-18908. DOI: https://doi.org/10.1021/acs.langmuir.3c02786.

Keizer, M; Van Riemsdijk, WH. 1998. ECOSAT. Department of Environmental Science, Subdepartment Soil Science and Plant Nutrition. Wageningen Agricultural University, Wageningen, Netherlands.

Kinniburgh D.G. 1993. FIT User Guide, Technical Report WD/93/ 23., Keyworth.

Koopmans, GF; Hiemstra, T; Vaseur, C; Chardon, WJ; Voegelin, A; Groenenberg, JE. 2020. Use of iron oxide nanoparticles for immobilizing phosphorus in-situ: Increase in soil reactive surface area and effect on soluble phosphorus. Science of The Total Environment 711:135220. DOI: https://doi.org/10.1016/j.scitotenv.2019.135220.

Langmuir, I. 1918. The adsorption of gases on plane surfaces of glass, mica and platinum. Journal of the American Chemical Society 40(9):1361-1403. DOI: https://doi.org/10.1021/ja02242a004.

Manceau, A; Gates, WP. 1997. Surface Structural Model for Ferrihydrite. Clays and Clay Minerals 45(3):448-460. DOI: https://doi.org/10.1346/CCMN.1997.0450314.

McLaughlin, JR; Ryden, JC; Syers, JK. 1981. Sorption of Inorganic Phosphate by Iron- and Aluminium- Containing Components. Journal of Soil Science 32(3):365-378. DOI: https://doi.org/10.1111/j.1365-2389.1981.tb01712.x.

Mendez, JC; Hiemstra, T. 2020. Ternary Complex Formation of Phosphate with Ca and Mg Ions Binding to Ferrihydrite: Experiments and Mechanisms. ACS Earth and Space Chemistry XXXX. DOI: https://doi.org/10.1021/acsearthspacechem.9b00320.

Mendez, JC; Hiemstra, T; Koopmans, GF. 2020. Assessing the Reactive Surface Area of Soils and the Association of Soil Organic Carbon with Natural Oxide Nanoparticles Using Ferrihydrite as Proxy. Environmental Science & Technology 54(19):11990-12000. DOI: https://doi.org/10.1021/acs.est.0c02163.

Murphy, J; Riley, JP. 1962. A modified single solution method for the determination of phosphate in natural waters. Analytica Chimica Acta 27:31-36. DOI: https://doi.org/10.1016/S0003-2670(00)88444-5.

Mwende Muindi, E. 2019. Understanding Soil Phosphorus. International Journal of Plant & Soil Science 31(2):1-18. DOI: https://doi.org/10.9734/IJPSS/2019/v31i230208.

Nanzyo, M. 2002. Unique properties of volcanic ash soils. Glob. Environ. Res. 6.

Nanzyo, M; Kanno, H. 2018. Primary Minerals. In Nanzyo, M; Kanno, H (eds.). Singapore, Springer. p. 11-35. DOI: https://doi.org/10.1007/978-981-13-1214-4_2.

Neall, V. 2006. Volcanic soils. Land Use and Land Cover, Encyclopaedia of Life Support Systems (EOLSS).

Neto, FCR; Schaefer, CEGR; Costa, LM; Corrêa, MM; Filho, EIF; Ibraimo, MM. 2004. Phosphorus adsorption, specific surface, and mineralogical attributes of soils developed from volcanic rocks from the Upper Paranaíba, MG (Brazil). Rev. Bras. Ciênc. Solo 28(6):953-964. DOI: https://doi.org/10.1590/S0100-06832004000600003.

Nizeyimana, E; Bicki, TJ; Agbu, PA. 1997. An assessment of colloidal constituents and clay mineralogy of soils derived from volcanic materials along a toposequence in Rwanda. Soil Science 162(5):361.

Olsen, SR. 1954. Estimation of Available Phosphorus in Soils by Extraction with Sodium Bicarbonate. s.l., U.S. Department of Agriculture. 20 p.

Qafoku, N; Sumner, M. 2000. Mineralogy and chemistry of some variable charge subsoils. Communications in Soil Science and Plant Analysis 31:1051-1070. DOI: https://doi.org/10.1080/00103620009370497.

Qafoku, N; Van Ranst, E; Noble, A; Baert, G. 2004. Variable Charge Soils: Their Mineralogy, Chemistry and Management. Advances in Agronomy 84:159-215. DOI: https://doi.org/10.1016/S0065-2113(04)84004-5.

Qin, Z; Shober, AL; Scheckel, KG; Penn, CJ; Turner, KC. 2018. Mechanisms of phosphorus removal by phosphorus sorbing materials. Journal of Environmental Quality 47(5):1232-1241. DOI: https://doi.org/10.2134/jeq2018.02.0064.

Rechberger, MV; Zehetner, F; Gerzabek, MH. 2021. Phosphate sorption-desorption properties in volcanic topsoils along a chronosequence and a climatic gradient on the Galápagos Islands. Journal of Plant Nutrition and Soil Science 184(4):479-491. DOI: https://doi.org/10.1002/jpln.202000488.

Sato, K; Hama, T; Ito, H; Kobayashi, K; Nakamura, K; Sakurai, S. 2024. Long-term stability of phosphate sorbed on an allophanic Andosol and a synthesized allophane. Soil Science Society of America Journal 88(6):1932-1941. DOI: https://doi.org/10.1002/saj2.20748.

Selim, HM. ed. 2018. Phosphate in Soils: Interaction with Micronutrients, Radionuclides and Heavy Metals. Boca Raton, CRC Press. 381 p. DOI: https://doi.org/10.1201/9781351228909.

Soil Survey Staff. 2022. Keys to Soil Taxonomy, 13th ed. USDA-Natural Resources Conservation Service.

Stoner, D; Penn, C; McGrath, J; Warren, J. 2012. Phosphorus removal with by-products in a flow-through setting. Journal of Environmental Quality 41(3):654-663. DOI: https://doi.org/10.2134/jeq2011.0049.

Strauss, R; Brümmer, GW; Barrow, NJ. 2005. Effects of crystallinity of goethite: II. Rates of sorption and desorption of phosphate. European Journal of Soil Science 48:101-114. DOI: https://doi.org/10.1111/j.1365-2389.1997.tb00189.x.

Strawn. 2015. Soil Chemistry, 4th Edition. 4 ed. Newark, Wiley-Blackwell. 394 p.

Takahashi, T; Dahlgren, RA. 2016. Nature, properties and function of aluminum–humus complexes in volcanic soils. Geoderma 263:110-121. DOI: https://doi.org/10.1016/j.geoderma.2015.08.032.

Tsai, CC; Chen, ZS; Kao, CI; Ottner, F; Kao, SJ; Zehetner, F. 2010. Pedogenic development of volcanic ash soils along a climosequence in Northern Taiwan. Geoderma 156(1-2):48-59. DOI: https://doi.org/10.1016/j.geoderma.2010.01.007.

Van Ranst, E; Mees, F; De Grave, E; Ye, L; Cornelis, J-T; Delvaux, B. 2019. Impact of andosolization on pedogenic Fe oxides in ferrallitic soils. Geoderma 347:244-251. DOI: https://doi.org/10.1016/j.geoderma.2019.04.013.

Van Ranst, E; Utami, SR; Vanderdeelen, J; Shamshuddin, J. 2004. Surface reactivity of Andisols on volcanic ash along the Sunda arc crossing Java Island, Indonesia. Geoderma 123(3):193-203. DOI: https://doi.org/10.1016/j.geoderma.2004.02.005.

Wang, L; Putnis, CV; Hövelmann, J; Putnis, A. 2018. Interfacial Precipitation of Phosphate on Hematite and Goethite. Minerals 8(5):207. DOI: https://doi.org/10.3390/min8050207.

Wang, X; Li, W; Harrington, R; Liu, F; Parise, JB; Feng, X; Sparks, DL. 2013. Effect of Ferrihydrite Crystallite Size on Phosphate Adsorption Reactivity. Environmental Science & Technology 47(18):10322-10331. DOI: https://doi.org/10.1021/es401301z.

Watanabe, T; Ueda, S; Nakao, A; Ze, AM; Dahlgren, RA; Funakawa, S. 2023. Disentangling the pedogenic factors controlling active Al and Fe concentrations in soils of the Cameroon volcanic line. Geoderma 430:116289. DOI: https://doi.org/10.1016/j.geoderma.2022.116289.

Zehetner, F; Rosenfellner, U; Mentler, A; Gerzabek, MH. 2003. Distribution of organic and inorganic phosphorus in a forested Andisol. Soil Science Society of America Journal 67(1):159–166. DOI: https://doi.org/10.2136/sssaj2003.1590.

Zheng, T-T; Sun, Z-X; Yang, X-F; Holmgren, A. 2012. Sorption of phosphate onto mesoporous γ-alumina studied with in-situ ATR-FTIR spectroscopy. Chemistry Central Journal 6(1):26. DOI: https://doi.org/10.1186/1752-153X-6-26.

Zhong, B; Stanforth, R; Wu, S; Chen, JP. 2007. Proton interaction in phosphate adsorption onto goethite. Journal of Colloid and Interface Science 308(1):40-48. DOI: https://doi.org/10.1016/j.jcis.2006.12.055.

3.7. SUPLEMENTARY INFORMATION

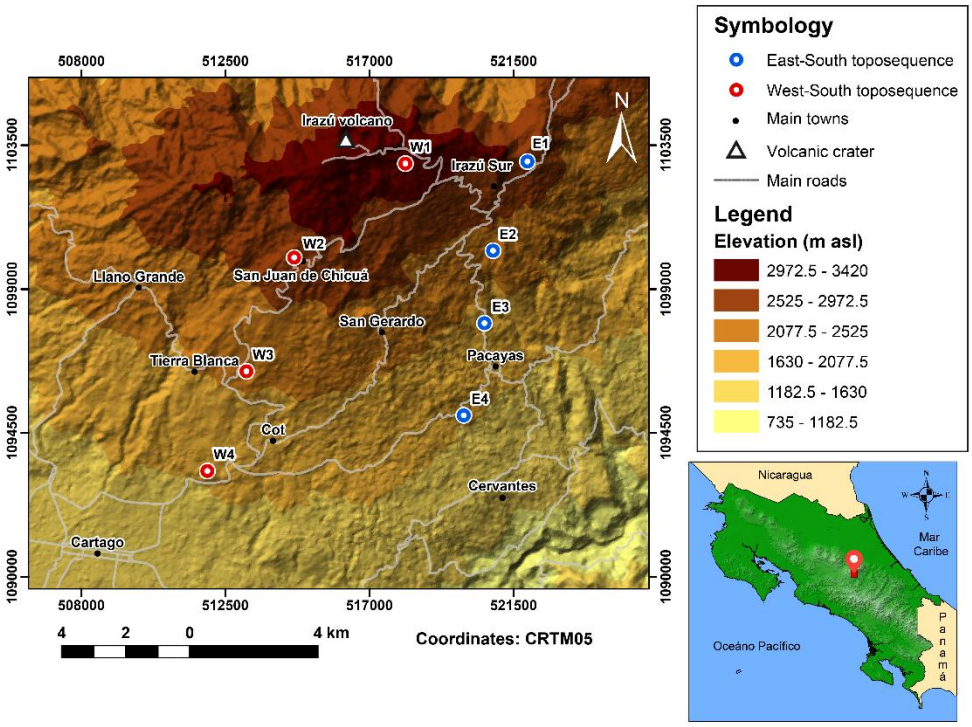

Figure S2. 1. Location of the soil sequences in the study area along the altitudinal profile in the southern flank of Irazú volcano, Costa Rica. East-South toposequence (blue dots) and West-South toposequences (red dots).

Table S2. 1. General characteristics of the sampled sites within two soil sequences located at the southern flank of Irazú volcano.

Profile	Depth (cm)	Elevation (m asl)	Anual average temperature (ºC)	Anual average precipitation (mm)	Soil order[a]	Moisture regime
West-South toposequence						
W1	0-80	3178	8 - 10	2000 – 3000	Entisol	Udic
W2	0-240	2777	10 – 12	1500 – 2000	Andisol	Udic
W3	0-120	2150	14 – 16	< - 1500	Andisol	Ustic
W4	0-70	1724	16 – 18	< - 1500	Alfisol	Ustic

East-South toposequence						
E1	0-96	2853	12 – 14	2000 – 3000	Andisol	Udic
E2	0-110	2355	14 – 16	2000 – 3000	Andisol	Udic
E3	0-120	1983	16 – 18	2000 – 3000	Andisol	Udic
E4	0-120	1734	16 – 18	2000 – 3000	Andisol	Udic

[a] According to the Soil Taxonomy (Soil Survey Staff 2022)

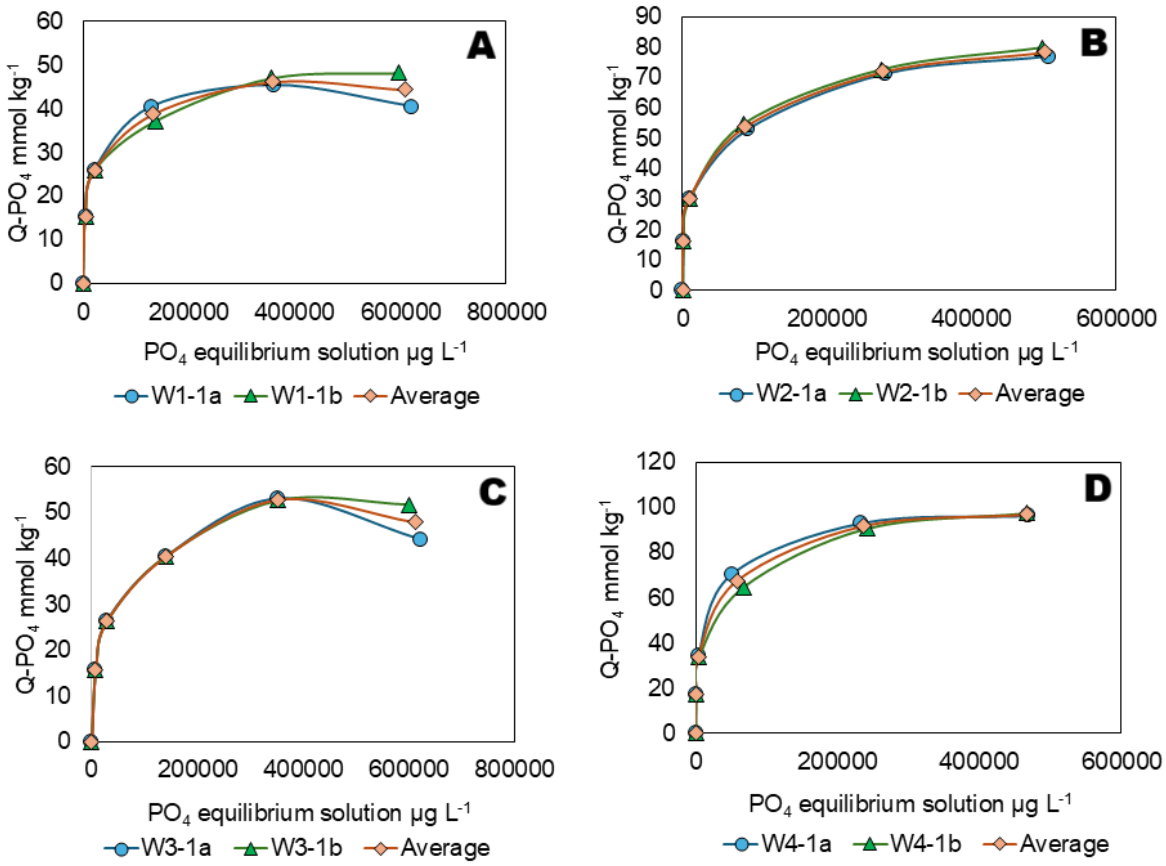

Figure S2. 2. Results of the duplicates and the average graph of phosphate sorption isotherms data of topsoils W1-1 (**A**), W2-1 (**B**), W3-1 (**C**) and W4-1 (**D**) from the West-South toposequence on the southern flank of Irazú volcano, Costa Rica.

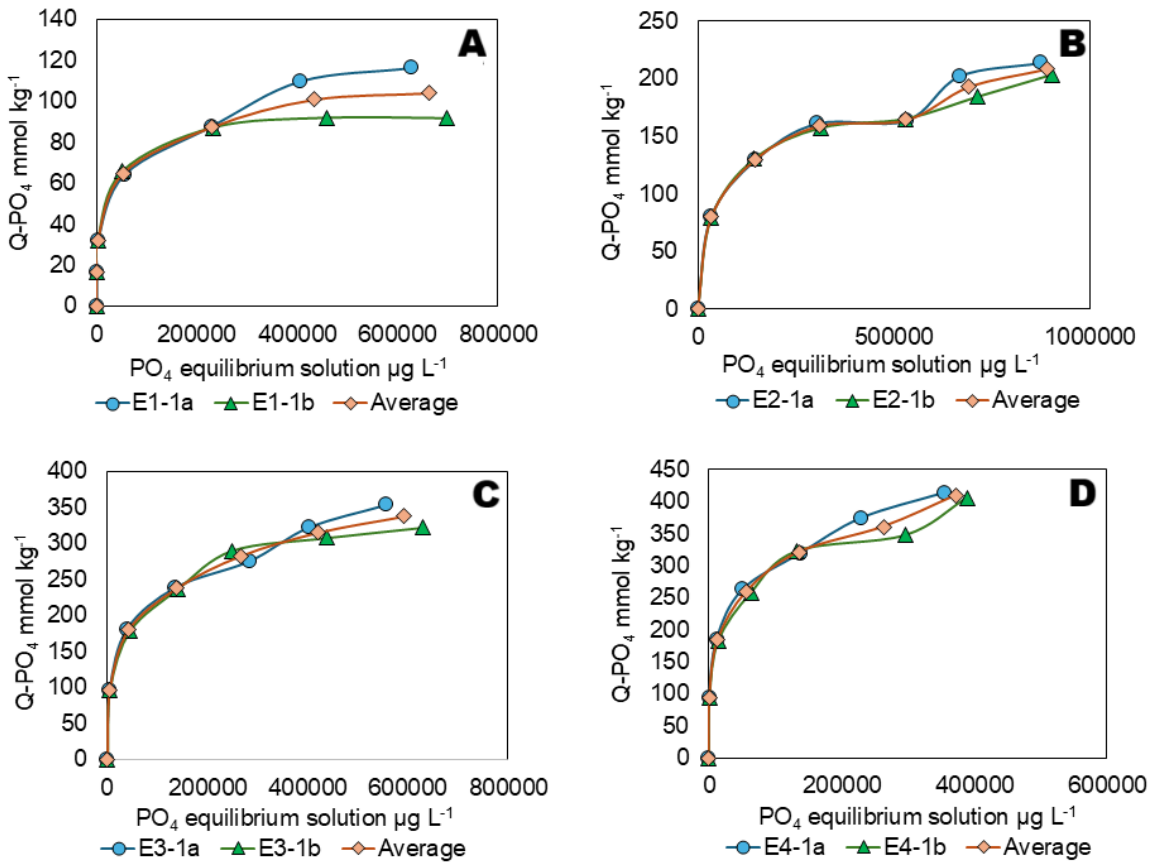

Figure S2. 3. Results of the duplicates and the average graph of phosphate sorption isotherms data of topsoils E1-1 (**A**), E2-1 (**B**), E3-1 (**C**) and E4-1 (**D**) from the East-South toposequence on the southern flank of Irazú volcano, Costa Rica.

Table S2. 2. Contents and ratios of aluminum (Alox), iron (Feox), phosphorus (Pox), phosphate ($P\text{-}PO_{4,ox}$) and silicon (Siox) Extracted with a 0.2 M ammonium oxalate (ox), aluminum (Alpy) extracted with 0.1 M sodium pyrophosphate, iron (Fedc) extracted with Dithionite-Citrate, phosphate ($P\text{-}PO_{4,ox}$) extracted with Olsen, and the reactive surface area (RSA) of Soil Profiles from the East-South toposequence.

West-South toposequence (WS)										
Sample ID	Depth (cm)	mmol kg^{-1} of soil								RSA
		Al_{py}	Al_{ox}	Fe_{ox}	Si_{ox}	P_{ox}	$P\text{-}PO_4^{3-}$ (ox)	Fe_{dc}	P-PO$_4$ Olsen	m^2/kg
3178 m asl										
W1-1	0-14	150	179	110.8	50.5	18	21.5	102.1	1.66	15.09
W1-2	14-40	160.8	156.6	114.8	44.7	12	13.0	117.8	0.70	7.46
W1-3	40-60	128.9	315.2	133.4	117	6	7.0	113.5	-	11.62
W1-4	60-80	149.2	437.9	183	160.5	7	5.0	154.6	-	14.57
2777 m asl										
W2-1	0-32	148.4	395.4	101.4	164.9	16	16.6	115.3	0.53	12.01
W2-2	32-80	114.6	433.1	113.4	221	10	7.4	130.5	0.08	17.51

W2-3	80-160	108.5	500.1	119.1	259.1	10	5.9	149.8	-	15.57
W2-4	160-210	81	435.9	133.9	245.9	12	8.2	145.2	-	13.63
W2-5	210-240+	74.3	918	248.6	560.3	19	11.6	236	-	12.72
					2150 m asl					
W3-1	0-20	83.4	378.6	261.4	226.7	19	17.9	397.5	1.75	13.81
W3-2	20-50	69.9	373.7	263.5	237.2	16	14.6	378.5	1.03	9.20
W3-3	50-100	76.2	299.1	216.8	191.2	10	9.0	411.4	-	7.22
W3-4	100-120+	57	288	209.6	187.1	9	8.3	434.3	-	3.21
					1724 m asl					
W4-1	0-26	290.7	177.8	288	46.2	3	4.7	818.9	0.09	22.33
W4-2	26-40	332	146.7	166.8	38.3	ND	ND	731.2	0.05	27.52
W4-3	40-70+	462.3	132.6	137.3	42.7	0	ND	669.4	-	30.09

Table S2. 3. Contents and ratios of aluminum (Alox), iron (Feox), phosphorus (Pox), phosphate (P-$PO_{4,ox}$) and silicon (Siox) Extracted with a 0.2 M ammonium oxalate (ox), aluminum (Alpy) extracted with 0.1 M sodium pyrophosphate, iron (Fedc) extracted with Dithionite-Citrate, phosphate (P-$PO_{4,ox}$) extracted with Olsen, and the reactive surface area (RSA) of Soil Profiles from the Eastern toposequence.

East-South toposequence (ES)										
Sample ID	**Depth (cm)**	**mmol kg^{-1} of soil**								**RSA**
		Al_{py}	**Al_{ox}**	**Fe_{ox}**	**Si_{ox}**	**P_{ox}**	**P-PO_4^{3-} (ox)**	**Fe_{dc}**	**P-PO_4 Olsen**	**m^2/kg**
					2853 m asl					
E1-1	0-26	183	698.8	156.5	233.6	21	21.2	138	1.09	22.54
E1-2	26-46	127.1	790.4	184.6	300.9	12	10.5	155	0.08	18.48
E1-3	46-63	178.1	796.9	185.4	260.9	9	6.2	201.1	-	30.69
E1-4	63-96+	147.7	981.9	186	353.7	9	5.3	232.5	-	33.09
					2355 m asl					
E2-1	0-15	264.1	864.9	195.3	297.1	42	38.9	281.5	1.48	34.69
E2-2	15-30	294.5	922.2	204.8	330.3	34	27.3	271.6	0.57	29.57
E2-3	30-50	278.6	802.8	147	284.2	28	19.6	192.4	-	27.14
E2-4	50-80	260.2	1155.9	300.6	412.9	16	5.9	371.9	-	39.06
E2-5	80-110+	272.6	1801.2	307.9	586.7	19	7.0	388.8	-	ND
					1893 m asl					
E3-1	0-25	324.5	1952.3	298.8	679.4	57	62.1	394.7	1.05	42.23
E3-2	25-40	295.4	2014.7	295.1	681	56	68.5	410.5	1.02	39.92
E3-3	40-60	235.3	2396.9	341.8	859	16	8.0	474.1	-	ND
E3-4	60-85	193.7	2313.2	315	878.9	14	18.6	466	-	ND
E3-5	85-120+	NA	2660.9	344.2	1014.9	22	22.6	480.4	-	ND
					1734 m asl					
E4-1	0-32	247.2	2913.7	393.7	1080.8	37	32.9	557.5	0.51	27.36
E4-2	32-60	274.4	3512	434.4	1236.1	12	10.7	565.7	0.04	ND
E4-3	60-90	254.9	4032.5	457.2	1579.6	12	13.7	724.7	-	ND
E4-4	90-120+	221.8	4413.3	611.6	1708.8	6	10.1	946.3	-	ND

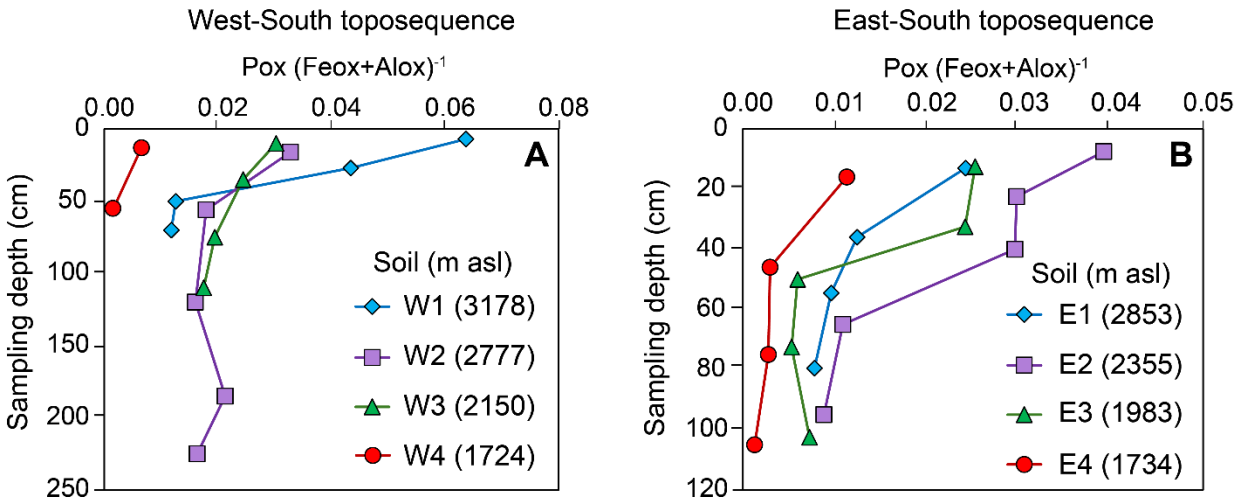

Figure S2. 4. Ratio of Pox(Feox+Alox)-1 extracted with a 0.2 M ammonium oxalate solution, plotted against sampling depth in soil profiles from the Western toposequence (A) and the Eastern toposequence (B) on the southern flank of the Irazú Volcano, Costa Rica. In the legend, the data of altitude (m asl) of each soil profile is provided.

4. GENERAL DISCUSSION

The findings from both chapters of this thesis are closely interconnected and their joint interpretation important insights into how pedogenic and climatic conditions shape the formation of short-range order (SRO) minerals and, in turn, how this influences phosphate (PO_4^{3-}) adsorption and phosphorus (P) availability in two toposequences of volcanic soil. The first chapter focused on studying the variation in content of SRO minerals along contrasting climatic gradients and within soil profiles. The second chapter investigated the reactivity of these minerals, with a focus on PO_4^{3-} sorption processes and their implications for P availability. Consequently, the results from the first chapter provided essential context and foundational information for interpreting the findings of the second chapter.

4.1. SOIL MOISTURE AS A DRIVER OF SRO MINERAL STABILITY ALONG TOPOSEQUENCES

The initial hypothesis for the first chapter proposed that in both the WS and ES toposequences, the content of SRO minerals would increase with decreasing altitudes along the topographic gradient due to enhanced weathering driven by higher temperatures at lower altitudes. Secondly, it was hypothesized that the soil moisture regime of each toposequence modulates the influence of altitude on soil mineralogy content and composition. The first hypothesis was confirmed only for the ES toposequence, whereas the second was supported for both. The different SRO mineral content–altitude patterns observed between the two toposequences were attributed to differences in soil moisture regimes: the ES toposequence maintained a constant Udic regime across elevations, while the WS toposequence shifted from Udic to Ustic conditions with decreasing altitude.

Previous studies have also reported a positive relationship between soil moisture and SRO mineral content in volcanic soil sequences (Nizeyimana *et al*. 1997; Zehetner *et al*. 2003; Tsai *et al*. 2010; Candra *et al*. 2019; Van Ranst *et al*. 2019; Watanabe *et al*. 2023), although in those cases, SRO content generally increased with increasing altitudes because higher elevations were associated with more humid conditions. Additionally, such studies focused on studied a single toposequences, whereas this research allowed to compared two toposequences located in the same study area with different climatic conditions.

Overall, soil humidity consistently emerged as a key factor promoting SRO mineral formation and persistence. The reason is because water molecules play an important role in stabilizing the

surface structure of SRO minerals, preventing the transformation of these minerals into more crystalline and less reactive phases (Manceau and Gates 1997; Jahinge *et al*. 2023). Consequently, the constant humid conditions in soils from the ES toposequence (i.e. Udic moisture regime) favored the formation and preservation of SRO minerals and increased their content with decreasing altitude, whereas in the WS, the transition from humid to drier conditions promoted transformation into more crystalline phases. This mineral transformation can be deduced from the Fe_{ox}/Fe_{dc} ratio, which has been used as a weathering index (Schwertmann 1958; Vacca *et al.* 2003). Lower Fe_{ox}/Fe_{dc} ratios indicated a higher proportion of crystalline iron oxides relative to poor crystalline forms, whereas higher ratios suggested the opposite. The results showed an increasing proportion of well-crystalline iron oxides relative to less crystalline forms at lower altitudes. A comparable trend may also occur in aluminosilicates, with more crystalline phases potentially becoming dominant at lower elevations. However, since this was not assessed in the present study, it remains a hypothesis that warrants investigation in future research.

4.2. IMPLICATION FOR PHOSPHORUS SORPTION AND AVAILABILITY

The implications of higher SRO mineral contents at lower altitudes for nutrient mobility were addressed in the second chapter, using phosphorus (P), a key plant nutrient with traditionally low availability in volcanic soils due to strong retention by SRO minerals (Nanzyo 2002; Qafoku *et al*. 2004; Zheng *et al*. 2012; Zhong *et al*. 2007; Elzinga and Sparks 2007; Sato *et al*. 2024). To establish links between chapters, the mineralogical patterns identified in the first chapter were evaluated in relation to mineral reactivity, PO_4^{3-} sorption, and P availability across the two toposequences. The altitudinal trends described in the first chapter aligned closely with those analyzed in the second, reinforcing the connection between SRO mineral distribution, reactivity, and nutrient availability.

The second chapter hypothesized that both mineral reactivity and PO_4^{3-} adsorption capacity would increase along the toposequences as SRO mineral content increased, while P availability would decrease due to adsorption onto these minerals. This pattern was confirmed for the ES toposequence, where SRO mineral content increased with decreasing altitude, leading to greater mineral reactivity and PO_4^{3-} sorption capacity. These trends were consistent with the SRO mineral distribution identified in the first Chapter, and the constant Udic moisture regime in the ES sequence further modulated these patterns. In contrast, the heterogeneous moisture regime of the WS toposequence hindered the detection of consistent altitudinal trends in SRO content, mineral reactivity, and PO_4^{3-} sorption capacity.

PO_4^{3-} adsorption on SRO minerals occurs primarily through ligand exchange reactions, also called specific adsorption or chemisorption, in which phosphate ions form mono- or bidentate complexes by replacing surface hydroxyl (-OH) groups with phosphate oxygen ligands (PO_4^{3-}) (Goldberg and Sposito 1985; Zheng *et al*. 2012; Elzinga and Sparks 2007; Zhong *et al*. 2007). As a consequence, Andisols have been characterized as having low availability of P, which represent a main challenge for soil fertility and therefore leading to the frequent application of high quantities of phosphate fertilizers in these soils (Nanzyo 2002). The low availability of P in volcanic soils was also evidenced in this research, were in both sequences, the fraction of available P, measured as P-Olsen, was generally low compared to the total P pool that is adsorbed to the reactive mineral surface, measured as P extractable in ammonium oxalate (P_{ox}). In topsoils from the ES toposequence this fraction of available P was lower than in soil availability due to its higher SRO mineral content. These results align with previous studies on volcanic soil toposequences, where SRO minerals and active Al and Fe compounds were positively correlated with P adsorption (Van Ranst *et al*. 2004; Rechberger *et al*. 2021; Chiu *et al*. 2021; Neto *et al*. 2004). However, those studies typically investigated a single toposequence rather than comparing multiple sequences simultaneously.

A distinctive aspect of this work was the incorporation of experimental measurements of reactive surface area (RSA), defined as the total surface area of SRO minerals in soil samples that effectively participate in adsorption processes (Hiemstra *et al*. 2010). The measurement of this soil property remains challenging, therefore literature on its application is scarce. To date, only Mendez *et al*. (2020), Mendez *et al*. (2022) have applied the Hiemstra et al. (2010) methodology in Dutch agricultural topsoils and in topsoils from sub-Saharan region, respectively. Also, recently Fallas-Corrales *et al*. (2025.) applied this method in volcanic tropical soils from Costa Rica. Other studies in volcanic toposequences have been focused on studying a similar soil property called the specific surface area (SSA) (Van Ranst *et al*. 2004; Rechberger *et al*. 2021; Neto *et al*. 2004). This property is defined as the total surface area of a soil per unit per mass ($m^2\ g^{-1}$) (SSSA 2008) that included surfaces that are available and not available for sorption processes, while RSA only determined the surfaces that are available to participate in sorption processes.

It is the first time that the method it has been used in a systematical way to compare internally consistent changes in the reactivity of a soil data set from two volcanic toposequences. Although the method has limitations, as discussed in Chapter 2, it provided internally consistent values for the RSA that allowed for comparative analysis between soils and the identification of altitudinal and depth patterns. Further research is needed to refine this methodology, including testing

alternative proxy materials that may better estimate RSA in soils with high SRO mineral content. Additionally, the addition of Ca^{2+} generally enhanced PO_4^{3-} sorption capacity, with the effect being more pronounced in soils with lower inherent sorption capacity, reduced SRO aluminosilicate content, and lower RSA. These findings have practical implications, as agricultural practices such as liming could influence P availability in volcanic soils. Further field-based research is therefore required to better understand the consequences of this interaction in the field.

4.3. IMPLICATIONS FOR P MANAGEMENT AND FUTURE RESEARCH DIRECTIONS

The findings of this study highlight the need to account for soil moisture regime, altitude, mineralogy, and reactivity when developing P management strategies in tropical volcanic soils. The higher PO_4^{3-} sorption capacity observed in ES toposequence soils suggests that conventional P fertilization may be inefficient or counterproductive in areas such as Pacayas, where highly reactive minerals dominate. In such soils, management should focus on mobilizing sorbed P through practices such as adjusting soil pH to alter mineral surface charge or applying organic amendments that provide competitive sorption sites to release PO_4^{3-}.

In contrast, soils of the WS toposequence, with lower reactivity and sorption capacity, may respond differently. In these soils, practices such as liming could enhance Ca-driven sorption, potentially reducing P availability if not carefully managed. Field monitoring is therefore essential to evaluate the effects of these amendments.

Future research should include long-term field trials to assess how different P sources interact with SRO minerals under varying climatic and topographic conditions. Integrating mineralogical analyses with chemical extractions will be critical for advancing our understanding of P binding mechanisms and improving nutrient-use efficiency in volcanic soils.

4.4. CONCLUSIONS AND RECOMMENDATIONS

This study demonstrates that both altitude and soil moisture regime strongly influence the formation of SRO minerals, their RSA, and associated P adsorption and P availability in volcanic soils of Irazú Volcano. Soils under a stable Udic regime (ES toposequence) showed higher SRO content, RSA, and P sorption capacity compared with those under a transitional Udic to Ustic regime (WS toposequence), where SRO minerals tended to transform into more crystalline forms. The consistently low P-Olsen fraction across all samples indicates strong P adsorption by SRO minerals, limiting P availability for plants. These findings emphasize the importance of considering soil mineral reactivity, altitude and moisture conditions when designing site-specific nutrient management strategies. Future research should focus on assessing the effects of fertilization,

liming, and organic amendments under field conditions to optimize P-use efficiency and sustain soil fertility in volcanic agroecosystems.

5. REFERENCES

Alvarado, A., Bertsch, F., Bornemisza, E., Cabalceta, G., Forsythe, W., Henríquez, C., Mata, R., Molina, E., Salas, R., 2001. Suelos derivados de cenizas volcánicas (Andisoles) de Costa Rica. ACCS, San Jose, Costa Rica.

Alvarado, A., Buol, S.W. 1985. Field Estimation of Phosphate Retention by Andepts. Soil Sci. Soc. Am. J. 49:911–914. https://doi.org/10.2136/sssaj1985.03615995004900040024x

Alvarado, A., Iturriaga, I., Smyth, J.T., Portuguez, E., Ureña J.M. 2009. Efecto Residual del Fertilizante Fosfatado Adicionado al Cultivo de la Papa en un Andisol de Juan Viñas, Costa Rica. Agronomía Costarricense 33(1): 63-76. https://revistas.ucr.ac.cr/index.php/agrocost/article/view/6735

Alvarado, A., Mata, R., Chinchilla, M. 2014. Arcillas identificadas en suelos de Costa Rica a nivel generalizado durante el período 1931-2014: II. mineralogía de arcillas en suelos con características vérticas y oxídico caoliníticas. Agron. Costarric. 38, 75–106. https://doi.org/10.15517/rac.v38i1.15161

Candra, I.N., Gerzabek, M.H., Ottner, F., Tintner, J., Wriessnig, K., Zehetner, F. 2019. Weathering and soil formation in rhyolitic tephra along a moisture gradient on Alcedo Volcano, Galápagos. Geoderma 343, 215–225. https://doi.org/10.1016/J.GEODERMA.2019.01.051

Castillo-Muñoz, R. 2019. Atlas Geoquímico de Costa Rica: Suelos: Fertilidad y Medioambiente. Primera edición. San José, Costa Rica: Edinexo.

Chiu, C-Y; Baillie, I; Jien, S-H; Hallett, L; Hallett, S. 2021. Sequestration of P fractions in the soils of an incipient ferralisation chronosequence on a humid tropical volcanic island. Botanical Studies 62(1):20. DOI: https://doi.org/10.1186/s40529-021-00326-5.

Cornell, R.M. and Schwertmann, U. 2003. The Iron Oxides: Structure, Properties, Reactions, Occurrences and Uses. 2nd Edition, Wiley-VCH, Weinheim. https://doi.org/10.1515/CORRREV.1997.15.3-4.533

Elzinga, EJ; Sparks, DL. 2007. Phosphate adsorption onto hematite: an *in situ* ATR-FTIR investigation of the effects of pH and loading level on the mode of phosphate surface

complexation. Journal of Colloid and Interface Science 308(1):53-70. DOI: https://doi.org/10.1016/j.jcis.2006.12.061.

Fallas-Corrales, RA; Mendez, JC; Meeussen, JCL. s. f. Boron Adsorption and Interaction With Phosphate in a Volcanic Soil From the Humid Tropic (online). Journal of Plant Nutrition and Soil Science n/a(n/a). DOI: https://doi.org/10.1002/jpln.70012.

Galvez, N., Barron, V., Torrent, J. 1999. Effect of phosphate on the crystallization of hematite, goethite, and lepidocrosite from ferrihydrite. Clays Clay Miner., 47, 304-311. https://citeseerx.ist.psu.edu/document?repid=rep1&type=pdf&doi=a9ef286b530c89af74f5d33848daf3dd2e1b5977

Gee, G.W., Or, D. 2002. Methods of Soil Analysis: Part 4. Physical Methods Chapter: 2.4. Soil Science Society of America, Inc.

Glossary of Soil Science Terms | Soil Science Society of America. 2025. (online). Consulted at 25 ago. 2025. Disponible en https://www.soils.org/publications/soils-glossary?q=publications/soils-glossary/.

Grieve, I.C., Proctor, J. and Cousins, S.A. 1990. Soil variation with altitude on Volcan Barva, Costa Rica. Catena, 17: 525 –534. https://doi.org/10.1016/0341-8162(90)90027-B

Hashimoto, Y., Kang, J., Matsuyama, N., Saigusa, M. 2012. Path analysis of phosphorus retention capacity in allophanic and nonallophanic Andisols. Soil Science Society of America Journal, 76: 441–448. http://doi.org/10.2136/sssaj2011.0196

Henmi, T., Nakai, M., Nakata, T., Yoshinaga, N. 1982. Removal of phosphorus by utilizing clays of volcanic ash soil and weathered pumice. Memoirs of the college of Agriculture, Ehime University, pp.17-24.

Henríquez, C. 2005. Sorción y desorción de fósforo en un Andisol de Costa Rica dedicado al cultivo del café, caña de azúcar y bosque. Agron. Costarric. 29:97–105. https://revistas.ucr.ac.cr/index.php/agrocost/article/view/6784

Hiemstra, T. 2013. Surface and mineral structure of ferrihydrite. Geochim. Cosmochim. Acta 105: 316-325. https://doi.org/10.1016/j.gca.2012.12.002

Hiemstra, T., Antelo, J., Rahnemaie, R., van Riemsdijk, W.H. 2010a. Nanoparticles in natural systems I: The effective reactive surface area of the natural oxide fraction in field samples. Geochim. Cosmochim. Acta 74: 41–58. https://doi.org/10.1016/j.gca.2009.10.018

Hiemstra, T., Antelo, J., van Rotterdam, A.M.D., van Riemsdijk, W.H. 2010b. Nanoparticles in natural systems II: The natural oxide fraction at interaction with natural organic matter and phosphate. Geochim. Cosmochim. Acta 74: 59–69. https://doi.org/10.1016/j.gca.2009.10.019

Hiemstra, T., Van Riemsdijk, W.H. 1996. A surface structural approach to ion adsorption: The charge distribution (CD) model. J. Colloid Interface Sci. 179: 488–508. https://doi.org/10.1006/jcis.1996.0242

Hiemstra, T., Van Riemsdijk, W.H. 2006. On the relationship between charge distribution, surface hydration, and the structure of the interface of metal hydroxides. J. Colloid Interface Sci. 301, 1–18. https://doi.org/10.1016/J.JCIS.2006.05.008

Hiemstra, T., Zhao, W. 2016. Reactivity of ferrihydrite and ferritin in relation to surface structure, size, and nanoparticle formation studied for phosphate and arsenate. Environ. Sci. Nano 3: 1265–1279. https://doi.org/10.1039/C6EN00061D

Hiemstra, T; Antelo, J; Rahnemaie, R; Riemsdijk, WH van. 2010. Nanoparticles in natural systems I: The effective reactive surface area of the natural oxide fraction in field samples. Geochimica et Cosmochimica Acta 74(1):41-58. DOI: https://doi.org/10.1016/j.gca.2009.10.018.

Jahinge, THL; Payne, MK; Unruh, DK; Jayasinghe, AS; Yu, P; Forbes, TZ. 2023. Characterization of Water Structure and Phase Behavior within Metal–Organic Nanotubes. Langmuir 39(51):18899-18908. DOI: https://doi.org/10.1021/acs.langmuir.3c02786.

Jenny, H. 1941. Factors of Soil Formation: A System of Quantitative Pedology. Foreword by Ronald Amundson. Dover Publications, New York, 281 p. https://doi.org/10.1016/j.geoderma.2021.114960

Kautz, C.R., Ryan, P.C. 2003. The 10 Å to 7 Å halloysite transition in a tropical soil sequence, Costa Rica. Clays and Clay Minerals, 51(3): 252–263. https://doi.org/10.1346/CCMN.2003.0510302

Keizer, M.G., van Riemsdijk, W.H., 1998. ECOSAT, Equilibrium Calculation of Speciation and Transport. Technical Report. Department of Soil Quality. Wageningen Univeristy.

Kinniburgh, D.G., 1993. Fit, Technical Report WD/93/23. Keyworth, Great Britain.

Koopmans, G.F.F., Hiemstra, T., Vaseur, C., Chardon, W.J.J., Voegelin, A., Groenenberg, J.E.E., 2020. Use of iron oxide nanoparticles for immobilizing phosphorus in-situ: Increase in soil reactive surface area and effect on soluble phosphorus. Sci. Total Environ. 711, 135220. https://doi.org/https://doi.org/10.1016/j.scitotenv.2019.135220

Landaeta, A., Lopez, C.A., Alvarado, A.1978. Caracterización de la fracción mineral de suelos derivados de cenizas volcánicas de la Cordillera de Talamanca, Costa Rica. Agron. Costarric. 2:117–129. https://www.mag.go.cr/rev_agr/v02n02_117.pdf

Li, M., Sugimoto, T., Yamashita, Y., Kobayashi, M. 2022. Aggregation and charging of natural allophane particles in the presence of oxyanions. Colloids and Surfaces A: Physicochemical and Engineering Aspects 649: 129413. https://doi.org/10.1016/j.colsurfa.2022.129413

Liu, J., Zhu, R., Ma, L., Fu, H., Lin, X., Parker, S.C., Molinari, M. 2021. Adsorption of phosphate and cadmium on iron (oxyhydr)oxides: A comparative study on ferrihydrite, goethite, and hematite. Geoderma 383: 114799. https://doi.org/10.1016/j.geoderma.2020.114799

Manceau, A., Gates, WP. 1997. Surface Structural Model for Ferrihydrite. Clays and Clay Minerals 45(3):448-460. DOI: https://doi.org/10.1346/CCMN.1997.0450314.

Martini, J.A., Mosquera, L. 1972. Properties of Five Tropepts in a Toposequence of the Humid Tropics in Costa Rica. Soil Sci. Soc. Amer. Proc., VOL. 36. https://doi.org/10.2136/sssaj1972.03615995003600030030x

Mehra, O.P., Jackson, M.L. 1960. IRON OXIDE REMOVAL FROM SOILS AND CLAYS BY A DITHIONITE–CITRATE SYSTEM BUFFERED WITH SODIUM BICARBONATE, in: Clays and Clay Minerals. Pergamon, pp. 317–327. https://doi.org/10.1016/b978-0-08-009235-5.50026-7

Meijer, E.L., Buurman, P. 2003. Chemical trends in a perhumid soil catena on the Turrialba volcano (Costa Rica). Geoderma 117:185–201. https://doi.org/10.1016/S0016-7061(03)00122-8

Mendez, J.C., Hiemstra, T. 2020. Surface area of ferrihydrite consistently related to primary surface charge, ion pair formation, and specific ion adsorption. Chemical Geology, 532, 119304. https://doi.org/10.1016/j.chemgeo.2019.119304

Mendez, J.C., Van Eynde, E., Hiemstra, T., Comans, R.N.J. 2022. Surface reactivity of the natural metal (hydr)oxides in weathered tropical soils. Geoderma 406, 115517. https://doi.org/10.1016/j.geoderma.2021.115517

Mendez, JC., Hiemstra, T., Koopmans, GF. 2020. Assessing the Reactive Surface Area of Soils and the Association of Soil Organic Carbon with Natural Oxide Nanoparticles Using Ferrihydrite as Proxy. Environmental Science & Technology 54(19):11990-12000. DOI: https://doi.org/10.1021/acs.est.0c02163.

Murphy, J., Riley, J.P. 1962. A modified single solution method for the determination of phosphate in natural waters. Anal. Chim. Acta 27, 31–36. https://doi.org/10.1016/S0003-2670(00)88444-5

Nanzyo M. 2002. Unique Properties of Volcanic Ash Soils. Global Environmental Research, Vol. 6, 2002, pp. 99-112. https://www.researchgate.net/publication/228797761_Unique_properties_of_volcanic_ash_soils

NCSS (National Cooperative Soil Survey). 2023 NCSS (National Cooperative Soil Survey) National Cooperative Soil Survey Characterization Database http://ncsslabdatamart.sc.egov.usda.gov/ (2023)

Neall, V.E. 2000. Volcanic Soils. Land Use and Land Cover – Vol. VII. https://edepot.wur.nl/484591

Neto, FCR., Schaefer, CEGR., Costa, LM., Corrêa, MM., Filho, EIF., Ibraimo, MM. 2004. Phosphorus adsorption, specific surface, and mineralogical attributes of soils developed from volcanic rocks from the Upper Paranaíba, MG (Brazil). Rev. Bras. Ciênc. Solo 28(6):953-964. DOI: https://doi.org/10.1590/S0100-06832004000600003.

Nieuwenhuyse, A., Verburg, P.S., Jongmans, A. 2000. Mineralogy of a soil chronosequence on andesitic lava in humid tropical Costa Rica. Geoderma 98:61–82. https://doi.org/10.1016/S0016-7061(00)00052-5

Nizeyimana, E., Bicki, TJ., Agbu, PA. 1997. AN ASSESSMENT OF COLLOIDAL CONSTITUENTS AND CLAY MINERALOGY OF SOILS DERIVED FROM VOLCANIC MATERIALS ALONG A TOPOSEQUENCE IN RWANDA. Soil Science 162(5):361.

Olsen, S.R., Cole, C.V., Watanabe, F.S., Dean, L.A. 1954. Estimation of available phosphorous in soils by extraction with sodium bicarbonate.

Parfitt, L.R., Kimble, M.J. 1989. Conditions for Formation of Allophane in Soils. Soil Sci. Soc. Am. J. 53:971-977. https://doi.org/10.2136/sssaj1989.03615995005300030057x

Qafoku, N., Van Ranst, E., Noble, A., Baert, G. 2004. Variable Charge Soils: Their Mineralogy, Chemistry and Management. Advances in Agronomy 84:159-215. DOI: https://doi.org/10.1016/S0065-2113(04)84004-5.

Ranst V.E., Mees F., De Grave E., Ye L., Cornelis J-T., Delvaux B. 2019. Impact of andosolization on pedogenic Fe oxides in ferrallitic soils. Geoderma 347: 244-251. https://doi.org/10.1016/j.geoderma.2019.04.013

Rechberger, MV., Zehetner, F., Gerzabek, MH. 2021. Phosphate sorption-desorption properties in volcanic topsoils along a chronosequence and a climatic gradient on the Galápagos Islands. Journal of Plant Nutrition and Soil Science 184(4):479-491. DOI: https://doi.org/10.1002/jpln.202000488.

Sato, K., Hama, T., Ito, H., Kobayashi, K., Nakamura, K., Sakurai, S. 2024. Long-term stability of phosphate sorbed on an allophanic Andosol and a synthesized allophane. Soil Science Society of America Journal 88(6):1932-1941. DOI: https://doi.org/10.1002/saj2.20748.

Saunders, W. M. H. 1959. Effect of phosphate topdressing on a soil from andesitic volcanic ash, New Zealand Journal of Agricultural Research, 2:4, 659-665. https://doi.org/10.1080/00288233.1959.10422824

Saunders, W. M. H. 1965. Phosphate retention by New Zealand soils and its relationship to free sesquioxides, organic matter, and other soil properties, New Zealand Journal of Agricultural Research, 8:1, 30-57. https://doi.org/10.1080/00288233.1965.10420021

Schwertmann, U. 1964. Differenzierung der Eisenoxide des Bodens durch Extraktion mit Ammoniumoxalat-Lösung. Zeitschrift für Pflanzenernährung, Düngung, Bodenkd. 105, 194–202. https://doi.org/10.1002/jpln.3591050303

Segura, M., Etxaleku, N., Castillo, A., Salazar, M., Alvarado, A. 2005. Respuesta a la Fertilización con P en Plantaciones de Jaúl (Alnus acuminata) en Andisoles de la Cuenca del Río Virilla, Costa Rica. Agronomía Costarricense 29(2): 121-134. https://dialnet.unirioja.es/servlet/articulo?codigo=6314484

Shoji, S., Fujiwara, Y. 1984. Active Aluminum and Iron in the Humus Horizons of Andosols from Northeastern Japan: Their Forms, Properties, and Significance in Clay Weathering. Soil Science. Volume 137 - Issue 4 - p 216-226

Simonsson, M., Berggren, D. and Gustafsson, J.P. 1999. Solubility of Aluminum and Silica in Spodic Horizons as Affected by Drying and Freezing. Soil Sci. Soc. Am. J., 63, 1116-1123. https://doi.org/10.2136/sssaj1999.6351116x

Soil Science Society of America (SSSA). 2008. Glossary of Soil Science Terms. Madison, WI, USA: Soil Science Society of America.

Soil Survey Staff. 2014. Kellogg Soil Survey Laboratory Methods Manual. Soil Survey Investigations Report No. 42, Version 5.0. R. Burt and Soil Survey Staff (ed.). U.S. Department of Agriculture, Natural Resources Conservation Service.

Soto, J. 1999. Formas de fósforo y su liberación en andisoles de la region central oriental de

Costa Rica. Universidad de Córdoba, Spain.

Strawn, D.G., Bohn, H.L., O'Connor, G.A. 2015. Soil Chemistry. Wiley-Blackwell 4th edition. 392 pp.

Takahashi, T., Dahlgren, R.A. 2016. Nature, properties and function of aluminum–humus complexes in volcanic soils. Geoderma 263:110–121. https://doi.org/10.1016/j.geoderma.2015.08.032

Theng, B.K.G., Russell, M., Churchman, G.J., Parfitt, R.L. 1982. Surface properties of allophane, halloysite, and imogolite. Clays Clay Miner. 30(2): 143-149. https://doi.org/10.1346/CCMN.1982.0300209

Tsai, C.C., Chen Z.S., Kao C.I., Ottner F., Kao S.J., Zehetner, F. 2010. Pedogenic development of volcanic ash soils along a climosequence in Northern Taiwan. Geoderma 156:48–59. https://doi.org/10.1016/j.geoderma.2010.01.007

Uchida, S., Hashimoto, Y., Takamoto, A., Noguchi, K., Klysubun, W., Wang, S.L. 2022. Phosphate binding to allophane and ferrihydrite with implications for volcanic ash soils. Soil Sci. Soc. Am. J. 1–11. https://doi.org/10.1002/saj2.20463

Uehara G., Gillman G.P. 1980. Charge Characteristics of Soils with Variable and Permanent Charge Minerals: I. Theory. Soil Sci. Soc. Am. J., VOL. 44. https://doi.org/10.2136/sssaj1980.03615995004400020008x

Van Dooremolen, W.A., Wielemaker, W.G., Van Breemen, N., Meijer, E.M., van Reewijk, L.P., 1990. Chemistry and mineralogy of andosols of various age in a soil chronosequence on andesitic lahars in Costa Rica. Chem. Geol. 84, 139–141. https://doi.org/10.1016/0009-2541(90)90190-I

van Erp, P.J., Houba, Y.J.G., Van Beusichem, M.L. 1998. One hundredth molar calcium chloride extraction procedure. part I: A review of soil chemical, analytical, and plant nutritional aspects. Commun. Soil Sci. Plant Anal. 29, 1603–1623. https://doi.org/10.1080/00103629809370053

Van Ranst, E., Mees, F., De Grave, E., Ye, L., Cornelis, J-T., Delvaux, B. 2019. Impact of andosolization on pedogenic Fe oxides in ferrallitic soils. Geoderma 347:244-251. DOI: https://doi.org/10.1016/j.geoderma.2019.04.013.

Van Ranst, E., Utami, SR., Vanderdeelen, J., Shamshuddin, J. 2004. Surface reactivity of Andisols on volcanic ash along the Sunda arc crossing Java Island, Indonesia. Geoderma 123(3):193-203. DOI: https://doi.org/10.1016/j.geoderma.2004.02.005.

Van Reeuwijk, L.P. 1993. n. International Soil Reference and Information Centre (ISRIC). Wageningen. Netherlands.

Verbeeck, M., Hiemstra, T., Thiry, Y., Smolders, E., 2017. Soil organic matter reduces the sorption of arsenate and phosphate: a soil profile study and geochemical modelling. Eur. J. Soil Sci. 68, 678–688. https://doi.org/10.1111/ejss.12447

Wada K., Henmi T., Yoshinaga N., Patterson S.H. 1972. Imogolite and Allophane Formed in Saprolite of Basalt on Maui, Hawaii. Clays Clay Miner. 20: 375–380. https://doi.org/10.1346/CCMN.1972.0200605

Wada, K. 1989. Allophane and imogolite, In: J.B. Dixon and S.B. Weed (eds.), Minerals in Soil Environments, 2nd Ed. Soil Science Society America Inc., Madison, Wisconsin, USA., pp.1051-1087. https://doi.org/10.2136/sssabookser1.2ed.c21

Wada, S.I., Kawabata K. 1991. Ion adsorption on variable charge materials and thermodynamics of ion exchange, Soil Science and Plant Nutrition, 37(2):191-200. https://doi.org/10.1080/00380768.1991.10415029

Warrinnier, R., Goossens, T., Amery, F., Vanden Nest, T., Verbeeck, M., Smolders, E. 2019. Investigation on the control of phosphate leaching by sorption and colloidal transport: Column studies and multi-surface complexation modelling. Appl. Geochemistry 100, 371–379. https://doi.org/10.1016/j.apgeochem.2018.12.012

Watanabe, T., Ueda, S., Nakao, A., Ze, AM., Dahlgren, RA., Funakawa, S. 2023. Disentangling the pedogenic factors controlling active Al and Fe concentrations in soils of the Cameroon

volcanic line. Geoderma 430:116289. DOI: https://doi.org/10.1016/j.geoderma.2022.116289.

Zehetner, F., Miller, WP., West, LT. 2003. Pedogenesis of Volcanic Ash Soils in Andean Ecuador. Soil Science Society of America Journal 67(6):1797-1809. DOI: https://doi.org/10.2136/sssaj2003.1797.

Zheng, T-T., Sun, Z-X., Yang, X-F., Holmgren, A. 2012. Sorption of phosphate onto mesoporous γ-alumina studied with in-situ ATR-FTIR spectroscopy. Chemistry Central Journal 6(1):26. DOI: https://doi.org/10.1186/1752-153X-6-26.

Zhong, B., Stanforth, R., Wu, S., Chen, JP. 2007. Proton interaction in phosphate adsorption onto goethite. Journal of Colloid and Interface Science 308(1):40-48. DOI: https://doi.org/10.1016/j.jcis.2006.12.055.